ACADEMIC REGISTRY

Research Thesis Submission

Name*:*	Eziuche Amadike Ugbogu		
School/PGI:	School of Life Sciences		
Version: *(i.e. First, Resubmission, Final)*		Degree Sought (Award and Subject area)	PhD in Biochemistry

Declaration

In accordance with the appropriate regulations I hereby submit my thesis and I declare that:

1) the thesis embodies the results of my own work and has been composed by myself
2) where appropriate, I have made acknowledgement of the work of others and have made reference to work carried out in collaboration with other persons
3) the thesis is the correct version of the thesis for submission and is the same version as any electronic versions submitted*.
4) my thesis for the award referred to, deposited in the Heriot-Watt University Library, should be made available for loan or photocopying and be available via the Institutional Repository, subject to such conditions as the Librarian may require
5) I understand that as a student of the University I am required to abide by the Regulations of the University and to conform to its discipline.

* *Please note that it is the responsibility of the candidate to ensure that the correct version of the thesis is submitted.*

Signature of Candidate*:*		Date:	

Submission

Submitted By (name in capitals):	
Signature of Individual Submitting:	
Date Submitted:	

For Completion in the Student Service Centre (SSC)

Received in the SSC by *(name in capitals):*			
Method of Submission (Handed in to SSC; posted through internal/external mail):			
*E-thesis Submitted (**mandatory for final theses)***			
Signature:		Date:	

The *PRS* gene family links primary metabolism and cell signalling in *Saccharomyces cerevisiae*

Submitted by

Eziuche Amadike Ugbogu

For the Degree of Doctor of Philosophy in Biochemistry

SCHOOL OF LIFE SCIENCES

HERIOT-WATT UNIVERSITY, EDINBURGH

September, 2014

This copy of the thesis has been supplied on condition that anyone who consults it is understood to recognize that the copyright rests with its author and that no quotation from the thesis and no information derived from it may be published without the prior written consent of the author or the University (as may be appropriate).

Table of Contents

Acknowledgements ix

Declaration x

Publications xi

Abbreviations xii

Symbols for Amino Acids xvi

Abstract xvii

1 Introduction 1

1.1 Human *PRS* genes and associated hereditary disorders 3

1.2 Prs-encoding genes in *Saccharomyces cerevisiae* 5

1.3 Cell wall integrity signalling pathway in *S. cerevisiae* 6

1.4 PPRP synthetase gene deletions in *S. cerevisiae* 12

1.5 Interaction of *PRS* genes with other genes 16

1.6 Aim of study 18

2 Materials and Methods 19

2.1 Strains 19

2.2 Plasmids 21

2.3 Media 26

2.3.1 LB (Luria-Bertani) medium 26

2.3.2 YEPD (Yeast Extract Peptone Dextrose) medium 26

2.3.3 SC (Synthetic Complete) media 26

2.3.4 Raffinose media 27

2.3.5 3xYeast Extract Peptone Galactose (YEPG) media 27

2.4 Strain maintenance 28

2.5 Determination of cell density 28

2.5.1 Sorbitol rescue of yeast strains' sensitivity to temperature and caffeine 28

2.6 Yeast transformation using the 'PLATE' method 29
2.7 Preparation of crude extract from *S. cerevisiae* 30
2.8 Determination of total protein in cell extracts 31
2.9 Analysis of proteins by SDS-polyacrylamide gel electrophoresis (SDS- PAGE) 34
2.9.1 Preparation of gels for SDS-PAGE 35
2.9.2 Preparation of protein samples 36
2.9.3 Coomassie staining and destaining of the gel 37
2.10 Western blotting 37
2.10.1 Electroblotting on PVDF (polyvinylidene difluoride) membrane 38
2.10.2 Immunodetection 39
2.10.3 Image detection 42
2.11 Co-immunoprecipitation 42
2.11.1 Co-immunoprecipitation of GFP-Prs1 and FLAG-tagged Slt2 42
2.11.2 Co-immunoprecipitation of His-tagged Prs1 and FLAG-tagged Slt2 46
2.12 Band quantification using the ChemiDoc™ XRS+ Imager Quantity One" software 47
2.13 Determination of β-galactosidase activity by the Thermo Scientific Yeast β-galactosidase assay kit 48
2.14 Determination of the *FKS2* expression 49
2.15 Preparation of cell extracts for isolation of His-tagged Prs5 50
2.16 Protein purification 50
2.16.1 Protein purification using the ÄKTA purifier Avant 250 50
2.16.2 Manual purification of His-tagged Prs5 using a His SpinTrap™ column 52
2.17 Mass spectrometry analysis 53
2.18 Statistical analysis 53
2.19 Database searches 54

3 Results 55

3.1 Monitoring the GFP signal generated by GFP-Prs1 in various *PRS* deletant strains 55

3.2 Growth of *PRS* deletant strains on 2% galactose at 30°C and 37°C 57

3.3 The interaction of Prs1 with Slt2 as demonstrated by co-immunoprecipitation 59

3.3.1 Temperature-dependent interaction of Prs1 with Slt2 60

3.4 Phenotypes of rescued YN97-14 (*prs1Δprs5Δ*) strains 63

3.4.1 Temperature sensitivity of YN97-14 rescued strains 65

3.4.2 Caffeine sensitivity of YN97-14 rescued strains 66

3.4.3 β-galactosidase activity as a measure of Rlm1 expression in viable transformants of YN97-14 (*prs1*Δ*prs5*Δ) 69

3.4.4 Phosphorylation status of Slt2 in rescued *prs1Δprs5Δ* deletant strains 71

3.5 Mutation of postulated phosphorylation sites of Prs5 influences temperature-induced Rlm1 expression 73

3.5.1 Influence of *in vitro* generated *PRS5* mutations on the phosphorylation status of Slt2 77

3.5.2 What is the individual contribution of the three postulated phosphorylated serine residues mutated in prs5(479) to Rlm1 expression following growth at elevated temperature? 80

3.5.3 Phosphorylation status of Slt2 following mutation of S_{364}, S_{367} and S_{369} aa residues of Prs5 82

3.5.4 Evaluation of Fks2 expression in the single mutations S_{364}A, S_{367}A and S_{369}A of Prs5 in comparison to Prs5 (WT) and prs5(479) 85

3.6 Introduction of Prs5 and *in vitro*-generated mutations thereof into YN97-14 rescued strains results in a synthetic growth defect and compromised CWI signalling 87

3.7 Detection of His-tagged Prs5 by Western blot analysis 91

3.7.1 Partial purification of His-tagged Prs5 proteins 92
3.7.2 Mass spectrometry (MS) analysis of His-tagged Prs5 95
4 Discussion 103
4.1 Interdependence of Prs1 and Prs3 112
4.2 Interaction of Prs1 with the CWI pathway 112
4.3 Isolation of the Prs5 polypeptide and associated proteins 115
Summary and perspective 118
References 147
Appendix ..... **Error! Bookmark not defined.**

List of Figures

Figure 1.1: The biosynthesis and metabolic fates of phosphoribosyl pyrophosphate (PRPP) 3
Figure 1.2: The structure of the five PRPP synthetase polypeptides 6
Figure 1.3: Scheme of the CWI signalling pathway 7
Figure 1.4: Functional entities and phenotypic minimal functional units of *S. cervisiae* Prs 12
Figure 2.1: Standard curve for quantifying total protein content in cell extracts, using BSA as the standard 33
Figure 2.2: Chemiluminescent reaction of Lumigen PS-3 with horseradish peroxidase 40
Figure 3.1: Monitoring the GFP signal in YN94-1 (WT), YN97-96 (*prs1*Δ::GFP-PRS1), YN98-8 (YN97-96 prs2Δ), YN98-11 (YN97-96 *prs3*Δ), YN98-12 (YN97-96 *prs4*Δ) and YN98-14 (YN97-96 *prs5*Δ). 56
Figure 3.2: Growth pattern of *PRS* deletant strains on YEP+2% galactose. 58
Figure 3.3: Principle of co-immunoprecipitation 59
Figure 3.4: Interaction of Slt2 with Prs1 61
Figure 3.5: Phosphorylation status of Slt2 dictates its interaction with Prs1 63
Figure 3.6: A schematic representation of *in vitro* mutated versions of *PRS1* capable of rescuing synthetic lethality 64
Figure 3.7: Temperature sensitivity of YN97-14 rescued strains 66
Figure 3.8: Effect of sorbitol on caffeine sensitivity of the rescued YN97-14 strains 68
Figure 3.9: Rlm1 expression at 30^{o}C and 37^{o}C as measured by β-galactosidase activity in the *prs1*Δ*prs5*Δ rescued strains 70
Figure 3.10: Phosphorylation status of Slt2 in rescued YN97-14 (*prs1*Δ*prs5*Δ) strains 71
Figure 3.11: Quantification of P-Slt2 status in YN97-14 (*prs1Δprs5Δ*) rescued strains 72
Figure 3.12: Influence of mutating the postulated phosphorylation sites in Prs5 on Rlm1 expression at 30^{o}C and 37^{o}C 76
Figure 3.13: Elevated incubation temperature influences the phosphorylation status of Slt2 in *PRS5* mutants 78

Figure 3.14: Quantification of P-Slt2 in strains carrying the *in vitro* mutated versions of Prs5 79
Figure 3.15: Rlm1 expression of single mutations of Prs5 in comparison with Prs5 (WT) and prs5(479) 81
Figure 3.16: Slt2 phosphorylation status of single serine residues, S364, S367 and S369, mutated in prs5(479) 83
Figure 3.17: Quantification of P-Slt2 status of single serine residues mutated in prs5(479) 84
Figure 3.18: Fks2 activity of individual mutations of S364A, S367A and S369A of Prs5 in comparison to Prs5 (WT) and prs5(479) 86
Figure 3.19: Temperature sensitivity of strains obtained by combining Prs1 and the *in vitro* mutations of Prs5 in YN97-14 87
Figure 3.20: Influence of Prs5 *in vitro* mutations on Rlm1 expression in YN97-14 rescued strains 89
Figure 3.21: Temperature sensitivity of prs1(Q133P) in combination with Prs5 WT and its derivatives 90
Figure 3.22: His-tagged Prs5 and GFP-Prs1 detection by Western blotting analysis of crude protein extracts of raffinose-grown and galactose-induced cultures of YN11-01 92
Figure 3.23: Purification profile of His-tagged Prs5 obtained from a 6 hr galactose-induced extract of YN11-01 94
Figure 3.24: Western blot analysis of YN11-01 crude extract of YN11-01 and the peak fractions eluted with 200 mM imidazole 95
Figure 3.25: SDS-PAGE and Western blot analysis of His-tagged Prs5 97
Figure 3.26: CID spectrum of the Prs5 peptide fragment, $_{117}$ENYTFESHPGTPVSSSLMTQRPGAESSLK$_{145}$ (gi: 6324511) 98
Figure 3.27: CID spectrum of the Prs1 peptide, $_{307}$EQLITLVGNVR$_{317}$ (gi: 6322667) 100
Figure 4.1: Model for activation of transcription by CWI signalling. 111
Figure 4.2: Interaction of Prs1 with Mpk1/Slt2 114

List of tables

Table 2.1: *S. cerevisiae* strains used in this study 19
Table 2.2: Plasmids 21
Table 2.3: Standard curve samples for Bradford protein assay 36
Table 3.1: Mutations of the triply phosphorylated aa residues of the Prs5 polypeptide 74
Table 3.2: Proteins and peptides identified by ESI-MS/MS analysis of YN11-01 and YN97-91 102
Table 5.1: Raw data of results presented in Figure 3.9. Rlm1 expression at 30^{o}C and 37^{o}C as measured by β-galactosidase activity in the *prs1Δ prs5Δ* rescued strains ..... **Error! Bookmark not defined.**
Table 5.2: Raw data of results presented in Figure 3.11. Quantification of phospho-Slt2 in *prs1Δprs5Δ* rescued strains based on the amount of Slt2 at 30^{o}C and 37^{o}C ..... **Error! Bookmark not defined.**
Table 5.3: Raw data of results presented in Figure 3.12. Influence of mutating the postulated phosphorylation sites in Prs5 on Rlm1 expression at 30^{o}C and 37^{o}C ..... **Error! Bookmark not defined.**
Table 5.4: Raw data of results presented in Figure 3.14. Quantification of phospho-Slt2 *in vitro* mutated versions of Prs5. All measurements were taken after 1 min exposure in the ChemiDoc imager ..... **Error! Bookmark not defined.**
Table 5.5: Raw data of the results presented in Figure 3.15. Rlm1 expression of single mutation of Prs5 in comparison with prs5(479) and Prs5 (WT) ..... **Error! Bookmark not defined.**
Table 5.6: Raw data of the results presented in Figure 3. 17. Phosphorylation of single mutations of Prs5 in comparison with prs5(479) and Prs5 (WT) ..... **Error! Bookmark not defined.**
Table 5.7: Raw data of result presented in Figure 3.18. Fks2 activity of single mutations of Prs5 in comparison with prs5(479) and Prs5 (WT) ..... **Error! Bookmark not defined.**
Table 5.8: Raw data of results presented in Figure 3.20. Influence of Prs1 and *in vitro* mutants of Prs5 on Rlm1 expression ..... **Error! Bookmark not defined.**

Table 5.9: Raw data of results presented in Figure 3.20. Influence of prs1(L115T) and *in vitro* mutants of Prs5 on Rlm1 expression.....**Error! Bookmark not defined.**

Table 5.10: Raw data of results presented in Figure 3.20. Influence of prs1(D326A) and *in vitro* mutants of Prs5 on Rlm1 expression.....**Error! Bookmark not defined.**

Table 5.11: Raw data of results presentedin Figure 3.20. Influence of prs1(D326A/H130A) and *in vitro* mutants of Prs5 on Rlm1 expression .....**Error! Bookmark not defined.**

Table 5.12: Raw data of results presented in Figure 3.22.....**Error! Bookmark not defined.**

Table 5.13: Interaction of Prs proteins with other proteins .....**Error! Bookmark not defined.**

Acknowledgements

My sincere gratitude goes to my supervisor Professor Michael Schweizer and Dr Lilian Schweizer for their parental advice, patience, encouragement and great kindness.

I remain grateful to Abia State University for their financial support. My special thanks go to my mentors and teachers: Professors Emmanuel I. Akubugwo, Chibuzo Ogbuagu, Uche Ikonne, Ogwo E. Ogwo, Reginald A. Onyeagba, Florence Nduka, Friday O.Uhegbu, Emeka Iweala, Ify Elekwa, Chuks I. Ogbonnaya, Nma Onyeike and Drs. Godwin C. Chinyere, Stanley Okereke.

I am grateful for assistance I received from Dr Ruth Fowler, Pauline White, Robin Galloway, Robert Rennie, Paul Cyphus, Hurst Roddy and Dr Lilian Schweizer with the yeast transformation experiments.

Thanks to Drs. Liz Dyrynda and Steve Euston, members of my PhD Review Committee and to Dr Wilf Mitchell, my second supervisor. I thank Balazs Kral for help with the preparation of figures.

A heartfelt “thank you” goes to all my wonderful friends, especially Jonathan, Lorna, Stewart, Julio, Ihechukwu, Mohammed, Amber, Ambrose, Ude, Chukuma and Fisayo for their encouragement.

Last but not least I owe a debt of gratitude to my parents, sisters and brothers, especially Dr Osita Ugbogu. I sincerely thank you all for your endless love, financial support and constant prayers.

God, I thank you for your wisdom and gift of life.

Declaration

I Eziuche Amadike Ugbogu, hereby declare that I am the author of this thesis. All work described in this thesis is my own, except where stated in the text. The work presented here has not been accepted in any previous application for a higher degree. All the sources of information have been consulted by myself and are acknowledged by means of references.

Eziuche Amadike Ugbogu

Publications

Published article

Ugbogu, E. A., Wippler, S., Euston, M., Kouwenhoven, E. N., De Brouwer, A. P., Schweizer, L. M. & Schweizer, M. (2013). The contribution of the nonhomologous region of Prs1 to the maintenance of cell wall integrity and cell viability. *FEMS Yeast Research,* 13, 291-301.

Conference proceeding

Ugbogu, E. A., Schweizer, L. M. & Schweizer, M. (2014). *PRS* gene family – a means of linking primary metabolism and cell signalling? *Genetic Society of America, Yeast Genetics Meeting,* Seattle, Washington, July 29th - August 3rd, 2014. Abstract number 315C.

Published conference proceeding

Schweizer, L. M., **Ugbogu, E. A**. & Schweizer, M. (2013). *PRS* gene family – a means of linking primary metabolism and cell signalling? *Yeast*, ***30***(S1), S183.

Unpublished conference proceedings

Ugbogu, E. A. (2013). *PRS* gene family – a means of linking primary metabolism and cell signalling. School of Life Sciences PhD Conference, Heriot-Watt University, Edinburgh.

Ugbogu, E. A. (2013). Biochemical studies of PRPP synthetase in *Saccharomyces cerevisiae*. *2nd year report*. School of Life Sciences, Heriot-Watt University, Edinburgh.

Ugbogu, E. A. (2012). Biochemical studies of PRPP synthetase in *Saccharomyces cerevisiae*. *1st year report*. School of Life Sciences, Heriot-Watt University, Edinburgh.

Abbreviations

aa	Amino acid
A_{280}	Absorbance at 280 nm
ADH	Alcohol dehydrogenase
ADP	Adenosine diphosphate
Amp^R	Ampicillin resistance
approx.	Approximately
ATP	Adenosine triphosphate
Bck1	Bypass of C kinase
bp	Base pairs
B. subtilis	*Bacillus subtilis*
BSA	Bovine Serum Albumin
°C	degrees centigrade
cAMP	Cyclic adenosine monophosphate
cDNA	Complementary DNA
CDK	Cyclin-dependent kinase
cf.	Compare
CFW	Calcofluor White
CGD	Candida Genome Database
CID	Collision-induced dissociation
CMTX5	Charcot-Marie-Tooth disease type 5
conc.	Concentration
COSHH	Control Of Substances Hazardous to Health
CTP	Cytidine triphosphate
CWI	Cell wall integrity
CWP	Cell wall protein
DCBS	Divalent-cation binding site
dist. H_2O	distilled water
DNA	Deoxyribonucleic Acid

E. coli	*Escherichia coli*
EC	Enzyme commission
EDTA	Ethylene diamine tetra-acetic acid
ERK	Extracellular signal-regulated kinase
ESI	Electrospray ionization
Fks2	FK506 sensitivity
Gal	Galactose
GAP	GTP-activating protein
GEF	GDP/GTP exchange factor
GFP	Green Fluorescent Protein
GlcNAc	N-acetyl glucosamine
GS	Glucan synthetase
GSK	Glycogen synthetase kinase
GTP	Guanosine triphosphate
HA	Human influenza hemagglutinin
hr	Hour(s)
kb	Kilobase pairs
KDa	Kilo Daltons
L	Litre
LB	Luria-Bertani medium
LiOAc	Lithium acetate
M	Molar
mA	milliAmpère
MADS	Mcm1, Agamous, Deficiens and Serum response factor
MALDI-TOF	Matrix-assisted laser desorption/ionization-Time-of-Flight
MAPK	Mitogen-activated protein kinase
MAP2K	Mitogen-activated protein kinase kinase
MAP3K	Mitogen-activated protein kinase kinase kinase
MAP4K	Mitogen-activated protein kinase kinase kinase kinase
MEK(K)	Mitogen ERK kinase (kinase)
Mg	Magnesium
mg	Milligram
Mid2	Mating-induced death

MIM	Mendelian Inheritance in Man
min.	Minute
Mkk1	Mitogen-activated protein kinase-kinase
Mkk2	Mitogen-activated protein kinase-kinase
ml	Millilitre
Mlp1	Mpk1-like kinase
mM	Millimolar
Mpk1	Mitogen-activated protein kinase
MS	Mass Spectrometry
Mtl1	Mid2-two like
NAD^+	Nicotinamide adenine dinucleotide
$NADP^+$	Nicotinamide adenine dinucleotide phosphate
NCBI	National Centre for Biotechnology Information
NHR	Non-homologous region
OD	Optical Density
o/n	Overnight
ORF	Open reading frame
PAF	Polymerase-associated factor
PAP	PRS-associated protein
PEG	Polyethyene glycol
pH	$-\log_{10}[H^+]$, where $[H^+]$ is hydrogen ion concentration
Pi	Inorganic phosphate
PIP_2	Phosphatidylinositol 4,5-bisphosphate
Pir	Protein with internal repeats
Pkc	Protein kinase C
PMSF	Phenymethanesulfonylfluoride
PRPP	Phosphoribosyl pyrophosphate
Prs	5-phosphoribosyl-1(α)-pyrophosphate synthetase
P-Slt2	Phosphorylated Slt2
PVDF	Polyvinylidene difluoride
Quad	Quadrupole
rpm	Revolutions per minute
Rho1	Ras homologue

Rlm1	Resistance to lethality of $MKK1_{p386}$ overexpression
Rom2	Rho1 multicopy suppressor
RT	Room temperature
SBF	SCB-binding factor
SC-U	Synthetic complete dextrose medium lacking uracil
S. cerevisiae	*Saccharomyces cerevisiae*
S.D	Standard deviation
SDS	Sodium dodecyl sulphate
SDS-PAGE	SDS-polyacrylamide gel electrophoresis
S.E.M.	Standard error of the mean
Sec.	Seconds
SGD	Saccharomyces Genome Database
Slt2	Suppressor of the lytic phenotype
Swi	Switching deficient
TBS	Tris-Buffered Saline
TBS-T	TBS with Tween 20
$Temp^e$	Temperature
TM	Trade mark
TOR	Target of rapamycin
Tris-HCl	Tris-buffered hydrochloric acid
Ura	Uracil
UTP	Uridine triphosphate
UV	Ultraviolet
µg	Microgram
µl	Microlitre
µM	Micrometre
V	Volt(s)
vol.	Volume
Wsc	Cell wall integrity and stress response component
(WT)	Wild type
(w/v)	Weight per volume
Y2H	Yeast two-hybrid
YEPD	Yeast Extract Peptone Dextrose

Symbols for Amino Acids

Single letter code	Abbreviation	Full name
A	Ala	Alanine
R	Arg	Arginine
N	Asn	Asparagine
D	Asp	Aspartic acid
C	Cys	Cysteine
Q	Gln	Glutamine
E	Glu	GlutamIic acid
G	Gly	Glycine
H	His	Histidine
I	Ile	Isoleucine
L	Leu	Leucine
K	Lys	Lysine
M	Met	Methionine
F	Phe	Phenylalanine
P	Pro	Proline
S	Ser	Serine
T	Thr	Threonine
W	Trp	Tryptophan
Y	Tyr	Tyrosine
V	Val	Valine

Abstract

The products of the five-membered *PRS* gene family in *S. cerevisiae* exist as three entities, Prs1/Prs3, Prs2/Prs5 and Prs4/Prs5, each capable of supporting cell viability. The signal generated from an integrated GFP-Prs1 construct is dependent on the presence of Prs3. Prs1 not only interacts with Prs3 but also with Slt2, the MAPK of the Cell Wall Integrity (CWI) pathway as shown by co-immunoprecipitation and confirming previous Y2H studies that the central region of Prs1, NHR1-1, is essential for the interaction with the CWI pathway. Point mutations in *PRS1* corresponding to missense mutations associated with human neuropathies or in the divalent cation- and/or PRPP-binding sites interfere with CWI signalling resulting in temperature and/or caffeine sensitivity. The synthetic lethality of a strain lacking *PRS1* and *PRS5* can only be rescued by versions of Prs1 containing NHR1-1, implying that impaired CWI contributes to this loss of viability. Prs5 is unusual in that it contains two NHRs, one, NHR5-2, contains three phosphorylation sites. Mutation of these amino acid residues impinges on the expression of the transcription factor, Rlm1, an endpoint of the CWI pathway and reduces the temperature-dependent transcription of *FKS2*, the gene encoding the stress-induced catalytic subunit of 1,3-β-glucan synthase essential for maintaining CWI. This finding emphasizes the functionality of the three phosphorylation sites located in NHR5-2 of Prs5. The data presented support the hypothesis that the *PRS* gene family has, as a result of gene duplication and acquisition of NHRs, evolved to link primary metabolism with CWI.

Introduction

1 Introduction

PRPP synthetase (5-phosphoribosyl-1(α)-pyrophosphate synthetase (Prs; E.C 2.7.6.1) catalyzes transfer of the terminal diphosphoryl group from ATP to the C_1-hydroxyl group of ribose-5-phosphate to generate phosphoribosyl pyrophosphate (PRPP) and AMP (Khorana, 1960, Miller *et al*., 1975, Becker, 2001) (Figure 1.1). It requires Mg^{2+} and inorganic phosphate (Pi) for activity and is also subject to feedback inhibition by ADP and GDP (Olszowy and Switzer, 1972, Garcia-Pavia *et al*., 2003, Tang *et al*., 2006).

The product of Prs, PRPP, is a key metabolite that plays a central role in many biosynthetic pathways, such as the *de novo* and salvage biosyntheses of purine, pyrimidine and pyridine nucleotides, NAD^+ and $NADP^+$ (Becker, 2001) and for the production of the amino acids histidine and tryptophan (Hove-Jensen, 1989, Hilden *et al*., 1995). Prs is of biochemical importance as it links carbon and nitrogen metabolism in the cell by connecting ribose-5-phosphate from the pentose phosphate pathway (PPP) with the nucleotide synthesis pathway (Miller *et al*., 1975, Hove-Jensen *et al*., *1986*, Tozzi *et al*., 2006, Kleineidam *et al*., 2009) and is therefore essential for life in all organisms with the exception of parasites, such as *Trypanosoma* and *Leishmania* that solely depend on the host's metabolism (Ullman and Carter, 1997). Prs enzymes have been identified in bacteria, fungi, plants and humans. For example, in *Mycobacterium tuberculosis*, the main cause of tuberculosis, there is only a single gene encoding *PRS*, *Mt-prsA* (Rv1017c), which has been shown to be essential for the maintenance of cell integrity because it provides the only source of PRPP for the cell wall biosynthetic precursor decaprenol-1-monophosphoarabinose and is therefore a potential drug target (Lucarelli *et al*., 2010, Alderwick *et al*., 2011).

There are three classes of Prs, based on its requirement for phosphate, allosteric regulation and specificity for the diphosphoryl donor (Eriksen *et al*., 2000, Kadziola *et al*., 2005, Li *et al*., 2007). Most PRPP synthetases belong to class I, also named "classical". Class I Prs enzymes are dependent on phosphate and Mg^{2+} ions for their activities and are regulated allosterically by ADP because of their exclusive use of either ATP or dATP as a diphosphoryl donor (Switzer, 1969, Kita *et al*., 1989, Li *et al*., 2007, Jiménez *et al*., 2008, Cherney *et al*., 2011). In *Bacillus subtilis* Prs, ADP is

a competitive inhibitor when it binds to the ATP-binding site and acts as an allosteric inhibitor when it competes with P_i at the allosteric site (Eriksen *et al*., 2000). It has been shown that the crystal structure of *Bacillus subtilis* forms a hexamer and is organised as a propeller with the N-terminal domain at the centre and the C-terminal domains at the outside. The catalytic site contains both ATP- and ribose-5-phosphate-binding sites (Eriksen *et al*., 2000). Structural determination of class I PRPP synthetase of *B. subtilis* (Eriksen *et al*., 2000), *Bacillus pseudomallei* (Cherney *et al*., 2011) and human *PRPS* (Li *et al*., 2007) showed 50% aa similarity in their monomeric sequences which aggregate to form a hexameric $(\alpha_2)_3$ quaternary structure organized as a trimer of dimers. Their allosteric sites are in proximity to the active site at the junction of three subunits, of which two of the subunits are in the same dimer while the third subunit comes from an adjacent dimer (Cherney *et al*., 2011).

Class II PRPP synthetases are specific to plants and do not require phosphate ions for activity. They have the ability to utilize a wide range of diphosphoryl donors, such as ATP, dATP, CTP, GTP and UTP and are not allosterically inhibited by ADP. They have the least sequence similarity (<20%) when compared with class I and class III enzymes (Krath *et al*., 1999, Krath and Hove-Jensen, 2001, Jiménez *et al*., 2008, Cherney *et al*., 2011, Breda *et al*., 2012).

Class III PRPP synthetases are a novel class of PRPP synthetases found in the Archaea *Methanocaldococcus jannaschii*. Its activation depends on phosphate ions and Mg^{2+}-ions. It uses ATP as the diphosphoryl donor and is not allosterically inhibited by ADP, but is tightly regulated by competitive inhibition (Kadziola *et al*., 2005). A sequence similarity of ≈ 23% with class I PRPP synthetase and 18% and 12% with class II PRPP synthetase from *Spinacia oleracea* isozyme 3 and 4, respectively, has been reported (Cherney *et al*., 2011).

Genes encoding Prs have been identified in a variety of organisms. Prokaryotes contain only one *PRS* gene while eukaryotes have more than one *PRS* gene. For example, *Arabidopsis thaliana* and *S. oleracea* possess five and four *PRS* genes, respectively (Krath *et al*., 1999). Five *PRS* genes have been identified in *S. cerevisiae* (Hernando *et al*., 1999), two in *Rattus norvegicus* (Taira *et al*., 1987) and

three in humans (Iizasa *et al*., 1989, Taira *et al*., 1989, Taira *et al*., 1990, Sonoda *et al*., 1991, Becker and Ahmed, 2000).

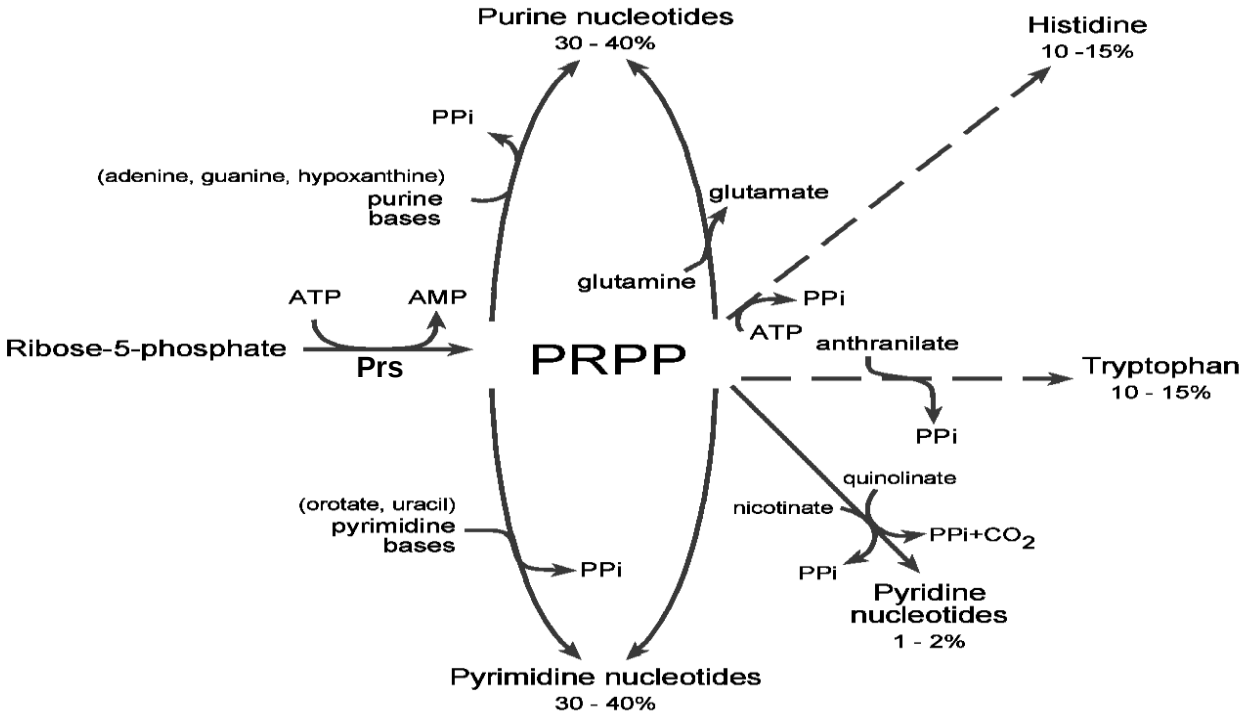

Figure 1.1: The biosynthesis and metabolic fates of phosphoribosyl pyrophosphate (PRPP)

Ribose-5-phosphate from the pentose phosphate pathway reacts with ATP to yield phosphoribosyl pyrophosphate (PRPP). This reaction is catalysed by the enzyme 5-phosphoribosyl-1(α)-pyrophosphate synthetase (Prs). Its product is utilized in the *de novo* synthesis and salvage pathway of nucleotides (purine, pyridine and pyrimidine) and synthesis of histidine and tryptophan in bacteria and yeast (taken from (Jensen *et al*., 2008)).

1.1 Human *PRS* genes and associated hereditary disorders

In humans there are three separate isoforms of PRPP synthetase, h*PRPS1* (MIM 311850), h*PRPS2* (MIM 311860) and h*PRPS1L1* (MIM 611566) which display high sequence homology (between h*PRPS1* and h*PRPS2* (95%); h*PRPS1* and h*PRPS1L1* (94.3%); h*PRPS2* and h*PRPS1L1* (91.2%)) (Li *et al*., 2007). The genes h*PRPS1* and h*PRPS2* are located on the X-chromosome and map to the long and short arms of the X-chromosome, respectively; they are expressed in all tissues while h*PRPS1L1* maps to chromosome 7 and appears to be testis-specific (Becker, 2001, Li *et al*., 2007). Studies on h*PRPS1* and h*PRPS2* showed that their cDNAs

hybridize with transcripts of 2.3 kb and 2.7 kb, respectively. Their tissue-specific expression indicates that h*PRPS1* may be constitutively expressed while h*PRPS2* may be activated by mitogenic agents (Becker, 2001).

In addition, Prs-associated proteins (PAPs) have been discovered in humans, thus increasing the complexity of human PRPP biosynthesis and its expression (Kita *et al*., 1989, Tatibana *et al*., 1995, Katashima *et al*., 1998). Human PAPs have a high degree of aa sequence similarity to the *h*PRPS proteins but contain mutations in residues conserved in Prs proteins of other organisms implying that their catalytic properties are compromised (Kleineidam *et al*., 2009). In rat liver, there is evidence that PAP39 interacts with PRPP synthetase and inhibits catalytic activity through reversible association (Tatibana *et al*., 1995).

In humans mutations in *PRPS* genes are associated with several syndromes, such as *PRS1* superactivity, Arts syndrome, Charcot-Marie-Tooth disease (CMTX5) and X-linked nonsyndromic sensorineural deafness (DFN2). Human PRPS1 superactivity is an X-linked disorder resulting from gain of function which causes superactivity of the enzyme thus leading to overproduction of uric acid which causes gout and leads to urolithiasis in men (Nyhan *et al*., 1969, Sperling *et al*., 1972, Becker *et al*., 1986, Becker *et al*., 1988, Becker *et al*., 1989, Roessler *et al*., 1993, Becker *et al*., 1996, Ahmed *et al*., 1999, Synofzik *et al*., 2014). It is also associated with the occurrence of infectious diseases in the upper respiratory tracts which can be fatal. On the other hand, reduced Prs activity is characteristic of certain neuropathies. Arts syndrome is characterized by mental retardation, delayed motor development, ataxia, hearing impairment and optic atrophy and is associated with two missense mutations in h*PRPS1*, L152P and Q133P (Arts *et al*., 1993). CMTX5, a neuropathic disorder characterized by loss of muscle tissue and touch sensation, has been linked to a missense mutation (M115T) in h*PRPS1*. CMTX5 affects approximately 1 in 2,500 people, and is one of the most common inherited disorders (Synofzik *et al*., 2014). DFN2 is associated with hearing impairment (Liu *et al*., 2010, de Brouwer *et al*., 2010). Another neuropathy, Rosenberg-Chutorian syndrome, is associated with the mutation E43D in *h*PRPS1 (Kim *et al*., 2007). Interestingly, there is high sequence similarity between *h*PRPS1 and *S. cerevisiae* Prs1, particularly between the region

of *h*PRPS1 harbouring the mutations associated with neuropathies mentioned above and the sequence of the N-terminal region of Prs1 (http://www.yeastgenome.org).

1.2 Prs-encoding genes in *Saccharomyces cerevisiae*

The *Saccharomyces cerevisiae* genome contains a family of five genes (*PRS1-PRS5*) located on different chromosomes, each containing characteristic motifs of Prs polypeptides capable of encoding PRPP synthetase: a divalent cation-binding domain located at the N-terminus and a PRPP-binding site close to the C-terminus (Hove-Jensen *et al*., 1986, Carter *et al*., 1994, Hernando *et al*., 1999).

PRS1 is located on chromosome XI, *PRS2* on chromosome V, *PRS3* on chromosome VIII, *PRS4* on chromosome II and *PRS5* on chromosome XV (Carter *et al*., 1997). *PRS2*, *PRS3* and *PRS4* each have a length of 318-320 aa with a corresponding molecular weight of 34.7 KDa, 35.1 KDa and 39 KDa, respectively, whereas *PRS1* and *PRS5* are longer and consist of 427 and 495 aa, respectively and molecular weights of 47 KDa for Prs1 and 53.5 KDa for Prs5 (Hernando *et al*., 1998, Schneiter *et al*., 2000, Kleineidam *et al*., 2009). The reason for the longer lengths of Prs1 and Prs5 is that they contain non-homologous regions (NHRs) that increase their lengths by at least one-third. These NHRs are in-frame insertions which are not introns (Carter *et al*., 1997, Hernando *et al*., 1998, Hernando *et al*., 1999, Vavassori *et al*., 2005b). Specifically, the NHR1-1 of Prs1 is an insertion of 105 aa residues bearing no homology to Prs2, Prs3, Prs4 or Prs5 and is located between the divalent cation-binding and PRPP-binding sites. Prs5 possesses two NHRs; NHR5-1 and NHR5-2. NHR5-1 consists of 70 aa and is located N-terminal to the divalent cation-binding site, NHR5-2 consists of 116 aa and is located at a similar position to NHR1-1 of Prs1, i. e. it separates the divalent cation- and PRPP-binding sites. Furthermore, as a result of phosphoproteome analysis Prs5 was found to be one of the 11 triply phosphorylated proteins in yeast (Ficarro *et al*., 2002). The three neighbouring phosphorylatable sites are located in NHR5-2 (Figure 1.2). Interestingly, it was postulated that Prs5 may be a protein kinase based on protein microarray assay (Fasolo *et al*., 2011). The authors have classified Prs5 as a protein

kinase possibly because of it being theoretically capable of donating a phosphate group to ribose-5-phosphate to yield PRPP.

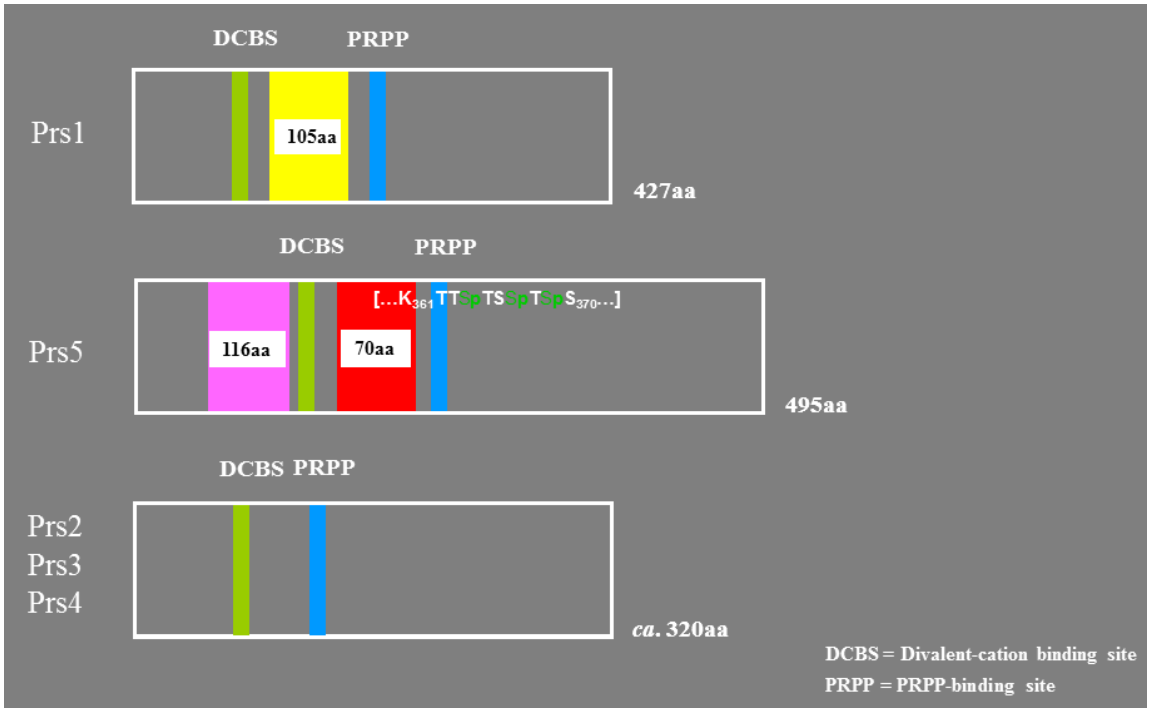

Figure 1.2: The structure of the five PRPP synthetase polypeptides

The figure shows the relative lengths of the Prs1- Prs5 polypeptides. Vertical green lines represent the divalent cation-binding sites (DCBS) and blue vertical lines show the PRPP-binding sites. The yellow rectangle indicates the location of NHR1-1 in Prs1.The magenta rectangle corresponds to the position of NHR5-1 while the red rectangle represents NHR5-2. The phosphosites (Ficarro *et al*., 2002) are indicated in green and followed by a "p" (phosphate group) (reproduced by kind permission of M Schweizer).

1.3 Cell wall integrity signalling pathway in *S. cerevisiae*

The cell wall of *S. cerevisiae* has four distinct functions. Firstly, it stabilizes the internal osmotic conditions of cytoplasm and limits the water influx that would perturb and cause swelling or rupture of the plasma membrane (Klis *et al*., 2006, Levin, 2011). Secondly, it serves as protection against mechanical damage, physical stress and maintains osmotic homeostasis of the cell through prevention of sheer and compression forces (Kim *et al*., 2008, Levin, 2011). Thirdly, the cell wall maintains cell shape which is essential for vegetative growth, cell division and during

pheromone-induced morphogenesis and pseudohyphal development (Klis *et al*., 2006). Fourthly, the cell wall functions as a scaffold for surface proteins; with the stress-bearing polysaccharides supporting the matrix of cell wall glycoproteins. These glycoproteins, especially those with *N*-linked carbohydrate side-chains, limit the permeability of the cell wall for macromolecules, and protect the glycan layer from the attack by cell wall-degrading enzymes or foreign proteins (Klis *et al*., 2006, Levin, 2011).

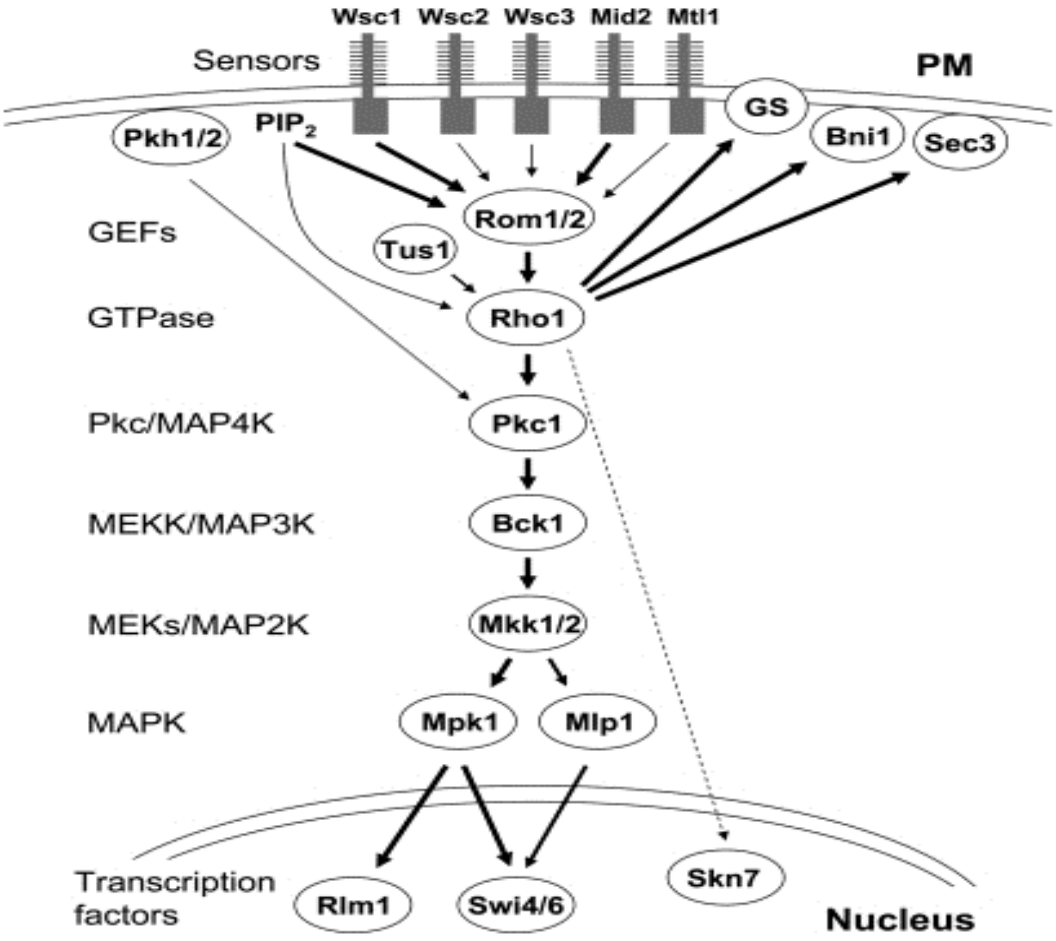

Figure 1.3: Scheme of the CWI signalling pathway

The nomenclature of proteins involved in MAPK signalling is indicated to the left of the components of the CWI pathway. Signals are initiated at the cell surface receptors traversing the plasma membrane (PM). Two transcription factors, Rlm1 and Swi4/Swi6 are activated through a cascade of MAPK from Rho1 which is activated by GEFs Rom1/2 following receptor stimulation. In addition to Pkc1 Rho1 activates four other effectors: β-1,3-glucan synthase (GS), the Bni1 formin protein, the exocyst component Sec3 and the Skn7 transcription factor which may contribute to the CWI transcriptional programme. PiP_2 = phosphatidylinositol-4,5-bisphosphate. Mpk1 and Slt2 are synonyms (taken from (Levin, 2011)).

S. cerevisiae invests a considerable amount of energy in the construction of its cell wall which comprises 10–30% of the cell's dry weight and 80-90% of the polysaccharide content (Aguilar-Uscanga and François, 2003, Klis *et al*., 2006). Specifically, the cell wall of *S. cerevisiae* consists of chitin, β-1,3-glucan, β-1,6-glucan, and glycoproteins which have the ability to form covalent complexes (Molina *et al*., 2000, Aguilar-Uscanga and François, 2003, Free, 2013). Electron microscopy has shown that the inner layer of the cell wall is comprised mainly of 1,3-β-glucan polymers and chitin. This layer is responsible for the elastic property and mechanical strength of the cell wall owing to the helical nature of β-1,3-glucan chains (Levin, 2011). Although chitin makes up only 1-2% of the cell dry weight, it has been found to be essential for *S. cerevisiae* viability and increases in content under cell wall stress (Klis *et al*., 2006) and this has been demonstrated in *PRS* deletant strains (Wang *et al*., 2004).

A linear series of protein kinases, known as Mitogen-Activated Protein Kinases (MAPK) relay signals by means of sequential phosphorylation (Manning *et al*., 2002, Zhang *et al*., 2003, Edmunds and Mahadevan, 2004, Qi and Elion, 2005, Akella *et al*., 2008) (http://kinase.com/scerevisiae/). The MAPK signalling pathways have been widely studied in *S. cerevisiae* and each comprises a highly conserved cascade of three protein kinases: MAP3K, MAP2k and MAPK. One of the five yeast MAPK pathways (Furukawa and Hohmann, 2013) is the well-studied cell wall integrity (CWI) pathway which is induced in response to cell wall stressors, such as increased temperature, hypo-osmotic shock, exposure to mating pheromone and agents that interfere with the cell wall, e.g. Congo red, caffeine, the chitin antagonist Calcofluor White or zymolyase (Stark, 2004, Levin, 2005, Kuranda *et al*., 2006, Chen and Thorner, 2007, Fuchs and Mylonakis, 2009, Rodicio and Heinisch, 2010, Heinisch and Dufrêne, 2010). The CWI signalling pathway is comprised of a family of five receptor proteins located at the plasma membrane: Wsc1-3, Mid2 and Mtl1 which are coupled to the small G-protein, Rho1 (Figure 1.3). It has been shown by single-molecule atomic force microscopy that Wsc1 is a sensor which in response to external stimuli reacts like a "nanospring" (Heinisch and Dufrêne, 2010). Rho1 encodes a GTP-binding protein and is involved in the maintenance of cell polarity and reorganisation of the actin cytoskeleton (Madden and Snyder, 1998) as well as activating a set of effectors which play essential roles in signalling events including

the CWI pathway. Rho1 binds and activates Pkc1, the yeast homologue of mammalian protein kinase C, which in turn controls the MAPK cascade (Nonaka *et al*., 1995, Heinisch, 2005). Yeast Pkc1 is much larger than the mammalian PKCs because it possesses a regulatory domain with all the subdomains that are distributed to the different isoforms of mammalian PKCs. Pkc1 is activated by the Phk1 and Phk2 kinases (Inagaki *et al*., 1999, Friant *et al*., 2001, Levin, 2005) and by TOR *via* nutrient depletion which results in dissociation of the Sit4/Tap42 complex and activation of the CWI pathway (Torres *et al*., 2002, Loewith and Hall, 2011, Yan *et al*., 2012). The CWI MAPK cascade consists of a MAP3K/MEKK (Bck1), a redundant pair of MAP2KK/MEK (Mkk1/2), and a MAPK (Mpk1/Slt2) (Levin *et al*., 1994, Kim *et al*., 2008, Kim and Levin, 2010, Lee *et al*., 2011). It has been observed that loss of Pkc1 function or any component of the MAPK cascade under the control of Rho1 results in a cell lysis defect (Levin, 2005, Kim *et al*., 2008). A further role for Rho1 is that it is an integral regulatory subunit of the 1,3-β-glucan synthase (GS) complex encoded by *FKS1* and *FKS2*. This enzyme complex synthesizes 1,3-β-glucan from UDP glucose thereby contributing to cell wall construction (Douglas *et al*., 1994, Mazur *et al*., 1995, Ram *et al*., 1995). In yeast the three nucleotide exchange factors (GEFs) Rom1, Rom2 and Tus1 activate Rho1 (Krause *et al*., 2012). Rom1 and Rom2 are homologous proteins whereas TUS1 is more distantly related and as a result of CDK phosphorylation ensures that Rho1 is recruited to the site of bud emergence (Levin, 2005, Kono *et al*., 2008, Yoshida *et al*., 2009). Rom2 is the major GEF responsible for transmitting signals from the cell surface to Rho1 for activation of the CWI pathway (Guo *et al*., 2009). Rom2 interacts with the plasma membrane *via* its pleckstrin homology domain which binds phosphatidylinositol-4,5-bisphosphate (PIP_2) and it also interacts with the cell surface receptor proteins, e. g. Wsc1 and Mid2 (Philip and Levin, 2001). During normal cell growth, Rom2 and Rho1 are co-localized to the bud neck (Manning *et al*., 1997) and are redistributed to the cell periphery in response to environmental stress where together with β-1,3-GS they are responsible for remodelling the cell wall (Guo *et al*., 2009).

Targets affected by the activation of Rho1 include Pkc1, β-1,3-GS, Bni1, Bnr1, Skn7 and Sec3. Bni1 and Bnr1 are formin proteins involved in actin filament assembly (Evangelista *et al*., 1997, Wen and Rubenstein, 2009). Rho1 oscillates between the active GTP-bound form and the inactive GDP-bound form which is regulated by

Rom2 resulting in the activation of the protein. The GTP-activating proteins (GAPs) are: Bem2, Sac7, Bag7 and Lrg1 (Martín *et al*., 2000, Schmidt *et al*., 2002). Following activation by Rho1 Pkc1 then switches on the MAPK cascade which amplifies the CWI signal. Specifically, Pkc1 phosphorylates Bck1 at several sites in a hinge region between its putative regulatory and catalytic domains (Levin *et al*., 1994). Bck1 then phosphorylates and activates Mkk1/Mkk2 based on Y2H interactions. Mkk1/Mkk2 then phosphorylates Mpk1/Slt2, a functional homologue of human ERK5, (Piper *et al*., 2006, Truman *et al*., 2006, Kim *et al*., 2008), on neighbouring threonyl and tyrosyl residues in a T-X-Y motif within the activation loop which is conserved in MAPKs and is analogous to Thr202/Tyr204 of mammalian p44/p42 MAPK (Erk) and can be detected by commercially available antibodies (Martín *et al*., 2000, de Nobel *et al*., 2000b). Interestingly, there is a paralogue of Mpk1/Slt2, Mlp1 (Mpk1-like protein). The two paralogues have 53% aa sequence identity but Mlp1 is not dually phosphorylated by Mkk1/Mkk2 since its T-X-Y motif is mutated to K-X-Y possibly allowing Mlp1 to be phosphorylated on Tyr192 (Kim *et al*., 2008).

The CWI pathway terminates in one of three targets: Rlm1, SBF and Sir3 (Jung and Levin, 1999, Jung *et al*., 2002, Ray *et al*., 2003, Garcia *et al*., 2004, Kim *et al*., 2008, Mascaraque *et al*., 2013). The transcription factor, Rlm1, a regulator of a wide array of cell wall biosynthetic genes, is phosphorylated on residues S_{427} and T_{439} by Mpk1/Slt2 (Jung *et al*., 2002, Heinisch and Dufrêne, 2010, Kim and Levin, 2011). Mlp1 is also a target of Rlm1 (Kim *et al*., 2008). Under non-stress conditions Mpk1/Slt2 is found mainly in the nucleus, however, in response to temperature stress some of the protein is rapidly moved to the cytoplasm (Kamada *et al*., 1995, Hahn and Thiele, 2002). Furthermore, a small proportion of Mpk1/Slt2 is found at sites of polarized cell growth since it shuttles constitutively between this location and the nucleus (Delley and Hall, 1999, van Drogen and Peter, 2002, Denis and Cyert, 2005, Li *et al*., 2013). In addition to regulation of gene expression Mpk1/Slt2 is also involved in the polarization of the actin cytoskeleton (Guo *et al*., 2009) and may be regarded as part of the checkpoint mechanism for morphogenesis (Harrison *et al*., 2001). Furthermore, Mpk1/Slt2 has been implicated in the cellular response to oxidative stress by controlling cyclin C degradation (Krasley *et al*., 2006). Mpk1/Slt2

interacts with Hog1, a functional homologue of mammalian p38 MAPK, in adaptation to zymolyase-mediated cell wall stress (Chen and Thorner, 2007).

The second target of Mpk1/Slt2 is SBF, a heterodimeric G_1-regulator composed of Swi4 and Swi6 which links CWI signalling to cell cycle metabolism (Madden *et al*., 1997, Baetz *et al*., 2001, Queralt and Igual, 2005, Heinisch and Dufrêne, 2010). The biological evidence that SBF participates in CWI signalling is: (i) the cell lysis defect of an *mpk1Δ* mutant is suppressed by overexpression of Swi4, (ii) Swi4 and Swi6 mutants are hypersensitive to Calcofluor White, (iii) Mpk1/Slt2 associates with the dimeric SBF *in vivo,* (iv) Swi6 is phosphorylated *in vivo* and *in vitro* by Mpk1/Slt2 in response to cell wall stress (Kim *et al*., 2008).

The transcriptional silencer Sir3 is another target of Mpk1/Slt2, thus implicating the CWI pathway in silencing and shortened lifespan (Ray *et al*., 2003). Mpk1/Slt2 is also regulated by four protein phosphatases – Msg5, Ptp2, Ptp3 and Sdp1 (Kamada *et al*., 1995, Keyse, 2000, Flandez *et al*., 2004, Martín *et al*., 2005, Marín *et al*., 2009). Furthermore, Mpk1/Slt2 is responsible for feedback regulation of the CWI pathway since Msg5, Rom2, and Mkk1/Mkk2 are among its targets (Jiménez-Sánchez *et al*., 2007, Guo *et al*., 2009, Molina *et al*., 2010).

Rlm1 and SBF cooperate in regulating the expression of Fks2, the 1,3-β-GS subunit which is activated under stress conditions (Levin, 2011, Kim and Levin, 2011). In addition, the pseudokinase paralogue of Mpk1, Mlp1, also interacts with the *FKS2* promoter as does the kinase-inactive form of Mpk1/Slt2 (mpk1/slt2-K54R) implying that *FKS2* transcription is not reliant on the kinase activity of Mpk1/Slt2 (Kim *et al*., 2008, Kim and Levin, 2010, Kim and Levin, 2011). In fact, the CWI signalling responsible for *FKS2* transcription is the result of a combination of the catalytic and non-catalytic functions of Mpk1 (Kim and Levin, 2011). In order for *FKS2* transcription to take place it requires the recruitment of Mpk1/Slt2, Swi4 and Swi6 to its promoter. Following recruitment of the Paf1C complex – one of the two RNA polymerase II complexes in yeast, which is responsible for the expression of less than 5% of yeast genes, including some whose products are involved in cell wall biosynthesis (Jaehning, 2010) – to the *FKS2* promoter Mpk1/Slt2 migrates from the Swi4/Swi6 complex to interact with Paf1C, thus promoting the transcription elongation of Fks2. It is known that Mlp1 is induced by Rlm1 activation thereby

providing an interesting feedback activation loop which enhances the non-catalytic function of Mlp1 expression (Kim and Levin, 2011).

1.4 PPRP synthetase gene deletions in *S. cerevisiae*

Genetic evidence shows that the *PRS* gene products of *S. cerevisiae* are organized into two functional interacting complexes, one of which is a heterodimer (Prs1/Prs3) and the other a heterotrimer (Prs2/Prs4/Prs5). Within these two interacting complexes three minimal essential functional units have been identified of which at least one combination must be present to guarantee viability (Hernando *et al*., 1999). Y2H analysis data have shown the existence of two interacting functional complexes in the cell which may have compensatory function since in the absence of one entity or a component thereof, the cell can still survive (Wang *et al*., 2004).

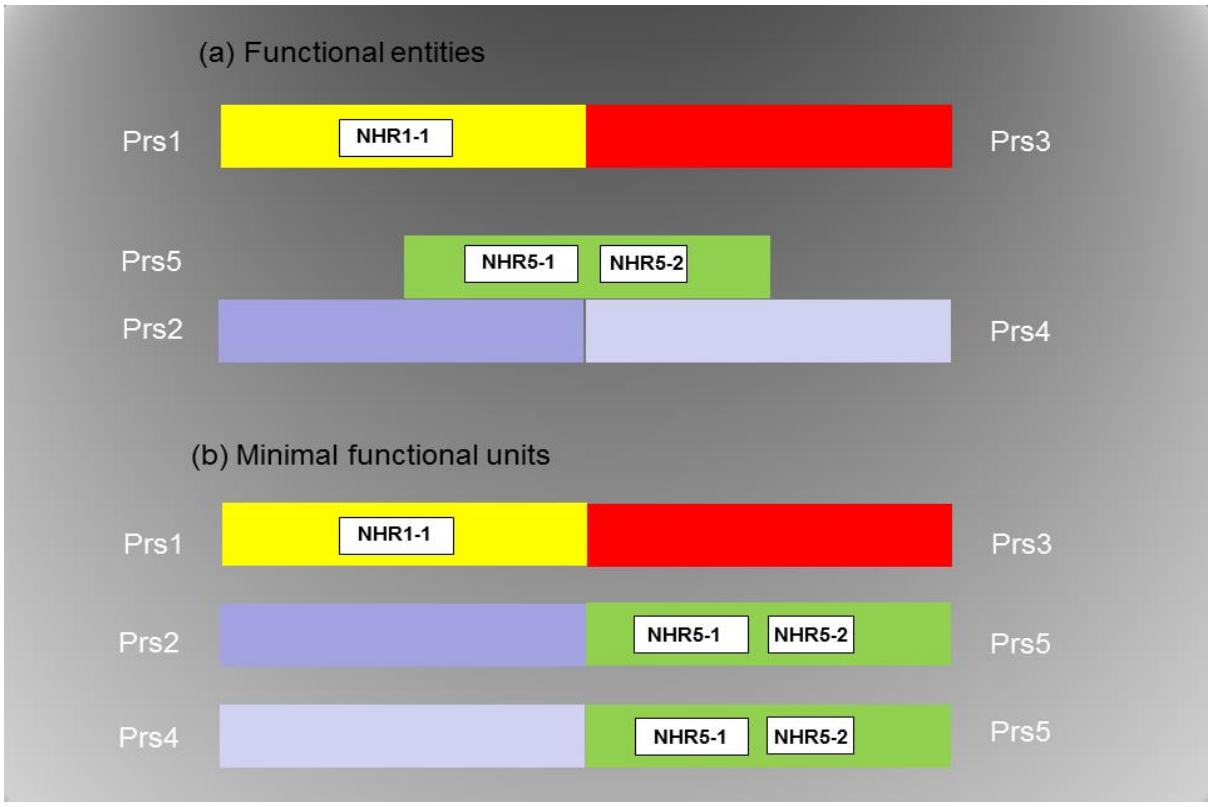

Figure 1.4: Functional entities and phenotypic minimal functional units of *S. cervisiae* Prs

(**a**) Functional entities: Prs1/Prs3 and Prs2/Prs4/Prs5. (**b**) Minimal functional units: Prs1/Prs3, Prs2/Prs5 and Prs4/Prs5. The non-homologous regions (NHRs) of Prs1 and Prs5 are indicated by white boxes.

It has been observed through systematic phenotypic analysis that: (i) synthetic lethality occurs when *PRS1* or *PRS3* is deleted from a strain lacking *PRS5* and also loss of *PRS1* or *PRS3* in combination with simultaneous deletion of *PRS2* and *PRS4* results in non-viability; (ii) deletion of *PRS1* and *PRS3* in combination with a lack of *PRS2* or *PRS4* results in reduction of growth rate, nucleotide content and enzymatic activity; (iii) combinatorial deletion of *PRS2*, *PRS4* and *PRS5* causes an 80% reduction in enzymatic activity but has no effect on growth rate and nucleotide content (Carter *et al*., 1994, Hernando *et al*., 1998, Hernando *et al*., 1999, Wang *et al*., 2004, Vavassori *et al*., 2005a).

There are three viable triple deletant combinations: *prs2Δprs4Δprs5Δ*; *prs1Δprs3Δ prs4Δ* and *prs1Δprs2Δprs3Δ*; each capable of synthesizing PRPP, thus defining the three minimal functional subunits, Prs1/Prs3, Prs2/Prs5 and Prs4/Prs5 (Hernando *et al*., 1998, Hernando *et al*., 1999, Wang *et al*., 2004).

Deletion of any single *PRS* gene is not a lethal event, a further indication that their products are to some degree compensatory. However, studies have shown that each *PRS* gene makes a contribution to cellular metabolism and physiology of *S. cerevisiae*. Loss of any of the Prs polypeptides has a severe effect on the expression of Rlm1, an output of the CWI pathway under normal growth conditions; e. g. deletion of *PRS5* reduced Rlm1 expression by 30% and lack of *PRS2* or *PRS4* alone or in combination with *PRS5* reduced Rlm1 expression by 80% whereas in *prs1*Δ and *prs3*Δ strains Rlm1 activation is reduced by over 90% and in *prs2*Δ and *prs4*Δ strains it is reduced to 20% (Wang *et al*., 2004, Vavassori *et al*., 2005b, Wang, 2005). Strains carrying single deletions of *PRS1* or *PRS3* have doubling times of 3 and 2.5 hr, respectively, indicating a slow growth phenotype when compared to the 1.6 hr doubling time of the WT. The double deletant strains lacking *PRS1* and *PRS3* or lacking *PRS1* or *PRS3* in combination with any other *PRS* deletant have doubling times of 3.5-4.0 hr whereas triple deletant strains *prs1*Δ*prs2*Δ*prs3*Δ *and prs1*Δ*prs3*Δ*prs4*Δ have a doubling time of approximately 5 hr (Hernando *et al*., 1999). Electron microscopic analysis showed that *prs2*Δ*prs4*Δ*prs5*Δ *and prs1*Δ*prs3*Δ*prs4*Δ have a high incidence of plasma membrane invaginations while cytoplasmic vesicle accumulation was observed in *prs1*Δ*prs3*Δ*prs4*Δ strains

indicating defects in growth polarization as well as impaired fusion of the non-targeted vesicles to the cell membrane (Schneiter *et al*., 2000).

It is well known that the mating pheromone, α-factor, induces morphological changes in the cell wall of yeast thus activating the CWI pathway (Buehrer and Errede, 1997). Treatment of *prs*Δ strains with 1 μM α-factor for 6 hr revealed that in comparison to the WT, strains lacking *PRS1* or *PRS3* displayed 46% and 73% reduction in viability, respectively, while simultaneous deletion of *PRS1* and *PRS3* had an additive effect. On the other hand the α-factor sensitivity of *prs1*Δ*prs3*Δ was overcome by the additional deletion of either *PRS2* or *PRS4* (Wang, 2005). Measuring Rlm1 expression following exposure to 2 μM α-factor of the WT or *prs5*Δ caused a 20% and 50% reduction, respectively, in Rlm1 activation whereas deletion of *PRS2* increases Rlm1 activation five-fold while deletion of *PRS4* caused a two-fold Rlm1 activation (Wang *et al*., 2004).

The expression of the *FKS2* gene, which encodes an alternative catalytic subunit of the 1,3-β-GS, in strains carrying deletions of *PRS* genes showed that Fks2 expression is reduced at 30°C and does not increase at elevated temperature when *PRS3* is absent. Lack of *PRS1* reduces the level of Fks2 expression at 30°C, but still allows an increase, albeit reduced in comparison to the WT, in Fks2 expression at 37°C. On the contrary, strains deleted for *PRS2* or *PRS4* were still able to activate Fks2 expression to a similar level to that of the WT. However, in *prs5*Δ and *prs1*Δ*prs3*Δ strains Fks2 expression was reduced at 30°C and reduced further at 37°C (Wang *et al*., 2004, Vavassori, 2005).

When the chitin content of *PRS* deletant strains was measured in the presence or absence of CFW, the strains deleted for *PRS2*, *PRS4* or *PRS5*, individually or in combination, responded in the same way as the WT, On the other hand, deletion of *PRS1* or *PRS3* caused a three-fold increase in chitin content and impairs the ability of the cell to increase its chitin content upon exposure to CFW. The *prs1*Δ, *prs3*Δ and *prs1*Δ*prs3*Δ*prs4*Δ strains showed resistance to CFW, whereas the double deletant *prs1*Δ*prs3*Δ and the triple deletant *prs1*Δ*prs2*Δ*prs3*Δ were sensitive to CFW (Wang *et al*., 2004, Wang, 2005).

Caffeine sensitivity is a characteristic phenotype of yeast strains with a compromised CWI pathway (Cid *et al*., 1995, Hampsey, 1997, Kuranda *et al*., 2006) although it is an atypical activator thereof since it causes additional phosphorylation of Mpk1/Slt2 via the DNA damage checkpoint pathway (Truman *et al*., 2009). Caffeine sensitivity of strains carrying *PRS* gene deletions has also been observed: (i) the WT strain is capable of growing at 6.5 mM caffeine as is a *prs2*Δ strain; (ii) deletion of either *PRS1* or *PRS3* results in inhibition of growth by 3.5 mM caffeine; (iii) *prs4*Δ and *prs5*Δ strains are inhibited by 6.0 mM and 5 mM caffeine, respectively; (iv) the double deletant strain *prs1*Δ*prs3*Δ fails to grow on 2 mM caffeine but the triple deletant strain *prs1*Δ*prs3*Δ*prs4*Δ is less sensitive to caffeine than *prs1*Δ*prs4*Δ and *prs1*Δ*prs2*Δ double deletants (Schneiter *et al*., 2000, Wang *et al*., 2004).

Furthermore, caffeine-associated release of alkaline phosphatase is restored by addition of 1 M sorbitol, an osmotic stabiliser, to the media (Schneiter *et al*., 2000), strongly indicating that the maintenance of CWI is compromised in these strains. Differential interference contrast (DIC) imaging of a GFP-PRS1 *prs3*Δ strain showed that this strain had highly vacuolated large spherical cells, a further indication that the CWI system is compromised (Schneiter *et al*., 2000).

In an approach to see whether or not h*PRPS1* mutations associated with human neuropathies exert an influence on CWI in yeast the corresponding mutations have been created in *PRS1* at the positions L115T and Q133P which correspond to CMTX5 and Arts syndrome, respectively (Monnier, 2010, Wilkiewicz, 2010, Gallacher, 2014). Furthermore, *in vitro*-generated mutations in the divalent cation-binding site (H130A), the PRPP-binding site (D326A) and the double mutation H130A/D326A have been created (Figure 3.6). In addition, *in vitro*-generated mutations of *PRS5* at the postulated phosphorylatable sites were also created (Gallacher, 2014). These mutations have been investigated for their impact on yeast physiology since an understanding of the effect of altering PRPP-synthesizing capacity and its link to CWI signalling may give new insight into MAPK activation and cell wall remodelling events which can be useful for future therapeutic purposes.

1.5 Interaction of *PRS* genes with other genes

Protein-protein interactions are essential for virtually all biological processes. A comprehensive understanding of how Prs polypeptides interact with other polypeptides, the function(s) of the interacting polypeptides and how Prs polypeptides are regulated is indispensable for uncovering all the cellular functions of yeast Prs. System-wide assays of Prs interactions with other polypeptides using high-throughput Y2H (Uetz *et al*., 2000, Ito *et al*., 2001), Principal Component Analysis (PCA) (Tarassov *et al*., 2008), mass spectrometry (tandem affinity capture-MS) analyses (Ho *et al*., 2002, Gavin *et al*., 2006) and reconstituted complex/protein microarrays (a powerful tool to study protein functions and interactions) (Fasolo *et al*., 2011), revealed that Prs polypeptides interact with a myriad of other proteins (Appendix, Table 2.1). Certain Prs polypeptide-interacting partners identified in high-throughput analysis have been confirmed and extended by Y2H analysis in various lab-based projects (Vavassori, 2005, Wang, 2005, Kleineidam *et al*., 2009). Most of the identified polypeptides are protein kinases; others are associated with protein synthesis, and CWI signalling components. It has been shown that Prs1 physical interacts with proteins, such as Chk1, Elm1, Esa1, Hrr25, Kcc4, Npr1, Swe1, Ptk2, Pho85, Rpn4 and Tpk1, Ygk3. Chk1 is a DNA damage check-point effector, Elm1, a regulator of cellular morphogenesis and cytokinesis, Hrr25 regulates vesicular trafficking, and DNA repair, Ygk3 is involved in the control of Msn2-dependent transcription and Npr1 stabilizes plasma membrane aa transporters (Fasolo *et al*., 2011). It has been reported by (Lin *et al*., 2009) that the Prs1 interacts with Esa1, a protein required for cell cycle progression and regulation of cellular acetylation balance.

Prs2 has been found to interact physically with Nuf2, a protein involved in chromosome segregation, and spindle checkpoint activity (Uetz *et al*., 2000). This interaction has been confirmed and extended by Y2H. It would appear that an intact Prs2/Prs4/Prs5 complex is required for the interaction (Wang, 2005). This is an interesting observation in light of the fact that Pkc1 localizes to the mitotic spindle *via* its N-terminal C2-like domain (Denis and Cyert, 2005).

Reports on high-throughput analysis showed that Prs3 also interacts with a number of proteins (for details see Table 2.1). It is worthy of mention that overexpression of Prs3 completely rescued the caffeine sensitivity of a mutant allele of *MPK1* (*mpk1*^{siw9}) (Binley *et al*., 1999), thus supporting the hypothesis that Prs polypeptides interact with the CWI pathway.

High-throughput analysis also shows that Prs4 and Prs5 physically interact with a variety of proteins including Ktr5 which is involved in protein glycosylation (Szappanos *et al*., 2011). The interaction of Prs5 and Bas1 is interesting since the latter induces expression of genes involved in purine and histidine biosynthesis (Fiedler *et al*., 2009).

The association of Prs polypeptides uncovered by high-throughput analysis using protein microarray screens shows that Mkk1 which is an element of the CWI pathway physically interacts with Prs1 and Prs4 and is postulated to phosphorylate the former (SGD PhosphoPep database) (Fasolo *et al*., 2011). Interestingly, Y2H analysis provided evidence that Mpk1/Slt2 also interacts with Prs1-Prs4 (Wang *et al*., 2004). Ubp3, a protein that responds to osmostress (Ossareh-Nazari *et al*., 2010) was found by means of tandem affinity capture-MS to interact physically with Prs1, Prs3 and Prs5. Another stress responsive protein, Ubi4, interacts with Prs1-Prs5 (Duttler *et al*., 2013, Swaney *et al*., 2013, Kolawa *et al*., 2013). Gnd1 a protein required for adaptation to oxidative stress (Szappanos *et al*., 2011) was identified by high through-put analysis to interact genetically with Prs2, Prs4 and Prs5.

Sro9, a protein involved in haem regulation and in the organization of actin filaments (Schenk *et al*., 2012) interacts with Prs2, Prs3 and Prs5. Rim11, a serine/threonine protein kinase and a homologue of mammalian glycogen synthase kinase 3 (Gsk3) was shown to interact with Prs2, Prs3 and Prs5 as shown by Y2H (Kleineidam *et al*., 2009) confirming affinity capture-MS findings (Ho *et al*., 2002). A list of the Prs-interacting proteins is provided in Appendix, Table 5.13.

1.6 Aim of study

The main objectives of this study are to gain a better understanding of the *S. cerevisiae* PRPP synthetase and its contribution to cell physiology by exploitation of the large collection of yeast strains mutated/deleted for one or more of the *PRS* genes and Prs plasmids available in the laboratory carrying either specific yeast *PRS* mutations or mutations associated with human neuropathies linked to altered human *PRPS* activity. These phenocopies emphasise the potential role of yeast as a model organism for human disease/biology. This was achieved by:

(i) Western blotting with GFP-tagged Prs1 in various *PRS* deletant strains to obtain biochemical evidence for the genetically defined Prs1/Prs3 complex,

(ii) expressing a His-tagged Prs5 construct in *prs5*Δ and *prs2*Δ*prs4*Δ*prs5*Δ strains followed by investigation of the Prs5-enriched extracts by MS/MS analysis to identify interacting proteins.

(iii) co-immunoprecipitation to provide supporting physical evidence for the Y2H interaction of Prs1 with the cell wall integrity (CWI) pathway. The approach taken involved the interaction of three different FLAG-tagged versions of Mpk1/Slt2 – WT, inactivated Mpk1/Slt2 or catalytically inactive ("kinase-dead") Mpk1/Slt2 with tagged Prs1,

(iv) detailed investigation of the *prs1*Δ*prs5*Δ synthetically lethal strain rescued by WT *PRS1* and various *in vitro*-generated mutated versions of *PRS1* in an attempt to determine the cause of synthetic lethality as demonstrated by Rlm1 expression and the phosphorylation status of Mpk1/Slt2 before and after exposure to mild heat shock and

(v) examining the functionality of the three postulated phosphorylatable residues of Prs5 as demonstrated by the transcriptional readouts, Rlm1 and Fks2, of the CWI pathway.

Materials and Methods

2 Materials and Methods

All chemicals used are of analytical grade and were purchased from Thermo Fisher Scientific (Loughborough, UK) or Sigma-Aldrich (Gillingham, UK) unless otherwise stated. All chemicals were handled and stored under conditions recommended by the suppliers and according to the University regulations. COSHH forms were completed as required.

2.1 Strains

Table 2.1: *S. cerevisiae* strains used in this study

Strain	Genotype	Sources
YN94-1	*MAT**a** ade2-1 his3-11 leu2-3,112 trp1-1 ura3-1 can1-100 ssd1-d2 GAL* (original strain)	Hernando *et al*. (1999)
YN96-65	YN94-1 *prs1*Δ::*loxP*	Carter *et al*. (1997)
YN96-68	YN94-1 *prs5Δ::loxP*	This study
	YN96-68 [pHPS100-Ura, $pGAD_{424}$]	This study
	YN96-68 [pHPS100-Ura, $pGAD_{424}$-Prs5]	This study
	YN96-68 [pHPS100-Ura, $pGAD_{424}$-prs5(479)]	This study
	YN96-68 [pHPS100-Ura, $pGAD_{424}$-prs5(362.2)]	This study
	YN96-68 [pHPS100-Ura, $pGAD_{424}$-prs5(365.5)]	This study
	YN96-68 [pHPS100-Ura, $pGAD_{424}$-prs5(365.1)]	This study
	YN96-68 [pHPS100-Ura, $pGAD_{424}$-prs5(S364A)]	This study
	YN96-68 [pHPS100-Ura, $pGAD_{424}$-prs5(S367A)]	This study
	YN96-68 [pHPS100-Ura, $pGAD_{424}$-prs5(S369A)]	This study
YN96-77	YN94-1 *prs3*Δ::*loxP*	Laboratory collection
YN97-5	YN94-1 *prs4*Δ::*loxP*	Laboratory collection
YN97-14	YN94-1 *prs1*Δ::*HIS3 prs5*Δ*::loxP* [pVT1]	Hernando *et al*. (1999)
	YN97-14 *prs1*Δ::*HIS3 prs5*Δ::*loxP* [pGBT9-Prs1]	This study

Table 2.1: (*continued*)

Strain	Genotype	Sources
	YN94-1 *prs1*Δ::*HIS3 prs5*Δ::*loxP* [pGBT9-prs1(L115T)]	Ugbogu *et al*. (2013)
	YN94-1 *prs1*Δ::*HIS3 prs5*Δ::*loxP* [pGBT9-prs1(Q133P)]	Ugbogu *et al*. (2013)
	YN94-1 *prs1*Δ::*HIS3 prs5*Δ::*loxP* [pGBT9-prs1(D326A)]	Ugbogu *et al*. (2013)
	YN94-1 *prs1*Δ::*HIS3 prs5*Δ::*loxP* [pGBT9-prs1(H130A/D326A)]	Ugbogu *et al*. (2013)
YN97-91	YN94-1 *prs2*Δ::*loxP prs4*Δ*::loxP prs5*Δ*::loxP* [pYES-DEST52-PRS5-His6X-V5::*URA3*]	This study
YN97-96	YN94-1 *prs1*Δ*::GFP-PRS1*	Schneiter *et al*. (2000)
YN97-157	YN97-96 *prs2*Δ::*GFP-PRS1*	Schneiter *et al*. (2000)
YN98-8	YN97-96 *prs2*Δ::*GFP-PRS1*	Schneiter *et al*. (2000)
YN98-11	YN97-96 *prs3Δ::kanMX4-loxP*	Schneiter *et al*. (2000)
YN11-01	YN94-1 *prs5Δ::kanMX4-loxP* [pYES-DEST52-PRS5-His6X-V5::*URA3*]	This study
YN98-12	YN97-96 *prs4Δ::kanMX4-loxP*	Schneiter *et al*. (2000)
YN98-14	YN97-96 *prs5Δ::kanMX4-loxP*	Schneiter *et al*. (2000)

2.2 Plasmids

Table 2.2: Plasmids

Plasmid	Description	Sources
pGBT9	*GAL4* DNA-binding domain cloning vector. *TRP1* is the selectable marker.	Laboratory collection
pGBT9-Prs1	A Y2H vector in which the *PRS1* coding region was fused to the DNA-binding domain of *GAL4*.	Hernando *et al*. (1999)
pGBT9-prs1(L115T)	A mutated version of *PRS1* created by *in vitro* mutagenesis to convert the leucine (L) residue at 115 to threonine (T).	Laboratory collection
pGBT9-prs1(Q133P)	A mutated version of *PRS1* created by *in vitro* mutagenesis to convert the glutamine (Q) residue at 133 to proline (P).	Laboratory collection
pGBT9-prs1(D326A)	A mutated version of *PRS1* created by *in vitro* mutagenesis to convert the aspartate (D) residue at 326 to alanine (A).	Laboratory collection
pGBT9-prs1(H130A/D326A)	A doubly mutated version of *PRS1* created by *in vitro* mutagenesis to convert the histidine (H) residue at 130 to alanine (A) and the aspartate residue (D) at 326 to alanine (A).	Laboratory collection

Table 2.2: (*continued*)

Plasmid	Description	Sources
pVT1	2-micron-based vector derived from pVT100-Ura containing a 1346-bp fragment that corresponds to the *PRS1* coding sequence plus 42 and 21 bp upstream and downstream. *URA3* is the selectable marker.	Hernando *et al*. (1999)
pGBT9-Prs5	A Y2H vector, in which *PRS5* was fused to the DNA-binding domain of *GAL4*.	Hernando *et al*. (1999)
$pGAD_{424}$	A *GAL4* activation domain cloning vector. *LEU2* is the selectable marker.	Laboratory collection
pGAD-Prs3	A Y2H vector, in which *PRS3* was fused to the *GAL4* activation domain.	Laboratory collection
pGAD-Prs5	A Y2H vector, in which *PRS5* was fused to the *GAL4* activation domain.	Hernando *et al*. (1999)
pGAD-prs5(479)	A triply mutated version of *PRS5* created by *in vitro* mutagenesis to convert the serine (S) residues at 364, 367 and 369 to alanine (A).	Laboratory collection

Table 2.2: (*continued*)

Plasmid	Description	Sources
pGAD-prs5(362.2)	A sextuply mutated version of *PRS5* created by *in vitro* mutagenesis to convert the threonine residues at 362, 363, 365 in pGAD-prs5(479) to alanine (A).	Laboratory collection
pGAD-prs5(365.1)	A sextuply mutated version of *PRS5* created by *in vitro* mutagenesis to convert the threonine (T) residues at 365 and 368 to alanine (A) and the serine (S) residue at 366 to alanine (A) in pGAD-prs5(479).	Laboratory collection
pGAD-prs5(365.5)	A spontaneous deletion of *PRS5* arising during *in vitro* mutagenesis in which 16 bp were removed causing the reading frame to be altered and resulting in a truncated version of Prs5 terminating 19 aa downstream of the deleted region.	Laboratory collection
pHPS100-Ura	A centromeric vector carrying a 3.2 kb *LexA-RLM1ΔN* construct under the control of the *ADH1* promoter and the *lacZ* reporter gene proceeded by five LexA-binding sites. *URA3* as the selectable markers. For measurement of Rlm1 transcriptional activation.	Kirchrath *et al*. (2000)

Table 2.2: (*continued*)

Plasmid	Description	Sources
pHPS100-Leu	A centromeric vector carrying a 3.2 kb *LexA-RLM1ΔN* construct under the control of the *ADH1* promoter and the *lac*Z reporter gene proceeded by five LexA-binding sites. *LEU2* as the selectable marker. For measurement of Rlm1 transcriptional activation.	Kirchrath *et al*. (2000)
p2313	YEp351[Slt2-FLAG], a high copy number expression vector of Slt2 with a C-terminal FLAG epitope (D-Y-K-D-D-D-K).	Kim *et al*. (2007)
p2316	YEp351[slt2(T190A,Y192F)-FLAG], a high copy number expression vector containing a C-terminally FLAG-tagged version of Slt2 doubly mutated at T190 and Y192 which can no longer be phosphorylated.	Kim *et al*. (2008)
p2317	YEp351[slt2(K54R)-FLAG], a high copy number expression vector containing a C-terminally FLAG-tagged version of Slt2 mutated at K54R which expresses an enzymatically inactive form of Slt2.	Kim *et al*. (2008)

Table 2.2: (*continued*)

Plasmid	Description	Sources
pYESDEST52	Contains a LR cloning site flanked by a V5-His6X C-terminal tag under the control of the *GAL1* promoter.	Life Technologies
pYESDEST52-PRS5-His6XV5::URA3	A fusion protein of Prs5 with a V5-His6X C- terminal tag. *URA3* is the selectable marker.	Fasolo *et al*. (2011)
pBG1805	An in frame fusion of *PRS1* with a C-terminal affinity tag consisting of 6xHis, HA, and 3C protease under the control of *GAL1* promoter. *URA3* is the selectable marker.	Open Biosystems
p*FKS2-lacZ*	Contains a *lac*Z gene from *E. coli* under the control of the *FKS2* promoter region between nts -701 and -1. *URA3* is the selectable marker.	de Nobel *et al*., (2000a)

The phenotypes of strains stored as glycerol stocks were checked before use by streaking on appropriate media (cf. 2.3 & 2.4). All plasmids used were checked by sequencing.

2.3 Media

2.3.1 LB (Luria-Bertani) medium

10.0 g Tryptone

5.0 g Yeast extract

10.0 g NaCl

15.0 g Agar (if plates are required)

Made up to 1 litre with distilled H_2O and autoclaved at 121°C for 15 min. For *Amp*^{R} selection, ampicillin was added to a final concentration of 100 μg/ml when the media had cooled to approximately 55°C.

2.3.2 YEPD (Yeast Extract Peptone Dextrose) medium

20.0 g Glucose (Formedium Ltd, UK)

10.0 g Yeast extract

20.0 g Bacteriological peptone

20.0 g Agar (if plates are required)

Made up to 1 litre with distilled H_2O and autoclaved at 121°C for 15 min.

2.3.3 SC (Synthetic Complete) media

20.0 g Glucose

1.70 g Yeast nitrogen base-without amino acids and ammonium sulphate

5.0 g Ammonium sulphate

25 ml Amino acid+adenine+uracil mix (see below)

20.0 g Agar (if plates are required)

Made up to 1litre with distilled H_2O and autoclaved at 121°C for 15 min.

'Amino acid + Adenine + Uracil' drop-out mix (40x):

0.10 g Adenine (hemi-SO_4)	0.20 g L-Arginine	0.10 g L-Histidine
0.60 g L-Isoleucine	0.60 g L-Leucine	0.40 g L-Lysine
0.10 g L-Methionine	0.60 g L-Phenylalanine	0.60 g L-Threonine
0.40 g L-Tryptophan	0.10 g Uracil	

Made up to 100 ml with distilled H_2O. 'Drop-out' mixes lacking the relevant component(s) were used for selective media.

2.3.4 Raffinose media

1.70 g Yeast nitrogen base-without amino acids and ammonium sulphate (Formedium Ltd, UK)

5.0 g Ammonium sulphate

25 ml ''Amino acid + Adenine-Uracil'' drop-out mix (2.3.3)

20% (w/v) raffinose (Formedium), autoclaved

Made up to 900 ml with distilled H_2O and autoclaved at 121°C for 15 min. 100 ml 20% (w/v) raffinose was added to 900 ml SC-Ura after the media had cooled to approximately 50^{o}C to give a final concentration of 2% raffinose.

2.3.5 3xYeast Extract Peptone Galactose (YEPG) media

3.0 g Yeast extract

6.0 g Peptone

6.0 g Galactose

Made up to 100 ml with distilled H_2O and autoclaved at 121°C for 15 min.

2.4 Strain maintenance (Guthrie and Fink, 1991, Ausubel *et al*., 1995)

For long-term storage at –70°C yeast strains were stored in YEPD media with 25% glycerol. To prepare glycerol stock cultures of *S. cerevisiae*, a fresh colony was picked from a YEPD plate and cells were re-suspended in 500 µl YEPD medium, in a 2 ml screw-cap tube (Fisher Scientific, UK). The tubes were then vortexed vigorously to thoroughly disperse the cells and 500 µl of sterile 50% (v/v) glycerol (Sigma-Aldrich) was added to the suspension to give a final glycerol concentration of 25% (v/v). For preparation of 'working' stock plates, a portion of the frozen glycerol stock was streaked onto YEPD or appropriate SC agar plates and incubated at 30°C.

When a mid-log phase culture was required, an appropriate amount of an o/n culture was transferred into the relevant medium to give a cell suspension with an OD_{600} of approximately 0.2-0.3 and incubated at 30°C for 3-5 hr with shaking (170 rpm, Gallenkamp™, Heraeus Instruments) to give a culture with an OD_{600} of 0.4-0.6. Transformed *S. cerevisiae* strains were stored on appropriate SC 'drop-out' media to maintain selective pressure on the plasmid.

2.5 Determination of cell density

The absorbance of a culture was determined spectrophotometrically at 600 nm (SmartSpec™ 3000, Bio-Rad). For reliable measurements, the culture was diluted to ensure the measured optical densities (OD) are not greater than 1. For *S. cerevisiae*, the OD_{600} = 1.0 is equivalent to 3×10^7 cells/ml (Groves *et al*., 1996).

Log phase growth of the yeast can be divided into three stages. Early-log phase was the period when the cell density is less than 10^7 cells/ml, mid-log phase is between $1\text{-}5\times10^7$ cells/ml and late-log phase occurred when the cell density was between 5×10^7- 2×10^8 cells/ml.

2.5.1 Sorbitol rescue of yeast strains' sensitivity to temperature and caffeine

A single colony of *S. cerevisiae* cells was inoculated in 10 ml appropriate medium at 30°C o/n with shaking. The OD_{600} of the o/n culture was determined as described

above and adjusted to OD_{600} 0.5 followed by 10-fold serial dilutions (10^{-1}-10^{-4}). To test for temperature and caffeine sensitivity or ability of sorbitol to rescue impaired growth 3 µl aliquots of the individual serial dilutions were spotted onto appropriate solid media with or without caffeine in the presence or absence of 1 M sorbitol (Formedium) at the indicated concentrations and incubated at 30°C or 37°C for 3 days. Growth at 30°C was routinely used as the control.

2.6 Yeast transformation using the 'PLATE' method (Elble, 1992)

Solutions:

Plate solution: 90 ml 45% (w/v) PEG 4000 (Fluka Chemicals, Switzerland)
10 ml 1 M LiOAc
1 ml 1 M Tris-HCl, pH 7.5
0.2 ml 0.5 M EDTA, pH 8.0

Carrier DNA: Herring sperm DNA (10 mg/ml).

10 ml distilled H_2O was added to 100 mg of herring sperm DNA and briefly vortexed. The mixture was boiled for 15 min and snap-cooled on ice for a further 15 min. The DNA was then sheared by repeated passage through a 20-gauge needle (Fisher Scientific, UK). The mixture was then boiled for an additional 15 min, aliquoted and stored at -20°C

Protocol:

The yeast strain of choice for transformation was streaked out for single colonies onto YEPD or appropriate selective media and incubated o/n at 30°C. A single colony was picked and grown o/n in 10 ml of the same media at 30°C with shaking (170 rpm). 0.5 ml of the culture was spun down in a microcentrifuge (Eppendorf 5415D, 1.0^{R}, Heraeus^{TM} Instruments) at 13000 rpm for 2 min and the supernatant was decanted by inversion. 10 µl of carrier DNA (100 µg) and 1 µg transforming DNA were then added (no transforming DNA was added for control) and vortexed. 0.5 ml

PLATE solution was added to the reaction mixture, vortexed and incubated o/n at RT. Cells were then pelleted at 13000 rpm for 2 min, washed and re-suspended in 100 µl sterile distilled H_2O. This was then plated directly onto selective media and incubated at 30°C for 3 days.

2.7 Preparation of crude extract from *S. cerevisiae*

Solutions:

Glass bead disruption buffer:	0.02 M Na-phosphate, pH 7.4
	0.5 M NaCl
	0.001 M PMSF

1 mM PMSF (a 100 mM stock solution was prepared in isopropanol and stored at -20 °C).

I tablet of protease inhibitor for each 10 ml glass bead disruption buffer (Roche Diagnostic, Germany).

425-600 µm acid-washed glass beads.

Protocol:

Single colonies of the yeast strains to be transformed were re-streaked onto appropriate fresh media and incubated at 30^{o}C for 3 days. A single colony from the fresh plate was then grown o/n in 10 ml of YEPD at 30^{o}C with gentle shaking (170 rpm). The cells were then diluted to the OD_{600} ≈ 0.2 in 50 ml of the selective media in 250 ml Erlenmeyer^{TM} flasks and incubated at 30^{o}C and 170 rpm until OD_{600} ≈ 1-1.2 was attained. The cells were harvested in 50 ml Greiner^{TM} tubes using a pre-cooled centrifuge (Megafuge 1.0^{R}, Heraeus Instruments) at 3000 rpm for 5 min at 4^{o}C, followed by washing twice with ice-cold H_2O. The wet weight of the cells was determined and the cells were frozen at -80^{o}C. The cells were lysed using 1 ml of glass bead disruption buffer containing I tablet of protease inhibitor with an equal

volume of 425-600 µm glass beads in a 50 ml Greiner tube. The suspension was vortexed for 1 min and ice-cooled for 1 min. This process was repeated 7x and an aliquot of the vortexed (broken) cells and intact (unbroken) cells viewed under the microscope (Zeiss Axiovert25^{R}) to check for breakage. The lysed cells were centrifuged at 3000 rpm for 5 min at 4^{o}C (Megafuge 1.0^{R}) and the supernatant decanted to a fresh tube. The pellet was re-suspended with 0.5 ml glass bead disruption buffer and vortexed twice followed by centrifugation. The two supernatants were combined and the protein concentration determined according to Bradford (1976).

2.8 Determination of total protein in cell extracts (Bradford, 1976)

Solutions:

Bovine Serum Albumin (BSA) standard solution (1.45 mg/ml, Bio-Rad) was re-suspended in 20 ml ultrapure H_20; this solution was then diluted to 100 µg/ml working solution by adding 1853 µl distilled H_2O to 147 µl BSA standard solution.

Protein assay dye reagent (Bio-Rad, #500-0006).

Protocol:

A standard curve was obtained by pipetting together the solution volumes listed in Table 2.3. The concentration range was from 0-16 µg/ml BSA and the final volume of all samples was 1 ml. 200 µl of the dye reagent was mixed with 800 µl of each BSA dilution in a 1 ml disposable cuvette (Fisher Scientific, Fisher brand, #FB55147) and incubated at RT for 10 min. The OD_{595} was then measured for each sample and the values were used to generate the calibration curve shown in Figure 2.1.

For each protein sample three dilutions (1:100, 1:500 and 1:1000) were prepared in 1 ml final volume with distilled H_2O. 800 µl of each dilution was mixed with 200 µl of the dye reagent and incubated for 10 min at RT. The protein concentration of the test samples was then determined and calculated from the standard curve taking into account the dilution factor.

Table 2.3: Composition of SDS-PAGE gels

BSA concentration (µg/ml)	Volume of BSA working solution (ul) (100 µg/ml)	Dist.H_2O (µl)
0	-	800
2	20	780
4	40	760
6	60	740
8	80	720
10	100	700
12	120	680
14	140	660
16	160	640
18	180	620

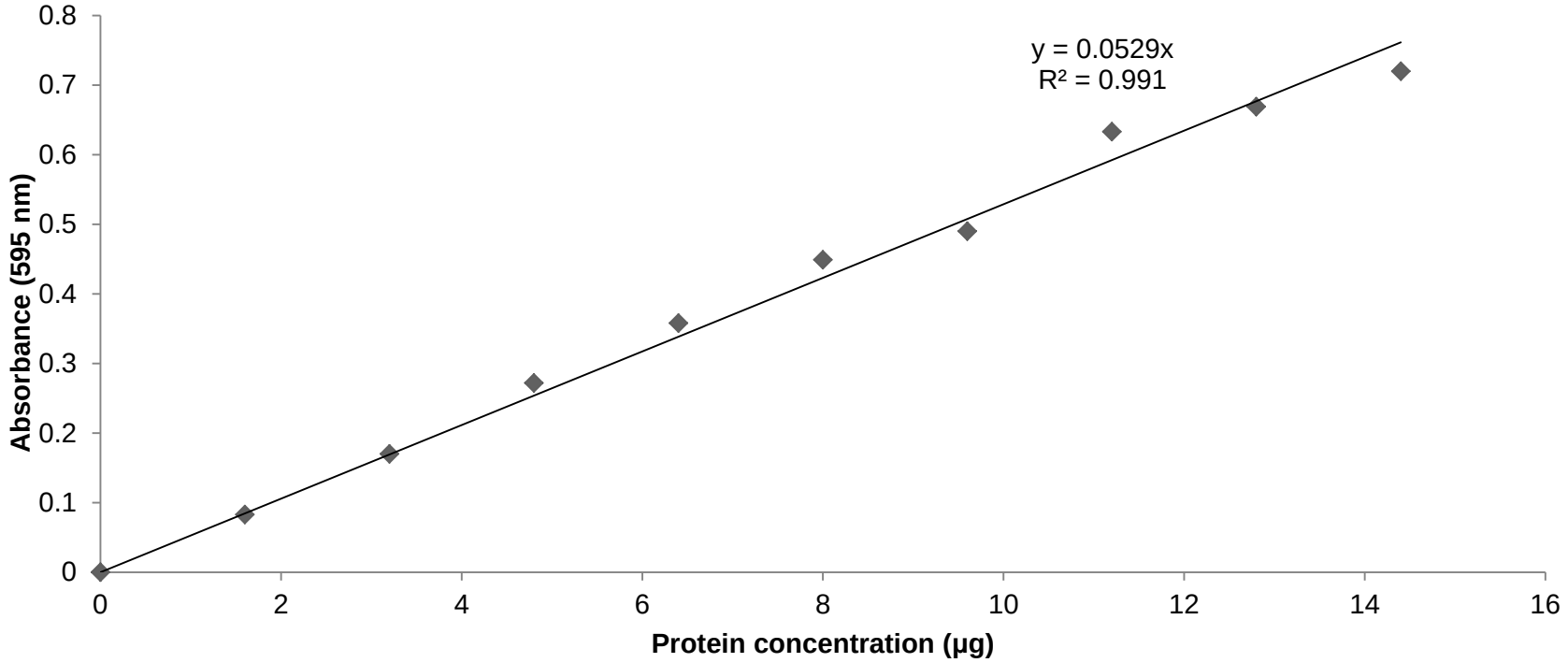

Figure 2.1: Standard curve for quantifying total protein content in cell extracts, using BSA as the standard

Aliquots of known amounts of BSA ranging from 0-16 µg were incubated for 10 min at RT with Bradford reagent and the absorbance measured at 595 nm. Means of triplicate determinations were used to plot the curve above. The protein content of experimental samples was calculated using the equation, x = a/y, of the standard curve and taking into consideration the dilution factor.

2.9 Analysis of proteins by SDS-polyacrylamide gel electrophoresis (SDS- PAGE) (Laemmli, 1970)

Solutions:

4x separating gel buffer:	1.5 M Tris-HCl, pH 8.8 10% (w/v) SDS
4x stacking gel buffer:	0.5 M Tris-HCl, pH 6.8 10% (w/v) SDS
1x electrophoresis buffer:	25 mM Tris-base 192 mM glycine 0.1% (w/v) SDS pH should be between 8.1-8.3
2x Laemmli sample buffer:	0.125 M Tris-HCl, pH 6.8 4% (w/v) SDS 5% (v/v) β-mercaptoethanol 20% (v/v) glycerol 0.01% (w/v) bromophenol blue

10% Ammonium persulphate (APS)

TEMED (N, N, N', N'-tetramethylene-ethylenediamine, Bio-Rad)

t-amyl ethanol (≥99%)

Protein markers:

Broad range pre-stained protein marker (Thermo Fisher Scientific, #sm1811). The marker is a -3-colour ladder with 10 proteins covering a molecular weight range from 10-170 KDa. The ladder contains two bright orange reference bands at 72 KDa and 27 KDa for easy band referencing and blot orientation.

Broad range pre-stained marker (Bio-Rad, #161-0376). The marker consists of 10 distinct bands with a molecular range from 10-250 KDa. The 25 and 75 KDa bands are stained orange.

Precision Protein™ Strep Tactin-HRP conjugate (Bio-Rad, #161-0380). The pre-stained marker contains 10 distinct bands with a molecular range from 10-250 KDa and is detectable using WesternC™blotting detection reagent which recognizes Precision Plus Protein™ WesternC™ Standards and enables simultaneous detection of protein standards and sample proteins.

All working solutions were stored at 4 °C except for the loading buffer which was stored in 0.5 ml aliquots at -20 °C. APS was prepared immediately prior to use.

2.9.1 Preparation of gels for SDS-PAGE

The plates were washed with distilled H_2O, rinsed with ethanol, dried and assembled according to the manufacturer's instructions (1 mm thick, Mini-Protean Cell®, Bio-Rad). Unless pre-cast gels obtained from Bio-Rad were used, a 10% separating gel was prepared in a 100 ml Erlenmeyer flask (Table 2.4) and introduced carefully into the gel sandwich using a 1 ml pipette to about 1.0 cm from the top of the front plate. The surface was overlaid by adding t-amyl ethanol to remove air bubbles and the gel was allowed to polymerize for 45 min at RT. The ethanol was poured off and the gel sandwich rinsed with distilled H_2O. A 5% stacking gel solution (Table 2.4) was then poured onto the separating gel and the comb carefully inserted without trapping air bubbles. The gel was allowed to polymerize for 30 min at RT. The gel sandwich was attached to the electrode assembly of the Mini-PROTEAN® Tetra Cell (Bio-Rad, #165-3301) and inserted into the electrophoresis tank. 1x electrophoresis buffer (700 ml) was added to the inner and outer reservoirs of the electrophoresis chamber, the comb carefully removed and the wells rinsed thoroughly with Ix electrophoresis buffer.

Table 2.3: Standard curve samples for Bradford protein assay

Solution	Separating gel 10% (20 ml)	Stacking gel 5% (10 ml)
40% acrylamide/0.8% bis-acrylamide stock solution	5 ml	1 ml
4x separating or stacking gel buffer	5 ml	2.5 ml
dist. H_2O	10 ml	6.4 ml
TEMED	20 µl	10 µl
APS 10% (added last)	200 µl	100 µl

2.9.2 Preparation of protein samples

25 or 50 µg of crude extract, as determined by the Bradford assay (Bradford, 1976), was mixed with twice the extract volume of the 2x Laemmli sample buffer in a 1.5 ml Eppendorf tube. Samples were then heated at 100 ^{o}C for 5 min and snap-cooled on ice and centrifuged for 1 min at RT in a microcentrifuge. Samples were loaded by means of a Hamilton^{R} syringe (Sigma-Aldrich, #20737 (100 µl)) into the rinsed wells of the gel. At least one well contained 5 µl of a standard pre-stained protein marker prepared according to the manufacturer's instructions (Bio-Rad, #161-0376). Electrophoresis was carried out at 200 V (constant voltage) until the bromophenol blue dye reached the bottom of the separating gel.

2.9.3 Coomassie staining and destaining of the gel

Coomassie Blue staining solution:	1% (w/v) Coomassie Blue R-250 45% (v/v) ethanol 10% (v/v) glacial acetic acid 45 ml distilled H_2O
Destaining solution:	40% (v/v) ethanol 10% (v/v) glacial acetic acid 50 ml distilled H_2O

The gels were soaked with gentle shaking (Mini Orbital Shaker SO5, Stuart Scientific) for 30 min in Coomassie Blue staining solution and were then transferred into the destaining solution. The destaining solution was replaced at least 3x until the gel background was destained. Documentation of gels was performed with the Bio-Rad ChemiDoc^{TM} XRS+ imager. The gel was placed on the white light conversion screen inside the Universal Hood 11 and the Epi-illumination switched on. Once the gel is satisfactorily positioned an image is obtained by running the appropriate protocol from the Image Lab software V4.1 (Bio-Rad). Images are stored on the dedicated computer.

2.10 Western blotting

Solutions:

1x transfer buffer:	25 mM Tris-base 192 mM glycine pH should be between 8.1-8.4
1xTris-Buffered Saline (TBS):	20 mM Tris-HCl pH 7.5 150 mM NaCl

TBS-T:	1xTBS + 0.1% Tween 20
Blocking solution:	non-fat dried milk (5% (w/v in TBS-T)
Ponceau S staining solution:	0.5% (w/v) Ponceau S (Bio-Rad) 1% (v/v) glacial acetic acid

Methanol (100%)

Kodak® processing chemicals for autoradiographic film: GBX developer/replenisher and GBX fixer/replenisher (Sigma-Aldrich, #P7167-56A).

ECL+Plus™ Western blotting detection reagent (GE Healthcare, #RPN2132) detects only sample proteins transferred to the membrane while WesternC™ blotting detection reagent also recognizes Precision Plus Protein™ WesternC™ Standards on account of the StrepTactin-HRP conjugate.

2.10.1 Electroblotting on PVDF (polyvinylidene difluoride) membrane

Electrotransfer of the separated proteins was performed using the Mini Trans-Blot® system from Bio-Rad. A PVDF sheet (GE Healthcare, Hybond-P™ 0.2 µm) was cut to fit the gel and pre-activated by soaking in 100% methanol for 30 sec. After a 5 min rinse in distilled H_2O, the membrane and the previously run SDS PAGE gel were equilibrated separately in pre-cooled 1x transfer buffer for 15-20 min with gentle shaking. Two sheets of Whatman 3 MM paper and two fibre pads (Bio-Rad, #1703932) were also soaked in transfer buffer for preparation of the gel-membrane sandwich in a shallow

tray. A frozen cooling unit (stored at -20°C) and a stirrer bar were placed into the tank filled with 1x transfer buffer (~ 900 ml). The sandwich cassette was inserted into the tank and the entire Trans-Blot apparatus placed on a magnetic stirrer (Fisher Scientific, #200042). The transfer was carried out at 100 V (constant voltage) for 1 hr.

2.10.2 Immunodetection

Immunodetection involves the transfer of proteins separated by SDS-PAGE from the gel onto a membrane which is subsequently probed with a specific primary antibody. Antibody/antigen interactions are detected by a secondary antibody which is coupled to the enzyme horseradish peroxidase (HRP). Addition of enzyme substrate results in a visible product at the location of the secondary antibody bound to the specific primary antibody/antigen complex. HRP-labelled antibodies catalyse the following reaction:

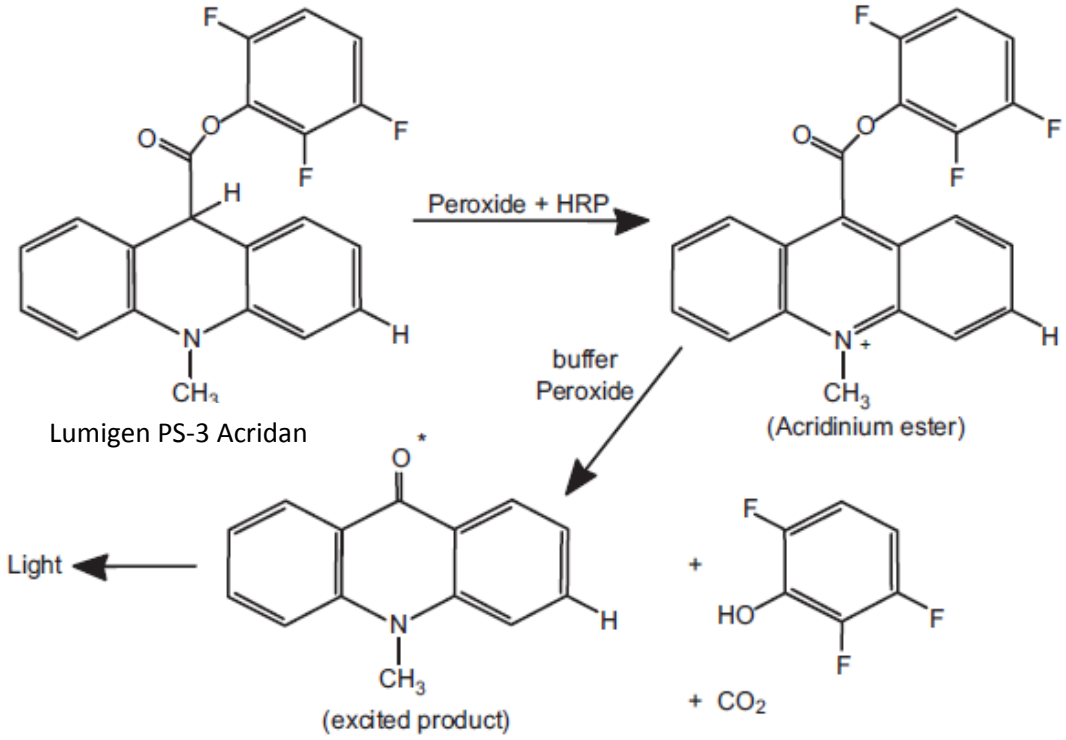

Figure 2.2: Chemiluminescent reaction of Lumigen PS-3 with horseradish peroxidase

(taken from Amersham ECL Plus Western Blotting Detection Reagents, Product Booklet, Life Sciences, GE Healthcare).

This reaction is based on the oxidation of Lumigen PS-3 Acridan substrate through a combined HRP and peroxide-catalysed reaction which generates thousands of acridinium ester intermediates per minute. These intermediates react with peroxide under slightly alkaline conditions to produce a sustained high intensity chemiluminescence with maximum emission at a wavelength of 430 nm. The resulting light is detected with the ChemiDoc^{TM} XRS+ imager.

Blocking the membranes:

All the incubation with antibodies and washing steps were carried out with gentle shaking at RT in a small square lidded container.

Following the electro-transfer, the membrane was washed in 1xTBS-T for 5 min and the gel stained in Coomassie Blue R-250 to monitor the transfer efficiency. Alternatively, the membrane was reversibly stained with 0.5% Ponceau S staining solution and de-stained in distilled H_2O. Non-specific protein binding sites were blocked by incubating the membrane in 5% non-fat dried milk in 1xTBS-T for 1 hr at RT or o/n at 4^{o}C, then the membrane was washed 2×2 min with 1xTBS-T.

Primary antibody incubation:

Primary antibody incubation was performed by probing the blocked membrane for 1 hr with specific primary antibody at dilutions 1:1000 to 1:300,000 (depending on the amount of protein sample being investigated) in 1xTBS-T containing 5% non-fat dried milk. The membrane was then briefly rinsed with two changes of 1xTBS-T followed by soaking in 1xTBS-T for 5 min and then 6x 5 min washing in 1xTBS-T.

FLAG primary antibody: monoclonal anti-FLAG M2 IgG_1 produced in mouse (Sigma-Aldrich, #F3165).

GFP antibody: mouse monoclonal IgG_1 (Santa Cruz, sc-73556).

P-Slt2 antibody: rabbit polyclonal IgG (anti-phospho-pThr^{202}/Tyr^{204}, Santa Cruz, sc-16982-R).

Mpk1/Slt2 antibody: rabbit polyclonal IgG (Santa Cruz, sc-20168)

His-probe antibody (H-3): mouse monoclonal IgG_1 (Santa Cruz, sc-8036)

Actin antibody: goat polyclonal IgG (C-11) (Santa Cruz, sc-1615).

Secondary antibody incubation:

The primary antibody was detected with secondary antibody used at different dilutions from 1:2000 to 1:100,000 (depending on the binding capacity of the primary antibody) incubated for 1 hr in 2% non-fat dried milk in 1xTBS-T. The membrane was then washed as described for the primary antibody.

FLAG, GFP and His-probe secondary antibody: goat anti-mouse IgG_1-HRP (Santa Cruz, sc-2060).

P-Slt2 and Mpk1/Slt2 secondary antibody: goat anti-rabbit IgG-HRP (Santa Cruz, sc-2004).

Actin secondary antibody: donkey anti-goat IgG-HRP (Santa Cruz, sc-2020).

2.10.3 Image detection

The washed membrane was placed on an acetate sheet for detection with the ECL+Plus™ system (Amersham Pharmacia Biotech) or the Western^c Bio-Rad detection kit. The detection reagents were mixed as described in the manufacturer's instruction manual and pipetted onto the membrane. Following 3-5 min incubation at RT excess detection reagent was drained off by holding the membrane with forceps and touching the edge against a tissue. A second acetate sheet was put on top of the membrane and the whole sandwich placed into the ChemiDoc^{TM} XRS+ imager for analysis.

For Western blots performed prior to acquisition of the ChemiDoc^{TM} XRS+ imager signals were obtained on X-ray film as follows: the membrane protected by two acetate sheets was placed into an X-ray film cassette with the protein side facing the light-tight seal of the cassette. In a dark room under red light, a sheet of autoradiographic film (Lumi-Film Chemiluminescent Detection Film 7.1x9.4 ins, Kodak®, #11666916001) was placed on top of the membrane for exposure times varying from 1-30 min, depending on the intensity of the signal.

2.11 Co-immunoprecipitation

2.11.1 Co-immunoprecipitation of GFP-Prs1 and FLAG-tagged Slt2

Solutions:

Lysis buffer:	50 mM Tris-HCl pH 7.5
	150 mM NaCl
	5 mM EDTA
	5 mM EGTA
	0.2 mM Na_3VO_4
	50 mM KF
	30 mM $Na_4P_2O_7$

I tablet of protease inhibitor for each 10 ml lysis buffer (Roche Diagnostic, Germany).

1 mM PMSF (a 100 mM stock solution was prepared in isopropanol and stored at -20^{o}C.

425-600 µm acid-washed glass beads

Restore^{TM} Western Blot stripping buffer (Thermo Fisher Scientific, #21059).

Western blotting solutions and techniques have been described in section (cf 2.10).

1xTris-Buffered Saline (TBS):	20 mM Tris-HCl pH 7.5 150 mM NaCl
Immunoprecipitation buffer I:	50 mM Tris-HCl pH 7.5 150 mM NaCl 5 mM EDTA 5 mM EGTA 0.2 mM Na_3VO_4 50 mM KF 30 mM $Na_4P_2O_7$ 1% NP-40
Immunoprecipitation buffer II:	50 mM Tris-HCl pH 7.5 150 mM NaCl 5 mM EDTA 5 mM EGTA 0.2 mM Na_3VO_4 1% NP-40

Buffer M:	25 mM MOPS (pH 7.5) 1 mM EGTA 0.1 mM Na_3VO_4 15 mM $C_6H_6NO_6P$
Kinase buffer:	25 mM MOPS (pH 7.5) 1 mM EGTA 0.1 mM Na_3VO_4 15 mM $C_6H_6NO_6P$ 25 mM $MgCl_2$
2x Laemmli sample buffer w/o β-mercaptoethanol:	0.125 M Tris-HCl, pH 6.8 4% (w/v) SDS 20% (v/v) glycerol 0.01% (w/v) bromophenol blue

ANTI-FLAG M2 affinity gel (Sigma-Aldrich, #A2220) is a purified murine IgG_1 monoclonal antibody covalently attached to agarose by hydrazide linkage. It is used for immunoprecipitation of FLAG fusion proteins (FLAG octapeptide: (D-Y-K-D-D-D-K).

Protocol:

A single colony, each of YN97-96 [p2313], YN97-96 [p2316] and YN97-96 [p2317], were re-streaked onto a fresh SC-Leu plate and incubated at 30 ^oC for 3 days. A single colony from each plate was inoculated into 10 ml of SC-Leu and incubated o/n at 30 ^oC with shaking. The cells were then diluted to OD_{600} ≈ 0.3 in four 250 ml Erlenmeyer flasks, each containing 50 ml SC-Leu and incubated at 30 ^oC at 170 rpm until OD_{600} ≈ 0.7 was reached. Two flasks per culture were then transferred to 37^oC and incubation continued for 1 hr. Cells were harvested in 50 ml Greiner^{TM} tubes using a pre-cooled centrifuge (Megafuge 1.0^R) at 3000 rpm for 5 min at 4^oC, followed by washing twice with ice-cold H_2O. The wet weight of the cells was determined and the cell pellets stored at -

80^{o}C prior to use. The cells were lysed using 1 ml lysis buffer with 1 ml of 425-600 µm glass beads in a 50 ml Greiner tube by vortexing for 1 min and ice-cooled for 1 min. This process was repeated 7x. The tubes containing the lysed cells were then centrifuged at 3000 rpm for 5 min at 4 ^{o}C and the supernatant decanted into a fresh Eppendorf tube for a second centrifugation at 13000 rpm for 10 min and the supernatant decanted into a fresh Eppendorf tube. Protein concentration of the supernatant was determined using the Bradford method (Bradford, 1976).

The ANTI-FLAG M2 affinity gel was thoroughly re-suspended in order to make a uniform suspension of the resin and immediately 40 µl of the gel suspension was transferred into a 1.5 ml Eppendorf tube and the resin centrifuged at 1000 rpm for 30 sec at RT. The resin was allowed to settle in the tube for 2-3 min and the supernatant removed from the resin with a narrow pipette tip. The packed gel was then washed twice with 0.5 ml 1xTBS and once with immunoprecipitation buffer I. Cell extract (250 µg of protein) was added to immunoprecipitation buffer I to a final volume of 0.5 ml. This mixture was incubated in the cold room for 2 hr on a roller drum (Model TC-7, New Brunswick Scientific Co. Inc, USA) at a speed of 1000 rpm. Following centrifugation the pellet obtained was washed 4x with immunoprecipitation buffer II, twice with buffer M and once with kinase assay buffer. All washing was done by re-suspending the beads with the pipette tip before centrifuging for 30 sec for 1000 rpm. 60 µl Laemmli sample buffer w/o β-mercaptoethanol was added to each sample, then heated at 100 ^{o}C for 5 min and snap-cooled on ice for 1 min. Samples were centrifuged at 1000 rpm for 30 sec to pellet the FLAG beads and the supernatant transferred into a fresh Eppendorf tube and centrifuged at 13000 rpm for 1 min. 10 µl of each sample was loaded into the wells of two 4-20% pre-cast SDS-PAGE gels (Mini-Protean^{R} TGX^{TM}, Bio-Rad, #456-1093) rinsed with 1x electrophoresis buffer. One well contained 5 µl of standard pre-stained protein marker prepared according to the manufacturer's instructions (Bio-Rad). Both gels were run at the same time. Electrophoresis was carried out at a 200 V (constant voltage) for 50 min until the bromophenol blue dye reached the bottom of the separating gel. Each gel was transferred to a PVDF membrane; one membrane was incubated sequentially with anti-FLAG primary antibodies (1:300,000 dilution) and 1:100,000 dilution of goat anti-mouse IgG_1-HRP and the other membrane was incubated with anti-GFP antibodies diluted at 1:1000 primary antibody and 1:50,000 anti-mouse IgG_1-HRP secondary antibody. The membranes were treated with

WesternC™ blotting detection reagent Bio-Rad kit and images generated in the ChemiDoc™ XRS+ imager.

10 µg of each crude extract was also subjected to SDS-PAGE on a 4-20% pre-cast gel followed by Western blotting with either FLAG- or GFP-antibodies as described above to detect input for the co-immunoprecipitation procedure.

2.11.2 Co-immunoprecipitation of His-tagged Prs1 and FLAG-tagged Slt2

A single colony, each of YN96-65 [pBG1805-Prs1 + p2313], YN96-65 [pBG1805-Prs1 + p2316] and YN96-65 [pBG1805-Prs1 + p2317], was re-streaked onto a fresh SC-Ura-Leu plate and incubated at 30°C for 3 days. A single colony from each plate was inoculated into 5 ml of SC-Ura-Leu and incubated o/n at 30°C with shaking. 1 ml of each of the o/n cultures was introduced into 25 ml SC-Ura-Leu+2% raffinose and incubated o/n at 30°C with shaking. The cells were then diluted to OD_{600} ≈ 0.3 in 9 x 100 ml of SC-Ura-Leu+2% raffinose in 500 ml Erlenmeyer flasks incubated at 30°C at 170 rpm until OD_{600} ≈ 1.2 was reached. Six flasks, two each for YN96-65 [pBG1805-Prs1 + p2313], YN96-65 [pBG1805-Prs1 + p2316] and YN96-65 [pBG1805-Prs1 + p2317], were induced with 50 ml of 3 x YEP+2% galactose and the three remaining cultures were not induced with 3 x YEP+2% galactose and served as the negative control. All cultures were incubated for 6 hr, after which three of the induced cultures were transferred to 37°C (New Brunswick Scientific Excella™ E25 temperature-controlled shaker) for heat shock for 1 hr. The cultures were harvested by centrifugation at 3000 rpm for 5 min at 4°C (Megafuge 1.0R) and washed twice with ice-cold H_2O. The wet weight of the cells was determined and the cell pellets stored at -80°C prior to use. The cells of the individual cultures were then re-suspended in 1.5 ml lysis buffer and an equal volume of 425-600 µm acid-washed glass beads added and subjected to vortexing for 1 min and ice-cooled for 1 min. This process was repeated 7x. The tubes containing the lysed cells were then centrifuged at 3000 rpm for 5 min at 4°C and the supernatants decanted into a fresh Eppendorf™ tubes, centrifuged at 13000 rpm for 15 min and the supernatants decanted into fresh tubes. Protein concentration of the supernatants was determined using the Bradford method (Bradford, 1976).

Following the transfer of the electrophoresed immunoprecipitates the four membranes were washed in 1xTBS-T for 5 min and blocked by incubating in 5% (w/v) non-fat dried milk in 1xTBS-T for 1 hr at RT, The membranes were then washed 2×2 min with 1xTBS-T. One membrane was incubated sequentially with anti-FLAG primary antibodies (1:150,000 dilution) and 1: 25,000 dilution of goat anti-mouse IgG_1-HRP, the secondary antibody. The second membrane was incubated sequentially with anti-His antibody (H-3), diluted 1:1000 and a 1:25,000 dilution of the secondary antibody, goat anti-mouse IgG_1-HRP. The third membrane was probed with anti-P-Slt2 (anti-phospho-pThr^{202}/Tyr^{204}) as primary antibody (1:1000 dilution) and anti-goat-rabbit secondary IgG-HRP antibody (1:5000 dilution). The fourth membrane was probed with actin IgG antibody (1:1000 dilution) and donkey anti-goat secondary IgG-HRP (1:10000 dilution). Incubation with primary and secondary antibodies was carried out for 1 hr each and washed 6x for 5 min in 1xTBS-T after each incubation. The membranes were treated with WesternC^{TM} blotting detection reagent Bio-Rad kit (#170-5060) and visualized in the ChemiDoc^{TM} XRS+ imager (ChemiDoc^{TM} XRS+ imager, version 4.1, Bio-Rad) at varying times ranging from 0-10 min.

10 µg of each of the crude extracts was also subjected to SDS-PAGE on a 4-15% gel followed by Western blotting with anti-FLAG, anti-His, anti-phospho-pThr^{202}/Tyr^{204} or anti-actin antibodies as described above to detect input for the co-immunoprecipitation.

2.12 Band quantification using the ChemiDoc^{TM} XRS+ Imager Quantity One" software

After transferring the protein gel to a PVDF membrane and processing (Material and Methods, section 2.11.1) images were obtained with the ChemiDoc^{TM} XRS+ imager using the Image Lab software, V4.1 (Bio-Rad) for the detection of bands corresponding to the separated polypeptides. The intensity of the protein bands detected after 1 min exposure was quantified using the "Volume Tool" analysis as follows: rectangular boxes of equal size were drawn around each band using the rectangular button. The boxes were labelled U1, U2, U3, U4 etc. 'U' stands for 'unknown' to distinguish them from the 'Background' volume. A rectangle of the same size is then drawn in the background area of the membrane. The value corresponding to the background pixels was

subtracted from the intensity of the detected bands. The background subtraction method was selected in the 'Volume Report Option' dialog box using 'Global' background subtraction which calculates and subtracts the background intensity for all detected bands to generate the 'Adjusted' volume.

The relative quantity of the control signal was obtained by defining the number of the bands in a box area using the 'Manual' method, then double clicking the band at 30^{o}C or 37^{o}C to assign a 'Reference' volume for a specific band to generate the relative quantity of the controls.

Finally the adjusted volumes obtained from the sample bands are divided by the relative quantity of the control bands at 30^{o}C or 37^{o}C to obtain the 'Relative' volume. The 'Relative' volumes obtained are then plotted for each sample.

2.13 Determination of β-galactosidase activity by the Thermo Scientific Yeast β-galactosidase assay kit

Solutions: Y-PER^{TM} Yeast Protein extraction reagent

2X β-galactosidase assay buffer

β-galactosidase assay stop solution (contains 1 M Na_2CO_3)

Protocol:

Three independent colonies of the appropriate strains were re-streaked individually onto fresh plates and incubated at 30^{o}C for 3 days. A single colony from each plate was grown o/n in 10 ml of the respective media at 30^{o}C with shaking at 170 rpm. The cells were then diluted to OD_{600}≈ 0.3 in 2x50 ml of the relevant media in 250 ml Erlenmeyer flasks. One flask from each strain was incubated at 30^{o}C and the other at 37^{o}C until OD_{660} ≈1 was attained. The β-galactosidase assay buffer was thawed on ice and an equal volume of Y-PER reagent was added to make a 1:1 'working' solution. A blank microcentrifuge tube was then prepared by mixing 350 µl of the culture medium (without cells), 350 µl 'working' solution and 300 µl β-galactosidase assay stopping solution. The remainder of the culture was placed on ice and retained for the preparation of crude extracts for Western blotting (cf. 2.10).

350 µl of each culture was transferred to an Eppendorf tube and an equal volume of the 'working' solution was added to each culture. After mixing the Eppendorf tubes were incubated at 37^{o}C in a water bath (Grant Instruments) until a pale yellow colour developed. The reaction was stopped by the addition of 300 µl stop solution and the samples vortexed for 15 sec before the reaction time was noted. The tubes were centrifuged at 13000 rpm for 30 sec to remove the cell debris and then the supernatant was transferred into a 1 ml disposable cuvette and the absorbance measured at 420 nm against the sample blank.

The following equation has been used to measure β-galactosidase activity is:

$$\beta - galactosidase\ activity\ (\text{Units}) = \frac{1000 \text{ x } A_{420}}{\text{t x V x } OD_{660}}$$

t = reaction time (in minutes).
V = volume of cells (ml) used in the assay.
The factor 1000 takes into account the conversion from µl to ml.

2.14 Determination of the *FKS2* expression

YN96-68 (*prs5*∆) was transformed with the vector (pGAD), pGAD-Prs5 (WT) or pGAD-derivatives containing *in vitro*-generated mutations of *PRS5* individually and the reporter plasmid *pFKS2-lac*Z (Table 2.2) by the 'Plate' method, described in section 2.7. The transformants were selected on Sc-Ura-Leu plates. Three independent colonies from each freshly re-streaked plate were used to inoculate o/n cultures in 10 ml SC-Ura-Leu media. After incubation the cells were diluted to OD_{600}≈ 0.5 in 2x50 ml of SC-Ura-Leu in 250 ml Erlenmeyer flasks. One flask from each strain was incubated at 30^{o}C and the other at 37^{o}C for 3 hr until OD_{660} ≈1 was attained. *Fks2* expression was measured from the β-galactosidase reporter plasmid, *pFKS2-lac*Z, as described in section 2.14.

2.15 Preparation of cell extracts for isolation of His-tagged Prs5 (Fasolo *et al*., 2011)

Fresh colonies of YN11-01 [pYESDEST52-PRS5-His6x-V5::URA3] and YN97-91 [pYESDEST52-PRS5-His6x-V5::URA3] (cf. Table 2.1) strains were grown o/n in 50 ml SC-Ura+2% glucose at 30^{o}C at 170 rpm for 24 hr. The cells were then diluted to an $OD_{600} \approx 0.1$ in four flasks containing 400 ml SC-Ura+2% raffinose each and grown at 30 ^{o}C at 170 rpm until an $OD_{600} \approx 0.6$ was attained. The flasks were then induced with 200 ml of YEP+2% galactose and incubated for a further 6 hr. The cells were harvested by centrifugation at 3000 rpm for 5 min at 4^{o}C and washed twice with ice-cold H_2O. The cells were then re-suspended in a 50 ml Greiner tube in 4 ml glass bead disruption buffer (as described in section 2.8) and an equal volume 0.425-600 µm acid-washed glass beads was added. The cells were lysed by eight cycles of vortexing for 1 min followed by 1 min incubation on ice. Cell breakage was monitored microscopically. The tubes containing the cell lysates were then centrifuged at 3000 rpm for 5 min at 4^{o}C and the supernatant decanted to a fresh tube. The pellet was then re-suspended with 3 ml glass bead disruption buffer, then vortexed twice followed by centrifugation. The supernatant obtained was combined with the previous one and the pellets discarded. The protein concentration of each extract was determined according to (Bradford, 1976) and the supernatant stored at -80^{o}C.

2.16 Protein purification

2.16.1 Protein purification using the ÄKTA purifier Avant 250 (Handbook from GE Healthcare, #11-0008-88 AF)

The ÄKTA purifier is a fully automated liquid chromatography system designed for method development and research applications. The ÄKTA Purifier Avant 250 is a standard system unit consisting of two pumps (A & B), each with buffer selection valves, a mixer unit, in-line filter, injection valve, detectors and outlet selection valve and fraction collector. It has the following features: an easy pump wash for quick solvent exchange without disturbing the column and routine; an automated system wash, automatic on-line buffer preparation from stock solutions; on-line UV-detection of up to three wavelengths simultaneously; on-line monitoring of conductivity; on-line

monitoring of pH and fraction collection options ranging from microtitre plates to large vessels.

Solutions:

Binding buffer:	0.02 M Na-phosphate, pH, 7.4 0.5 M NaCl 0.02 M imidazole, pH 7.4
Elution buffer:	0.02 M Na-phosphate, pH, 7.4 0.5 M NaCl 0.5 M imidazole, pH 7.4

HisTrap™ FF column, 1 ml (GE Healthcare, # 11-0008-88 AF)

Protocol:

A sterile 1 ml syringe (Thermo Scientific, # 14-823-261) was filled with 1 ml distilled H_2O. After the stopper was removed from the HisTrap™ FF column, 1 ml the syringe was connected to it and, to avoid the introduction of air bubbles, 1 ml distilled H_2O was loaded drop-wise into the column. The snap-off end at the column outlet was then removed and connected to the adaptor (1/16 male) of the chromatography system and then ethanol was washed out of the ÄKTA purifier system with 3 to 5 column volumes of distilled H_2O and the column equilibrated with 10 column volumes of binding buffer at a flow rate of 1 ml/min. The protein suspension was then applied to the column at a flow rate of 1 ml/min using a syringe fitted to the 'Luerconnector'. After sample application the column was washed with 10 volumes of binding buffer at a flow rate of 1 ml/min and the His-tagged Prs5 protein eluted with a continuous gradient of 0% to 100% elution buffer in 20 column volumes at a flow rate of 1 ml/min.

After elution of the His-tagged protein the column was washed with five column volumes of elution buffer followed by five column volumes of binding buffer and the column stored at -4^{o}C for re-use. The ÄKTA Avant250 system (Handbook from GE

Healthcare, #18-1142-75 AD) was then washed with 20% ethanol in readiness for the next run.

2.16.2 Manual purification of His-tagged Prs5 using a His SpinTrap™ column

(Handbooks from GE Healthcare, #11-0036-91 AA)

His SpinTrap™ column (GE Healthcare, #28-4013-53)

2-ml Eppendorf tubes and Eppendorf™ 5415D, 24 fixed-angle rotor centrifuge were used throughout the purification process.

Solutions:

Commercially available His buffer kit (GE Healthcare, #11-0034-00) and consisted of:

Binding buffer:	0.02 M Na-phosphate
	0.5 M NaCl
	0.01 M imidazole, pH 7.4

Binding buffer:	0.02 M Na-phosphate
	0.5 M NaCl
	0.05-0.3 M imidazole, pH 7.4

(Handbook from GE Healthcare, #11-0036-91 AA).

Protocol:

The crude extracts prepared as described in section 2.17 were diluted 1:1 with binding buffer before applying to the His SpinTrap™ column. The column was inverted and shaken repeatedly to re-suspend the beads in the storage buffer. The top cap of the column was loosened by a one-quarter turn and after removing the snap-off end the column was placed in a 2-ml Eppendorf tube and centrifuged at 1000 rpm to remove the storage buffer. The cap was removed and the column equilibrated with 600 µl binding buffer followed by application of 600 µl of the sample added in ‘one-go’ and centrifuged at 1000 rpm for 30 s. The column was then washed twice with 600 µl

binding buffer by centrifugation at 1000 rpm for 30 s. The His-tagged Prs5 polypeptide was eluted by applying increasing imidazole in elution buffer ranging from 0.05-0.3 M imidazole to the column. The protein concentration was measured according to (Bradford, 1976) and subjected to SDS-PAGE and Western blot.

2.17 Mass spectrometry analysis

The samples for MS analysis were obtained by excision of a band identified by Western blotting as His-tagged Prs5 (section 3.18, Figure 3.28(b)) from a Coomassie-stained 4-20% pre-cast SDS-Page gel. In addition, two discrete bands eluting with 200 mM imidazole but not cross-reacting with anti-His antibodies (result section, 3.18 Figure 3.28(a)) were also excised from the gel. The three samples were stored at -80^{o}C before dispatching to BMS Mass Spectrometry and Proteomics Facility at the University of St. Andrews where they were analysed by MALDI-TOF and interrogation of the NCBI protein database (http://www.ncbi.nlm.nih.gov/pubmed) identified specific peptide mass fingerprints.

In a second experiment crude extracts of YN11-01 [pYESDEST52-PRS5-His6x-V5::URA3] and YN97-91 [pYESDEST52-PRS5-His6x-V5::URA3] (cf. Table 2.1) were purified on His SpinTrap^{TM} and subjected to 4-20% SDS-PAGE gel (1x1 mm) thickness gel. A ‘chunk’ approximately containing protein material ranging from 30 to 100 KDa from each His SpinTrap^{TM} purified extract was analysed by ESI-QUAD-TOF at the University of St Andrews. The peptides obtained were used to interrogate the NCBI yeast database (http://www.ncbi.nlm.nih.gov/pubmed) and matched with the MASCOT search engine (https://bsrcmascot.st-andrews.ac.uk/mascot/x-cgi/ms-review.exe).

2.18 Statistical analysis

Statistical analysis was performed using One-way and Two-way analysis of variance (ANOVA) with the R^{TM} Statistic software package, version 3.0.3. The normal distribution of the data and the homogeneity of variance were tested by Bartlett homogeneity test. Two-way ANOVA model (GLM) was developed to test the significance of the independent variables, plasmid and temperature and their interactions (plasmid x temperature). If the interaction term was significant simple effects within treatments

were investigated by One-way ANOVA with a Tukey test post-hoc to identify differences among groups. A *p*-value of ≤0.05 was considered statistically significant.

2.19 Database searches

The peptide search was performed with MASCOT (Version: 2.5.0) (Perkins *et al*., 1999) (www.matrixscience.com) using NCBI (http://www.ncbi.nlm.nih.gov/pubmed) and SGD (http://www.yeastgenome.org). Information on putative phosphorylation sites was obtained using the PhosphoGRID (Stark *et al*., 2010) (http://www.phosphogrid.org/) and PhosphoPep (Bodenmiller *et al*., 2008) (http://www.phosphopep.org/) databases available at SGD.

Results

3 Results

3.1 Monitoring the GFP signal generated by GFP-Prs1 in various *PRS* deletant strains

At least one of the three minimal functional units which have been previously defined genetically as Prs1/Prs3, Prs2/Prs5 and Prs4/Prs5, each consisting of a Prs polypeptide with an NHR and one without, is necessary for the survival of *S. cerevisiae* (Hernando *et al*., 1998, Hernando *et al*., 1999). Genetic evidence and Y2H analysis data have shown the existence of two interacting functional complexes, Prs1/Prs3 or Prs2/Prs4/Prs5, with compensatory functions, since in the absence of one entity or a component thereof, the cell can still survive (Hernando *et al*., 1998, Wang *et al*., 2004). To extend these findings, an experiment was designed to gain more information on the *S. cerevisiae* PRPP synthetase complex(es) by means of biochemical evidence to confirm or refute the genetic evidence for the postulated enzyme complexes Prs1/Prs3 and Prs2/Prs4/Prs5.

Various *PRS* deletant strains containing a GFP-tagged *PRS1* integrated at the *PRS1* locus (Schneiter *et al*., 2000) were monitored for the GFP signal. The *PRS* deletant strains, YN97-96 (*prs1*Δ*::GFP-PRS1*), YN98-8 (YN97-96 *prs2Δ*), YN98-11 (YN97-96 *prs3Δ*), YN98-12 (YN97-96 *prs4Δ*), YN98-14 (YN97-96 *prs5Δ*) were subjected to Western blot analysis and the results are shown in Figure 3.1. As expected, no GFP-signal was visible in lane (2) since YN94-1 does not express GFP. However, the GFP-Prs1 signal with an apparent molecular weight of 74 KDa is detectable in lanes (3-4 & 6-7) but not in lane (5) which contains the extract of YN98-11 from which *PRS3* has been deleted. The absence of the band in lane (5) may be due to the instability of Prs1 in the absence of Prs3. The extract in lane (9) was prepared from YN98-11 (YN97-96 *prs3Δ*) transformed with a plasmid-borne copy of *PRS3*, pGAD-Prs3, thus re-creating the WT situation. The extract of YN98-11 [pGAD-Prs3] contained the band corresponding to GFP-Prs1 whereas the extract in lane (8) which is YN98-11 [pGAD], showed no visible band of the same size as the GFP-Prs1 band. The lower MW signal in lanes (2–9) is that of an unknown protein recognized by anti-GFP antibodies and also appears in the negative control (lane (2)) and therefore may be regarded as a loading control. The results show that in the absence of *PRS3*, Prs1 is unstable (Ugbogu *et al*., 2013).

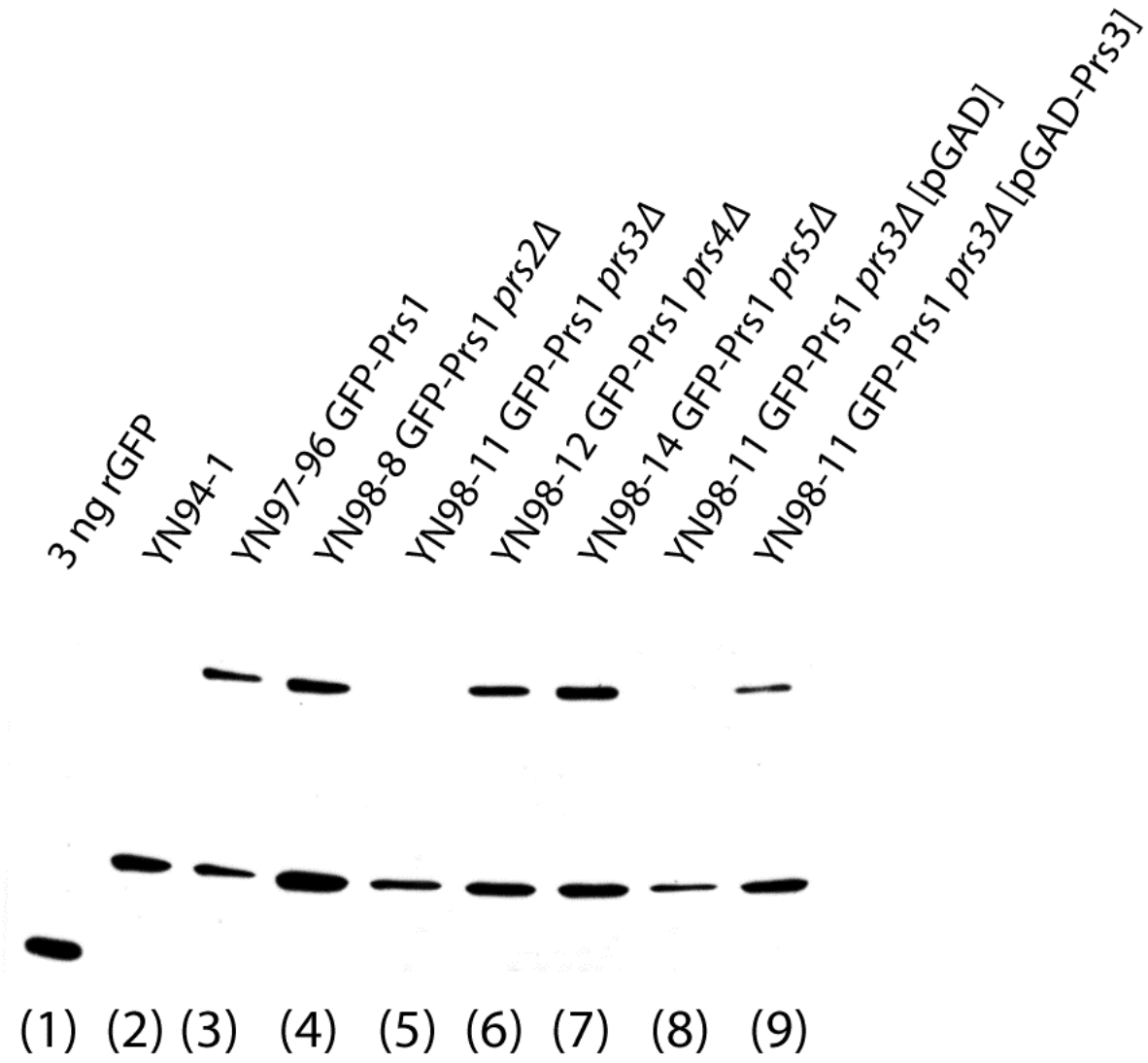

Figure 3.1: Monitoring the GFP signal in YN94-1 (WT), YN97-96 (*prs1*Δ::GFP-PRS1), YN98-8 (YN97-96 prs2Δ), YN98-11 (YN97-96 *prs3*Δ), YN98-12 (YN97-96 *prs4*Δ) and YN98-14 (YN97-96 *prs5*Δ).

Whole cell extracts were prepared as described (Materials & Methods, section 2.7). 25 µg total protein of each of the crude extracts was separated on a 10% SDS-PAGE gel. The separated proteins were transferred to a PVDF membrane, blocked with 5% non-fat milk and incubated sequentially with anti-GFP antibodies diluted 1:1000 (sc-73556, primary antibody) and a 1:50,000 dilution of anti-mouse IgG-HRP (sc-2060, secondary antibody). The membrane was treated with ECL detection solution (GE Healthcare) and exposed to X-ray film. 3 ng of commercially available recombinant GFP (rGFP) served as the positive control. The high MW signal corresponds to GFP-Prs1 and the lower MW signal in lanes (2-9) to an unknown protein which cross-reacts with anti-GFP antibodies and serves as a loading control. Western blots were performed on three biological replicates. A representative experiment is shown.

3.2 Growth of *PRS* deletant strains on 2% galactose at 30°C and 37°C

Previous studies on growth characteristics of the WT and various *prsΔ* strains using YEPD solid media at elevated temperature have shown an impaired growth at 37°C for *prs1Δ* and *prs3Δ* strains (Wang *et al*., 2004). Hypersensitivity to caffeine of *prs1Δ* and *prs3Δ* strains and their ability to release more alkaline phosphatase than the WT strain have also been reported (Schneiter *et al*., 2000). The temperature and caffeine sensitivities of these strains may be due to an alteration in cell signalling mechanisms. With a view to obtaining more information on the phenotypic characteristics of *PRS* deletants, their growth was examined and compared with the WT strain by spotting YN94-1 (WT), YN96-65 (*prs1Δ*), YN97-157 (*prs2Δ*), YN96-77 (*prs3Δ*), YN97-5 (*prs4Δ*) and YN96-68 (*prs5Δ*) on YEP+2% galactose plates, incubating them for a period of 3 days and documenting them on the second and third days. The reason for choosing galactose as the sole carbon source is that galactose-bound metabolites, e.g. UDP-galactose, are involved in cell wall synthesis (Klis *et al*., 2002, Timson, 2007). As shown in Figure 3.2 the strains which are *prs2Δ*, *prs4Δ* or *prs5Δ* have a similar growth pattern to that of the WT at 30°C and 37°C. However, strains lacking *PRS1* or *PRS3* display distinctively slower growth at 30°C when compared to the other strains and growth is almost abolished at 37°C. This result may be interpreted to mean that in the absence of the Prs1/Prs3 complex galactose metabolism is impaired and is further evidence for the importance of the Prs1/Prs3 complex in cell metabolism.

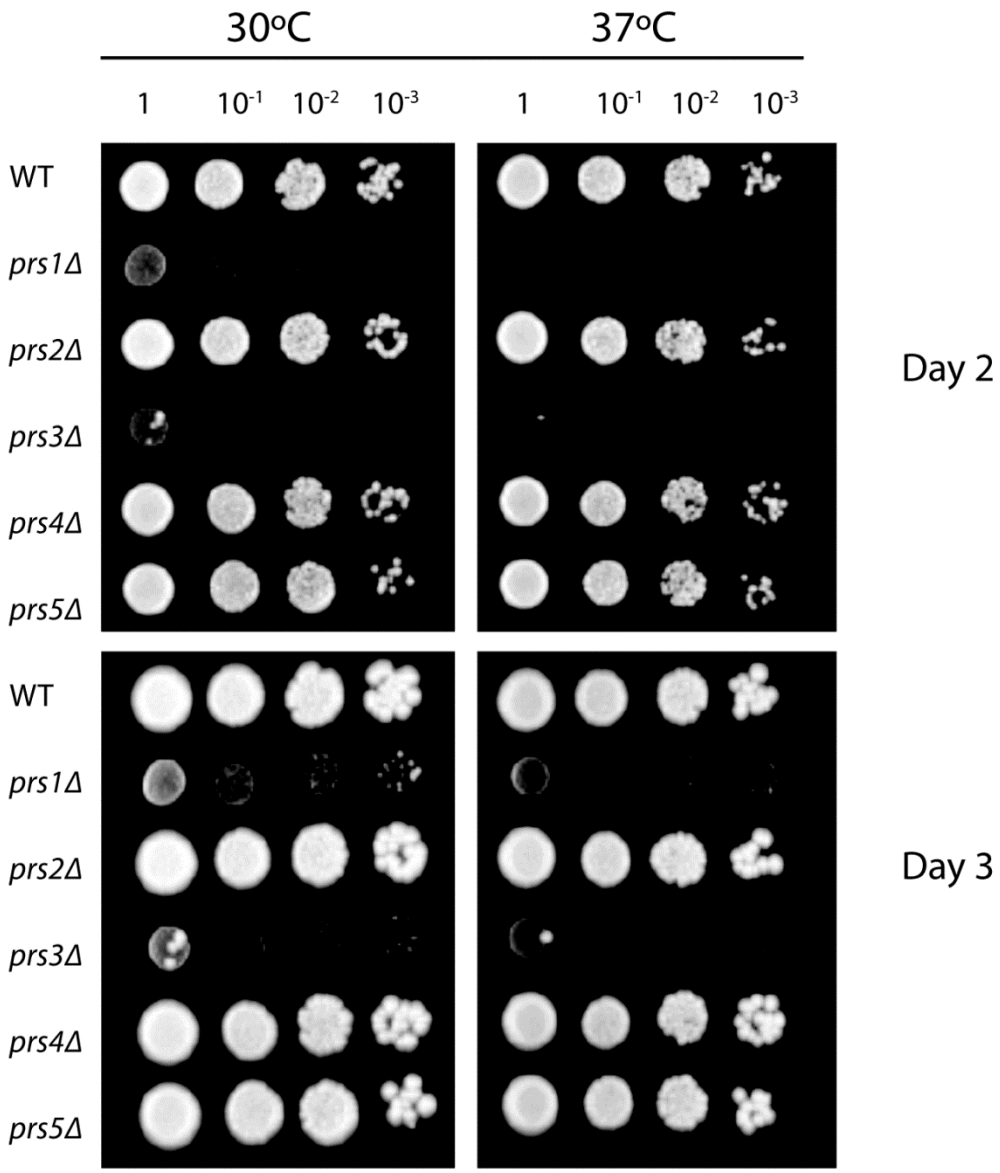

Figure 3.2: Growth pattern of *PRS* deletant strains on YEP+2% galactose.

The strains deleted for *PRS1* (YN96-65), *PRS2* (YN97-157*)*, *PRS3* (YN96-77*)*, *PRS4* (YN97-5) or *PRS5* (YN96-68) were grown in YEPD o/n. OD_{600} was determined and adjusted to OD_{600} = 0.5 for each culture. The cultures were serially diluted (10^{-1}, 10^{-2}, and 10^{-3} in sterile distilled H_2O. 3 µl aliquots of each of the dilutions were spotted onto YEP+2% galactose and incubated for 3 days and photographed after the second and third days.

3.3 The interaction of Prs1 with Slt2 as demonstrated by co-immunoprecipitation

Co-immunoprecipitation is one of the most powerful tools for detecting physical interactions between two or more proteins of interest by using target protein-specific antibodies which indirectly capture proteins of interest that are bound to the specific target protein. The basic approach to immuno-precipitating tagged proteins from whole-cell extracts is illustrated below (Phizicky and Fields, 1995, Dwane and Kiely, 2011).

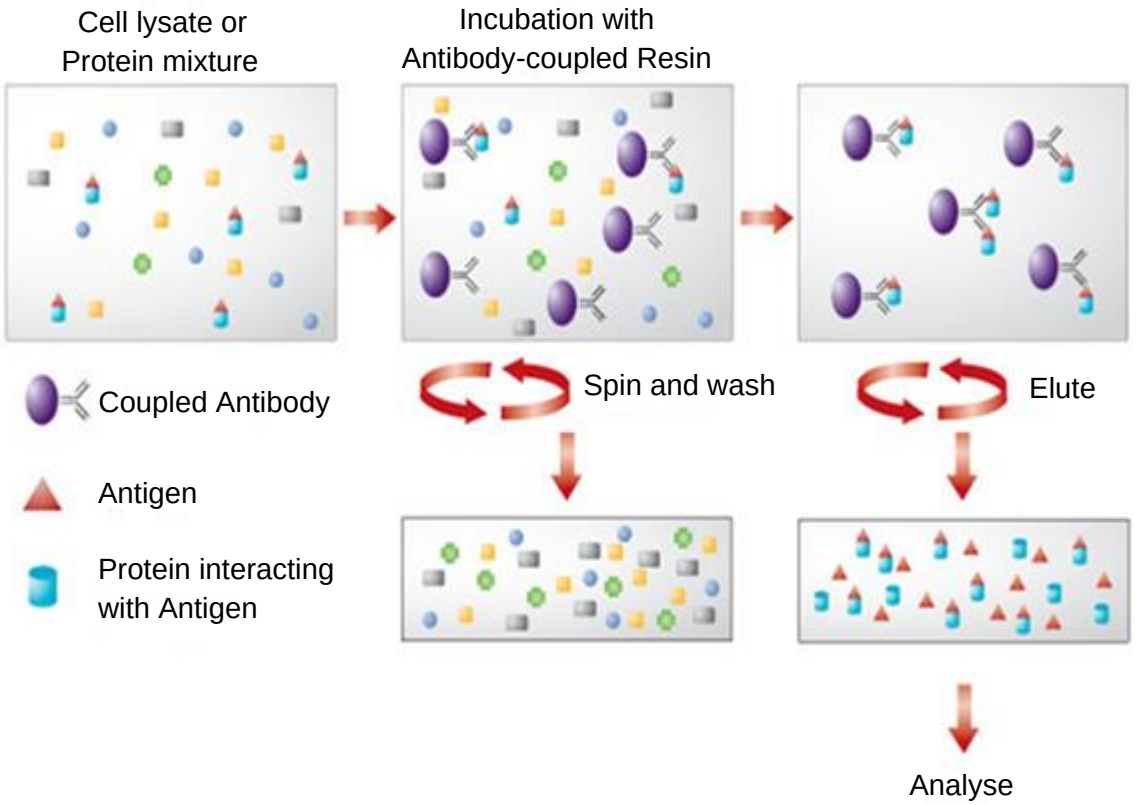

Figure 3.3: Principle of co-immunoprecipitation

The coupled antibody (purple/grey) is a purified murine IgG monoclonal antibody covalently attached to resin beads by hydrazide linkage. The coupled antibody allows the tagged protein (antigen, red triangle) and any other protein(s) interacting with it (blue cylinder) to be precipitated from a mixture of specific and unspecific proteins (grey, green and yellow). The precipitated complex is then pelleted by centrifugation and washed to remove proteins which are not bound to the coupled antibody. The protein(s) of interest that bind to the coupled antibody, i. e. proteins interacting with the antigen is/are eluted and subjected to SDS-PAGE followed by Western blotting (taken from www.piercenet.com).

3.3.1 Temperature-dependent interaction of Prs1 with Slt2

It was previously shown by Y2H analysis that Prs1 interacts with Slt2, suggesting that at least one Prs polypeptide can interact with the CWI pathway (Wang *et al*., 2004). It was also observed that deletion of NHR1-1 of *PRS1* completely abolished the Prs1/Slt2 interaction whereas it has been reported that removal of NHR1-1 has no effect on the interaction of Prs1 with other Prs polypeptides (Carter *et al*., 1997, Wang *et al*., 2004). To exclude the possibility that the interaction of Prs1 and Slt2 was not a false positive (Vidalain *et al*., 2004, Bruckner *et al*., 2009), a result which can occur in Y2H, co-immunoprecipitation was performed. Specifically, YN97-96 which contains an amino-terminally GFP-tagged version of Prs1 (Schneiter *et al*., 2000) integrated at the *PRS1* locus was transformed with FLAG-tagged WT Slt2 and two mutated versions thereof. The FLAG-tagged versions of Slt2 were kindly provided by Dr. D. E. Levin, Boston University. Plasmid p2313 expresses a FLAG-tagged WT version of Slt2 and p2316 is a FLAG-tagged version of Slt2 mutated at positions T190 and Y192 and expresses a non-activatable form of Slt2 which cannot be phosphorylated by Mkk1/Mkk2. Plasmid p2317 has a mutation in the ATP binding site at position K54 of Slt2 and expresses an enzymatically inactive form of FLAG-tagged Slt2 (Kim *et al*., 2008).

The FLAG-tagged versions of Slt2 were immuno-precipitated from crude extracts of the transformants YN97-96 [p2313], YN97-96 [p2316] and YN97-96 [p2317] grown at 30^{o}C or exposed to mild temperature stress (37^{o}C for 1 hr) as described in Materials and Methods, 2.11.1. The immuno-precipitated extracts were then subjected to incubation with anti-FLAG antibody to detect Slt2 or with GFP antibody to detect associated Prs1. As shown in Figure 3.4 for the crude extracts (CE), GFP-Prs1 and Slt2-FLAG signals are visible in lanes ((1-2), (7-8) and (13-14)). GFP-Prs1 co-precipitated with WT FLAG-tagged Slt2 (p2313) at 30^{o}C (lane (3)) and 37^{o}C (lane (4)) with an increased GFP-Prs1 signal under thermal stress conditions. However, the non-phosphorylatable version of Slt2 (p2316, slt2(T190A,Y192F)-FLAG) does not associate with Prs1 since there is no GFP signal in lanes (9-10). The kinase inactive version of Slt2 (p2317, slt2(K54R)-FLAG) interacts with Prs1 only under thermal stress resulting in a strong signal (lane (16)) whereas no signal is visible at 30^{o}C (lane (15)). No bands were detected when the extracts were incubated with protein A-affinity beads (no-antibody control, lanes ((5-6), (11-12) and (17-18)) and serve as the negative controls.

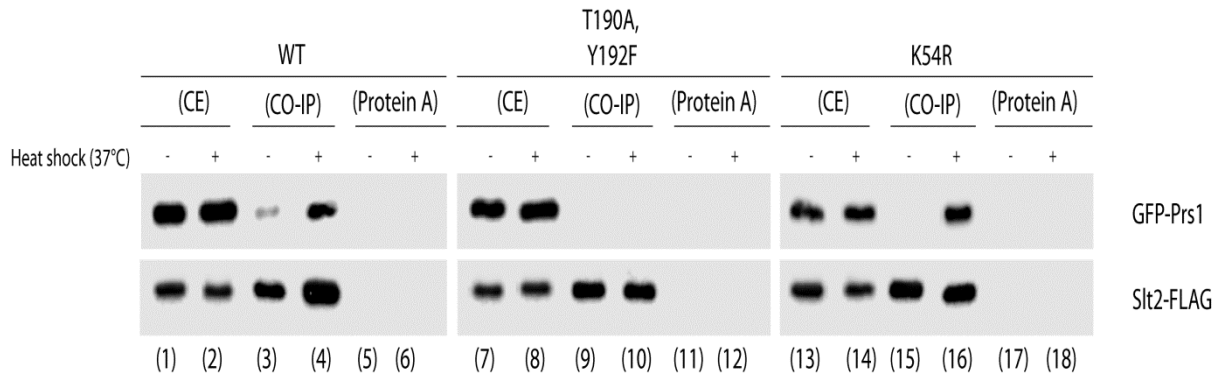

Figure 3.4: Interaction of Slt2 with Prs1

YN97-96 in which the endogenous *PRS1* was replaced by the GFP-tagged Prs1 construct was transformed either with a high copy plasmid p2313 expressing WT Slt2-FLAG (WT) or a non-phosphorylatable mutant, p2316 (slt2(T190A,Y192F)-FLAG (T190A Y192F) or the kinase inactive mutant, p2317 (slt2-K54R)-FLAG) (K54R). YN97-96 [p2313], YN97-96 [p2316] and YN97-96 [p2317] were grown in duplicate flasks to mid-log phase in SC-Leu at 30^{o}C and one flask per strain was subjected to heat shock at 37^{o}C for 1 hr. 10 µg of each crude extract (CE, lanes (1-2), lanes (7-8) and lanes (13-14) was prepared as described (Materials and Methods, section 2.7). For co-immunopreciptation 300 µg of each CE was treated as described in Materials and Methods, section 2.11.1 using FLAG (M2)-affinity beads or protein A-affinity beads (no-antibody control). The precipitates were washed with immunoprecipitation buffers and 10 µl of each sample was subjected to electrophoresis on 4-15% SDS-PAGE gel and analysed by immunoblotting with anti-GFP and anti-FLAG antibodies. The GFP-Prs1 signal was detectable in lanes (3)-(4) and (16) whereas the Slt2 signal was detected in lanes (3-4), (9-10) and (15-16) after the membrane was treated with ECL detection solution and visualized in the ChemiDoc XRS+ imager (ChemiDoc, version 4.1, Bio-Rad). No signals were detected in the protein A-treated extracts lanes ((5-6), (11-12) and (17-18)). Western blots were performed on three biological replicates and a representative blot is shown.

For further verification that Slt2 interacts with Prs1 as observed in Figure 3.4, the experiment was repeated with a different set of transformed strains. The plasmid, pBG1805, an in-frame construct of Prs1 with a C-terminal affinity tag consisting of 6xHis, HA, and 3C protease under the control of the *GAL1* promoter (Materials and Methods, Table 2.2) was co-transformed into YN96-65 (*prs1Δ*) with the high copy plasmid expressing WT Slt2-FLAG (p2313), the mutant (p2316, slt2(T190A,Y192F)-FLAG) or (p2317, slt2(K54R)-FLAG). The strains were grown to OD_{600} ≈1.2 in SC-Ura-Leu+2% raffinose and subsequently transferred into YEP+2% galactose for 6 hr at 30^{o}C to induce expression of Prs1 and subjected to heat shock at 37^{o}C for 1 hr (cf. Materials and Methods, section 2.11.2)**.** 300 µg CE from the non-heat treated or heat treated-cultures were used for co-immunoprecipitation. The CE and immuno-precipitated

extracts were subjected to SDS-PAGE and Western blotting (cf. Materials and Methods, sections 2.9.1 and 2.10).

In the crude extract Prs1 was not detectable in Figure 3.5, lanes (1), (4) and (7) for WT Slt2-FLAG (p2313), mutant (p2316, slt2(T190A,Y192F)-FLAG) and (p2317, slt2(K54R)-FLAG), respectively, as expected because they are un-induced cells and cannot express His-tagged Prs1 whereas a signal was observed when the cells were grown in galactose (lanes (2)-(3), (5)-(6) and (8)-(9)) which did not vary in intensity after heat shock (37^{o}C). No signal was observed in CE (lanes (5) and (6)) when the membrane was challenged with anti P-Slt2 antibodies and confirms the elimination of the two phosphorylation sites in the activation domain of Slt2 in this mutant. A P-Slt2 signal was visible in CE of the WT and K54R mutant (lanes (2-3) & (8-9)), respectively. Slt2-FLAG was detected in every strain (lanes (1-9)) independent of galactose induction or heat shock thus indicating correct expression of Slt2-FLAG. The signal obtained for actin was detectable in all lanes and served as the loading control.

The His-tagged Prs1 and P-Slt2 co-precipitated with either WT Slt2-FLAG (p2313) or (p2317, slt2(K54R)-FLAG), both of which showed an increased signal following galactose induction and heat shock (lanes (2)-(3) and (8)-(9)). However, as was the case for GFP-labelled Prs1 (Figure 3.4), there was no co-immunoprecipitation for Prs1 and Slt2 with the non-phosphorylatable version of Slt2 (p2316) (lanes (5-6)) following galactose induction and heat shock. Since Prs1 failed to interact with the non-phosphorylatable mutant of Slt2 (p2316), it is reasonable to postulate that Slt2 must be in the phosphorylated state in order to associate with Prs1. In agreement with this hypothesis Slt2 lacking kinase activity, (p2317, slt2(K54R)-FLAG), does interact with Prs1.

Both co-immunoprecipitation approaches gave comparable results, although the versions of Prs1 used were either N-terminally labelled and integrated (Figure 3.4) or C-terminally tagged, galactose-inducible and plasmid-borne (Figure 3.5) versions. In summary the results obtained with either approach are consistent with the Prs1/Slt2 interaction being dependent on the phosphorylation status of Slt2.

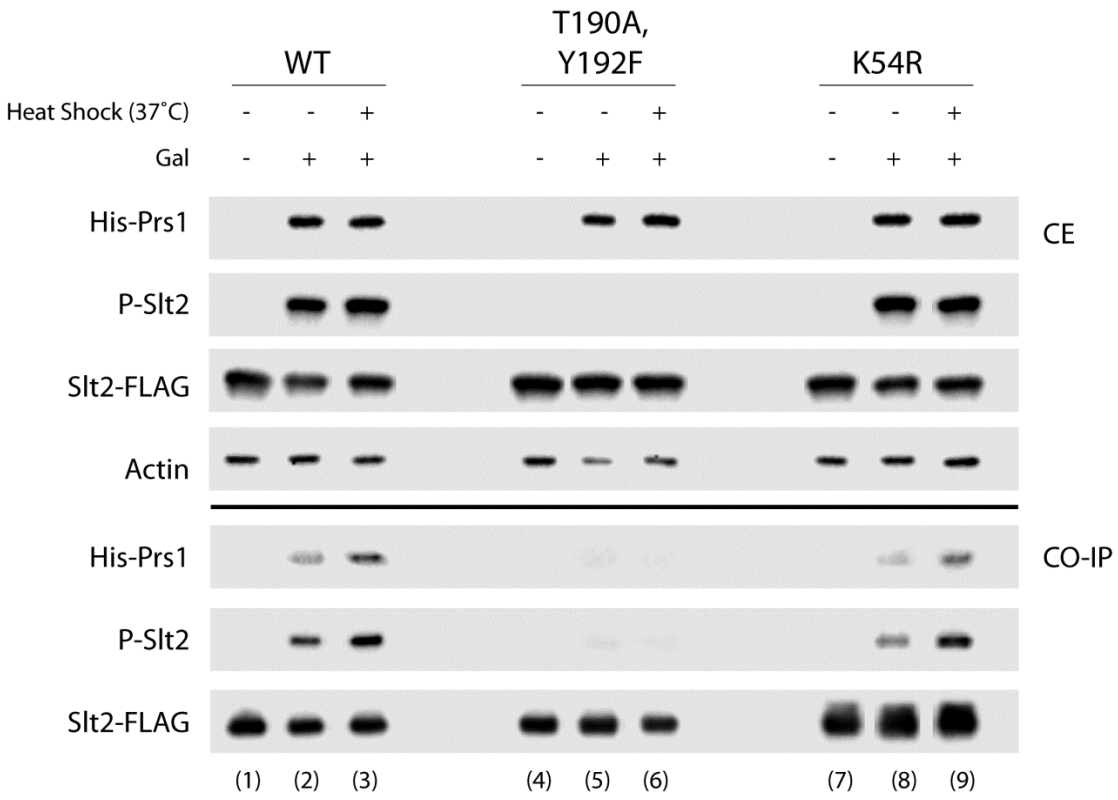

Figure 3.5: Phosphorylation status of Slt2 dictates its interaction with Prs1

YN96-65 (*prs1Δ*) [pBG1805-Prs1] was transformed either with a high copy plasmid expressing WT [Slt2-FLAG, (p2313)], [T190A, Y192F (slt2(T190A,Y192F)-FLAG), (p2316)] or [K54R (slt2(K54R)-FLAG), (p2317)]. The transformants were grown to an OD_{600} ≈1.2 in SC-Ura-Leu+2% raffinose and subsequently induced with YEP+2% galactose for 6 hr at 30^{o}C in duplicate flasks to permit expression of Prs1 and then one flask was subjected to heat shock at 37^{o}C for 1 hr. For co-immunoprecipitation 300 µg crude extract (CE) was treated as described in Materials and Methods, section 2.11.2 with FLAG (M2)-affinity beads to precipitate Slt2-FLAG. Western blotting with His-antibodies was used to detect Prs1, anti-FLAG antibodies detected Slt2 and the phosphorylation status of Slt2 (P-Slt2) was monitored by anti-phospho-pThr^{202}/Tyr^{204} antibodies (Materials and Methods, section 2.11.2). Western blots were performed on three biological replicates and representative membranes are shown.

3.4 Phenotypes of rescued YN97-14 (*prs1Δprs5Δ*) strains

In addition to interacting with Prs3, Prs1 also interacts with Prs5 (Hernando *et al*., 1999). Simultaneous deletion of *PRS1* and *PRS5* causes cell death (Hernando *et al*., 1998). The strain YN97-14 (*prs1Δprs5Δ*) is kept alive since it contains a plasmid-borne version of *PRS1* (pVT1) which has the *URA3* gene as the selective marker. In order to determine if any mutant versions of *PRS1* could restore viability of YN97-14 plasmid shuffling experiments (Sikorski and Boeke, 1991) were carried out with various mutated versions of *PRS1* (Ugbogu *et al*., 2013). To this end, each of the

following plasmids (pGBT9, pGBT9-Prs1, pGBT9-prs1(L115T), pGBT9-prs1(H130A), pGBT9-prs1(Q133P), pGBT9-prs1(D326A), pGBT9-prs1(H130A/D326A), pGBT9-prs1(deltaNHR1-1), pGBT9-prs1(ΔC600), pGBT9-prs1 (Δ*Eco* RI/*Bam* HI) and pGBT9-prs1(Δ*Bam* HI/*Pst* I) (cf. Figure 2 in Ugbogu *et al*. (2013)) was transformed individually into YN97-14 by selecting for tryptophan prototrophy since the mutated versions of *PRS1* are contained in plasmids having *TRP1* as the selectable marker. Plasmid shuffling experiments exploit the fact that in the presence of 5-fluoroorotic acid (5-FOA) a strain can only survive if it is an uracil auxotroph (Boeke *et al*., 1984). The Trp^+-transformants were grown in the presence of 5-FOA to determine which of the plasmid-borne mutated versions of *PRS1* could rescue the synthetic lethality caused by the simultaneous deletion of *PRS1* and *PRS5* (Ugbogu *et al*., 2013). Only five of the plasmids tested maintained the viability of the double deletant strain, *viz* pGBT9-Prs1, pGBT9-prs1(L115T), pGBT9-prs1(Q133P), pGBT9-prs1(D326A) and pGBT9-prs1(H130A/D326A) and they are illustrated in Figure 3.6.

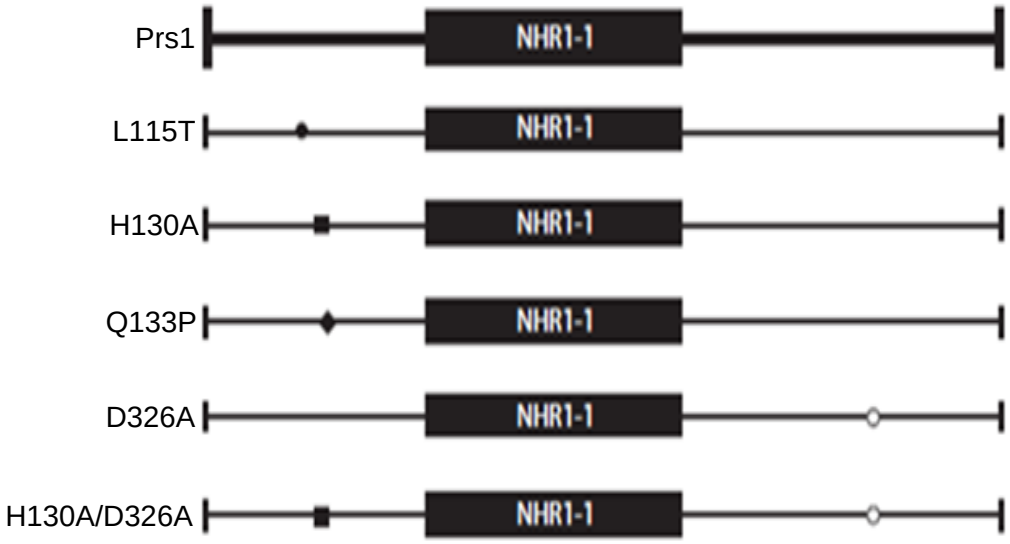

Figure 3.6: A schematic representation of *in vitro* mutated versions of *PRS1* capable of rescuing synthetic lethality

The closed and open symbols indicate the positions of the *in vitro*-generated point mutations in *PRS1*. NHR1-1, non-homologous region of Prs1 (taken from (Ugbogu *et al*., 2013)).

3.4.1 Temperature sensitivity of YN97-14 rescued strains

Yeast cells have no internal temperature regulator, therefore the higher the temperature the more damage to the yeast cell, thereby causing rapid decline of cell viability (Walker, 1998). Response to mild heat-shock (37-39°C) involves activation of specific heat shock proteins that enable the cells to adapt and survive (Ye *et al*., 2009, Rikhvanov *et al*., 2014). Heat shock affects many cellular processes: these include transient cell division arrest, build-up of misfolded proteins, uncoupling of oxidative phosphorylation, damage and defects of cell wall biosynthesis (Richter *et al*., 2010), thus reducing significantly the rate of protein synthesis by focusing on the synthesis of heat shock proteins for the repair or remodelling of the cells and also for cell survival (Jarolim *et al*., 2013).

The response of YN97-14 [(prs1-L115T)], YN97-14 [(prs1-Q133P)], YN97-14 [(prs1-D326A)] and YN97-14 [(prs1-H130A/D326A)] to mild heat-shock was examined by spotting the cultures on solid media and incubating the plates at 30^{o}C and 37^{o}C. Single colonies from each of the above-named strains containing the Rlm1 expression plasmid were inoculated individually into SC-Ura-Trp and grown o/n at 30^{o}C with shaking. Serial dilutions of the o/n cultures were spotted onto appropriate media (Materials and Methods, section 2.5.1). The plates were incubated for 3 days at 30^{o}C and 37^{o}C. Figure 3.7 shows that in all the strains no growth was observed at 37^{o}C. Interestingly, the growth impairment of the strains at 37^{o}C was corrected if 1 M sorbitol was included in the media. However, it was observed that YN97-14 [(prs1-Q133P)] grew less well than the other strains at either temperature, implying that the Q133P mutation may affect Prs1 more severely than the other mutants.

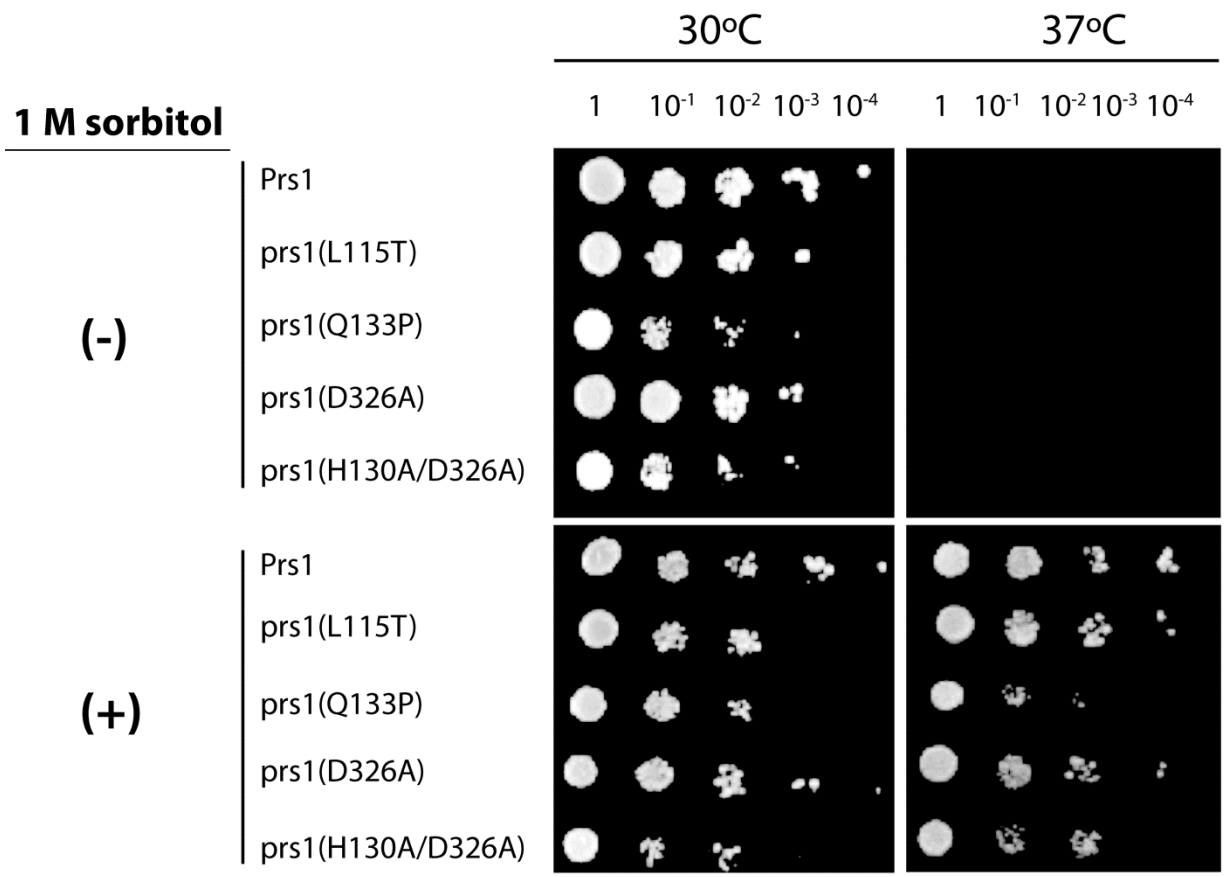

Figure 3.7: Temperature sensitivity of YN97-14 rescued strains

The rescued strains YN97-14 [(prs1-L115T)], YN97-14 [(prs1-Q133P)], YN97-14 [(prs1-D326A)] and YN97-14 [(prs1-H130A/D326A)] were grown o/n at 30°C with shaking. OD_{600} was determined and adjusted to 0.5 for each culture. The cultures were serially diluted in sterile distilled H_2O. 3 µl of the individual dilutions were then spotted onto appropriate selective media (SC-Ura-Trp plates) with and without I M sorbitol. The plates were incubated for 3 days at 30°C and 37°C.

3.4.2 Caffeine sensitivity of YN97-14 rescued strains

S. cerevisiae must have a functional PKC1 to cope with cell wall stresses caused by environmental changes and toxic substances to guarantee CWI essential for cell viability and survival (Levin, 2005, Fuchs and Mylonakis, 2009, Soriano-Carot *et al*., 2012). To gain further insight into possible links between Prs polypeptides and the CWI pathway, the ability of the rescued strains to grow in the presence of caffeine was tested. Sensitivity to the purine analogue, caffeine, (Hampsey, 1997) is a diagnostic phenotype of yeast strains with a compromised CWI pathway (Martín *et al*., 2000, Levin, 2011). Compromised CWI has been observed in strains deleted for one of or more of the five *PRS* genes, in particular, those lacking Prs1/Prs3, one of

the minimal functional complexes, required for cell viability (Schneiter *et al*., 2000, Wang *et al*., 2004).

The effect of caffeine on the growth of YN97-14 rescued by WT Prs1 or one of the *in vitro*-generated Prs1 point mutations L115T, Q133P, D326A or the double mutation, H130A/D326A was tested. After spotting, the plates were incubated for 3 days at 30^{o}C. As shown in Figure 3.8 each of the rescued strains was sensitive to caffeine. YN97-14 [prs1(L115T)], YN97-14 [prs1(D326A)] and YN97-14 [prs1(H130A/D326A)] showed a similar growth pattern on 2 mM and 3 mM caffeine as YN97-14 [Prs1]. However, YN97-14 [prs1(Q133P)] was more sensitive being unable to grow even at the lowest dilution on 3 mM caffeine. As can be seen the inclusion of 1 M sorbitol in the media corrected the caffeine sensitivity to the extent that YN97-14 [prs1(Q133P)] could grow on 3 mM caffeine. However, the caffeine sensitivity of the strain containing the H130A/D326A mutation was more pronounced than in the other strains. Exposure of the strains to caffeine and elevated temperature simultaneously in the presence of sorbitol prevented growth of YN97-14 [prs1(Q133P)] and permitted growth of the other strains only with the undiluted o/n culture. The correction of the caffeine sensitivity by 1 M sorbitol is similar to the correction of temperature sensitivity illustrated in Figure 3.7.

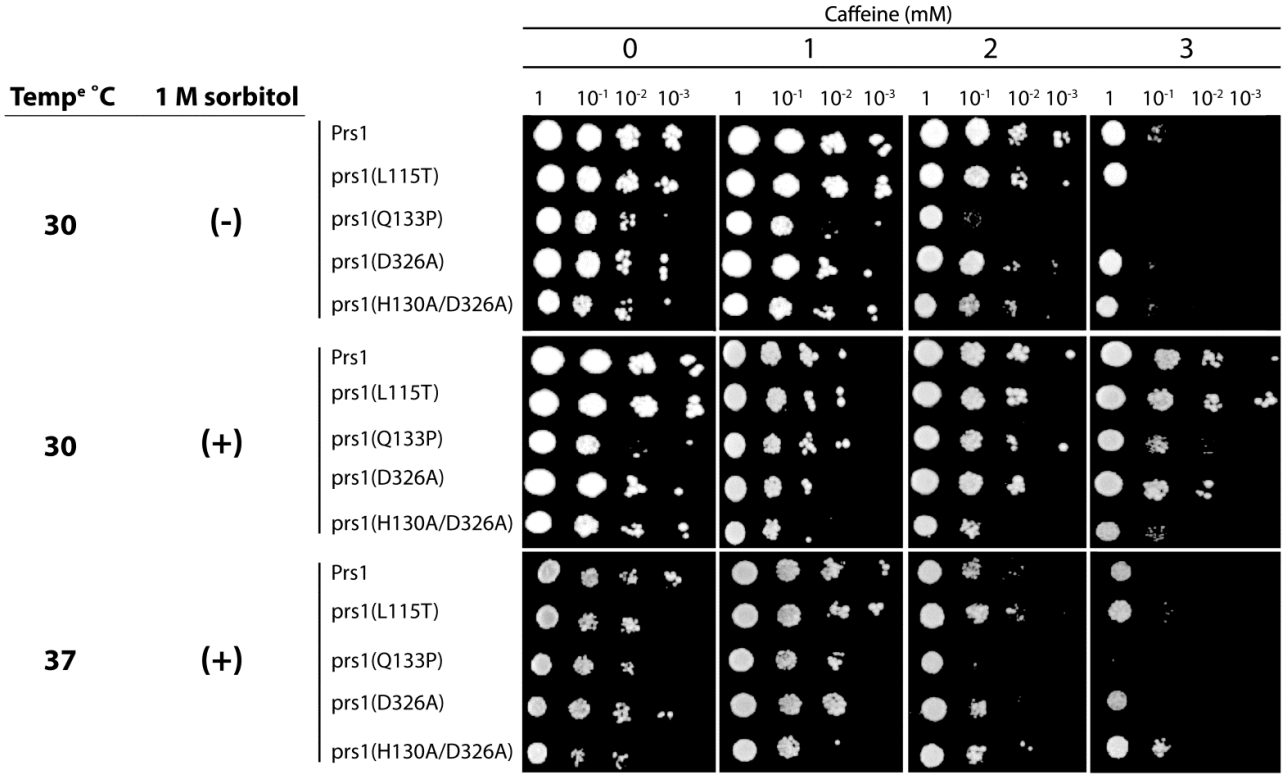

Figure 3.8: Effect of sorbitol on caffeine sensitivity of the rescued YN97-14 strains

YN97-14 [Prs1], YN97-14 [prs1(L115T)], YN97-14 [prs1(Q133P)], YN97-14 [(prs1(D326A)] and YN97-14 [prs1(H130A/D326A)], each containing the Rlm1 reporter plasmid [pHPS100-Ura] were grown o/n at 30^{o}C with shaking. The OD_{600} of the o/n cultures were measured and subsequently adjusted to 0.5 followed by 10-fold serial dilutions (10^{-1}-10^{-3}). 3 µl of the individual dilutions were then spotted onto SC-Ura-Trp with and without caffeine or caffeine in the presence of I M sorbitol and incubated at 30°C or 37°C for three days.

3.4.3 β-galactosidase activity as a measure of Rlm1 expression in viable transformants of YN97-14 (*prs1*Δ*prs5*Δ)

Since it has been hypothesized that impaired CWI signalling contributes to the synthetic lethality of the *prs1*Δ *prs5*Δ strain (Ugbogu *et al*., 2013), it was decided to examine the phosphorylation status of Slt2 in these rescued strains. This was done indirectly since expression from the Rlm1 reporter plasmids occurs only when Slt2 is phosphorylated. Although, as shown in Figure 3.7, the rescued strains are unable to grow at 37^{o}C on solid media, it was decided to see how the strains behaved at 37^{o}C in liquid media. Rlm1 expression was measured by means of β-galactosidase activity after incubation at 30^{o}C and 37^{o}C. The transformed strains were grown o/n and diluted into 2x50 ml of the same media to an OD_{600}≈ 0.3. One flask was incubated at 30^{o}C and the other at 37^{o}C until mid-log phase (OD_{660} ≈ 1.0) was achieved. Not unexpectedly the cultures incubated at 37^{o}C grew slowly but did reach OD_{660} = 1.0 after 8 hr. Nevertheless β-galactosidase activity was measured in cultures from both temperatures. The data obtained for the 30^{o}C cultures showed variation in Rlm1 expression. When WT Prs1 is the rescuing plasmid the value is lower than that for YN96-68 (*prs5*Δ) (see inset of Figure 3.9), although both are lacking *PRS5*. For the remaining rescuing plasmids only Q133P has reduced Rlm1 expression at 30^{o}C with respect to the other strains tested. The Rlm1 expression measured at 37^{o}C should be treated with caution since, as shown above, they are incapable of growing at 37^{o}C in the absence of an osmotic stabilizer (Figure 3.7) and the time taken to reach OD_{600} 1.0 was 8 hr.

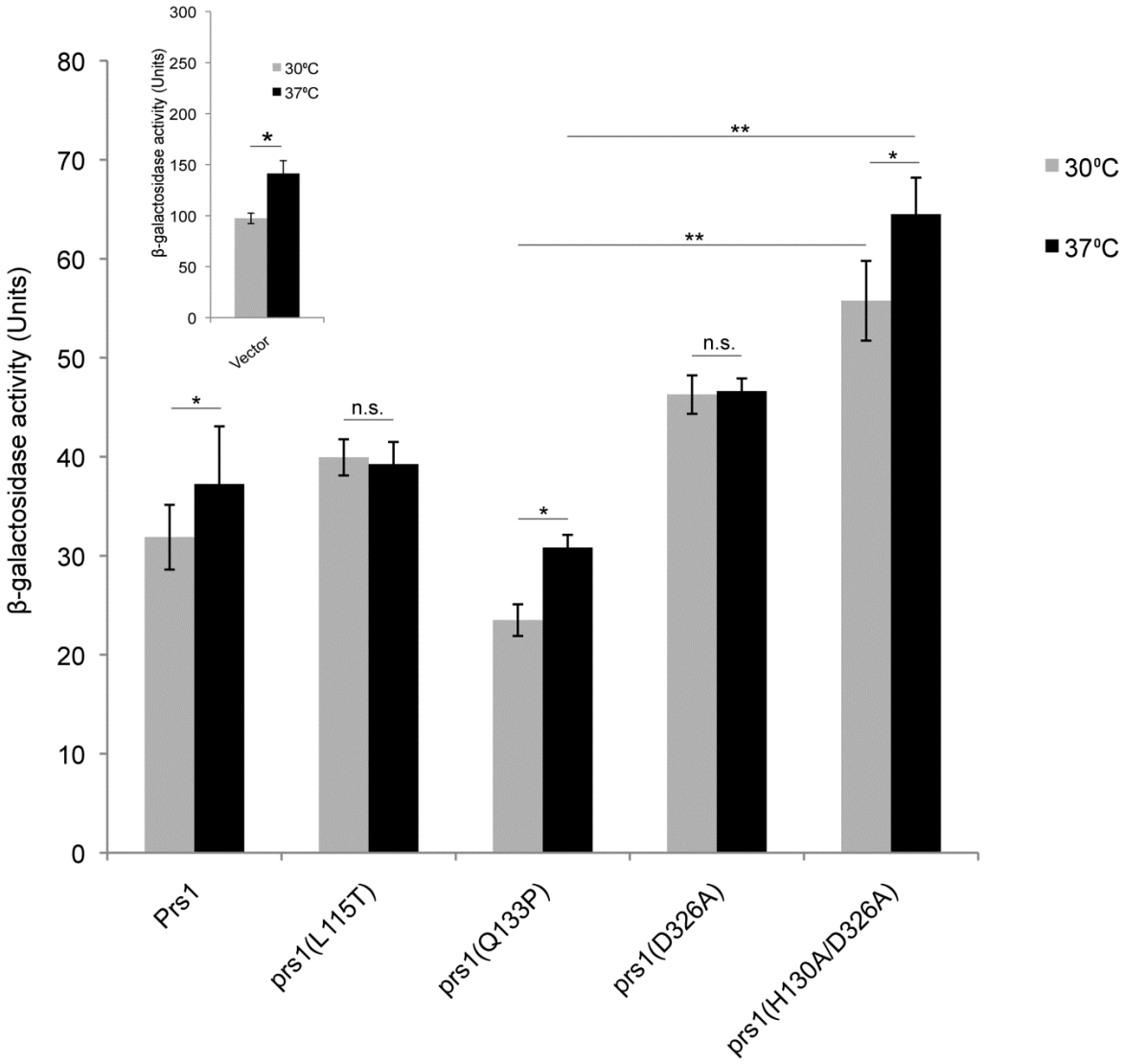

Figure 3.9: Rlm1 expression at 30°C and 37°C as measured by β-galactosidase activity in the *prs1*Δ*prs5*Δ rescued strains

Rlm1 activation was measured in YN97-14 (*prs1*Δ*prs5*Δ*)* strains containing the Rlm1 reporter and a pGBT9-based plasmid carrying the WT or mutated versions of *PRS1* which rescued synthetic lethality (Ugbogu *et al*., 2013). The histogram was obtained by duplicate or triplicate measurements of Rlm1 expression in three independent transformants for each combination. The data is represented as the mean ± s.d., **p*<0.05, ***p*<0.01 (TukeyHSD test), n.s., not statistically significant. The raw data are shown in the Appendix, Table 5.1. The inset is taken from Figure 3.12 and shows temperature-dependent Rlm1 expression in YN96-68 (*prs5*Δ) [pGAD].

3.4.4 Phosphorylation status of Slt2 in rescued *prs1Δprs5Δ* deletant strains

Previous work on Prs has shown that deletion of NHR1-1 abolished the temperature-induced Rlm1 expression of Prs1 (Ugbogu *et al*., 2013). It has been found that the NHR1-1 region of *PRS1* gene is vital for the Prs1 polypeptide to interact with Slt2 (Wang *et al*., 2004, Vavassori *et al*., 2005a, Vavassori *et al*., 2005b), suggesting that the observed *prs1Δ prs5Δ* synthetic lethality may be associated with perturbation of the CWI pathway (Ugbogu *et al*., 2013). Therefore, it was decided to check the phosphorylation status of Slt2 in the rescued *prs1Δprs5Δ* deletant strains by Western blotting. The Western blot was performed using the same cultures which had been used for measuring Rlm1 expression (Figure 3.9). The intensity of the P-Slt2 signal in each instance is stronger at 37^{o}C than at 30^{o}C and with the exception of Q133P the P-Slt2 signal of the mutants is weaker than that obtained with the strain rescued by WT Prs1 (Figure 3.10). The strength of the P-Slt2 signals relative to the corresponding Slt2 signal is illustrated in Figure 3.11 and they reflect the modest increase in Rlm1 expression following incubation at 37^{o}C.

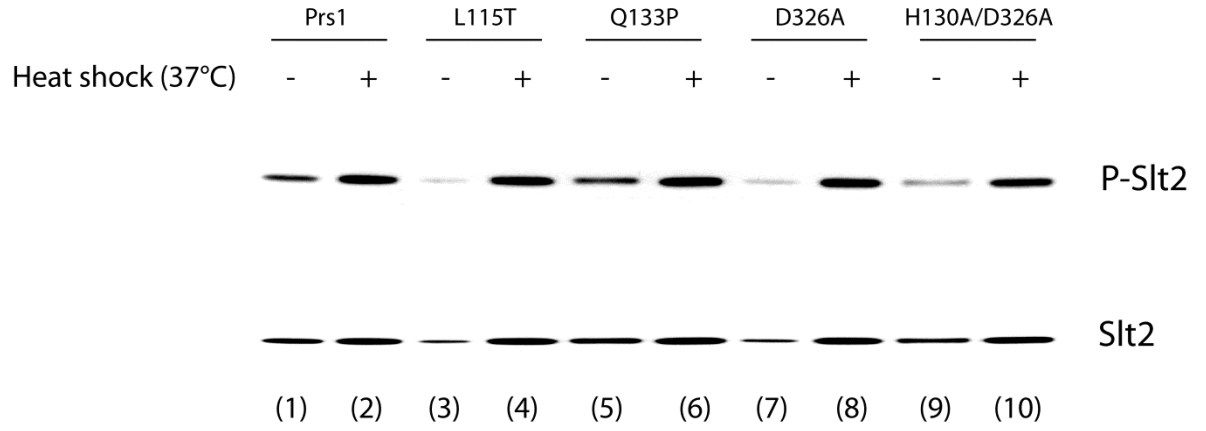

Figure 3.10: Phosphorylation status of Slt2 in rescued YN97-14 (*prs1*∆*prs5*∆) strains

For each strain crude extract equivalent to 15 µg protein per lane was separated on a 4-20% SDS-PAGE gel, transferred to a PVDF membrane and incubated against P-Slt2 (anti-phospho-pThr^{202}/Tyr^{204}) as the primary antibody (sc-16982-R, 1:5000 dilution) for 1 hr followed by incubation with goat anti-rabbit IgG-HRP (sc-2004, 1:5000 dilution). The membrane was stripped and re-probed to detect Slt2 with the primary antibody against Slt2 for 1 hr (sc-20168, 1:1000 dilution) followed by incubation with goat anti-rabbit IgG-HRP (sc-2004, 1:5000 dilution). The relative Slt2 activation was quantified by dividing the density of P-Slt2 band by the density of the corresponding Slt2 band. Western blots were performed on three biological replicates.

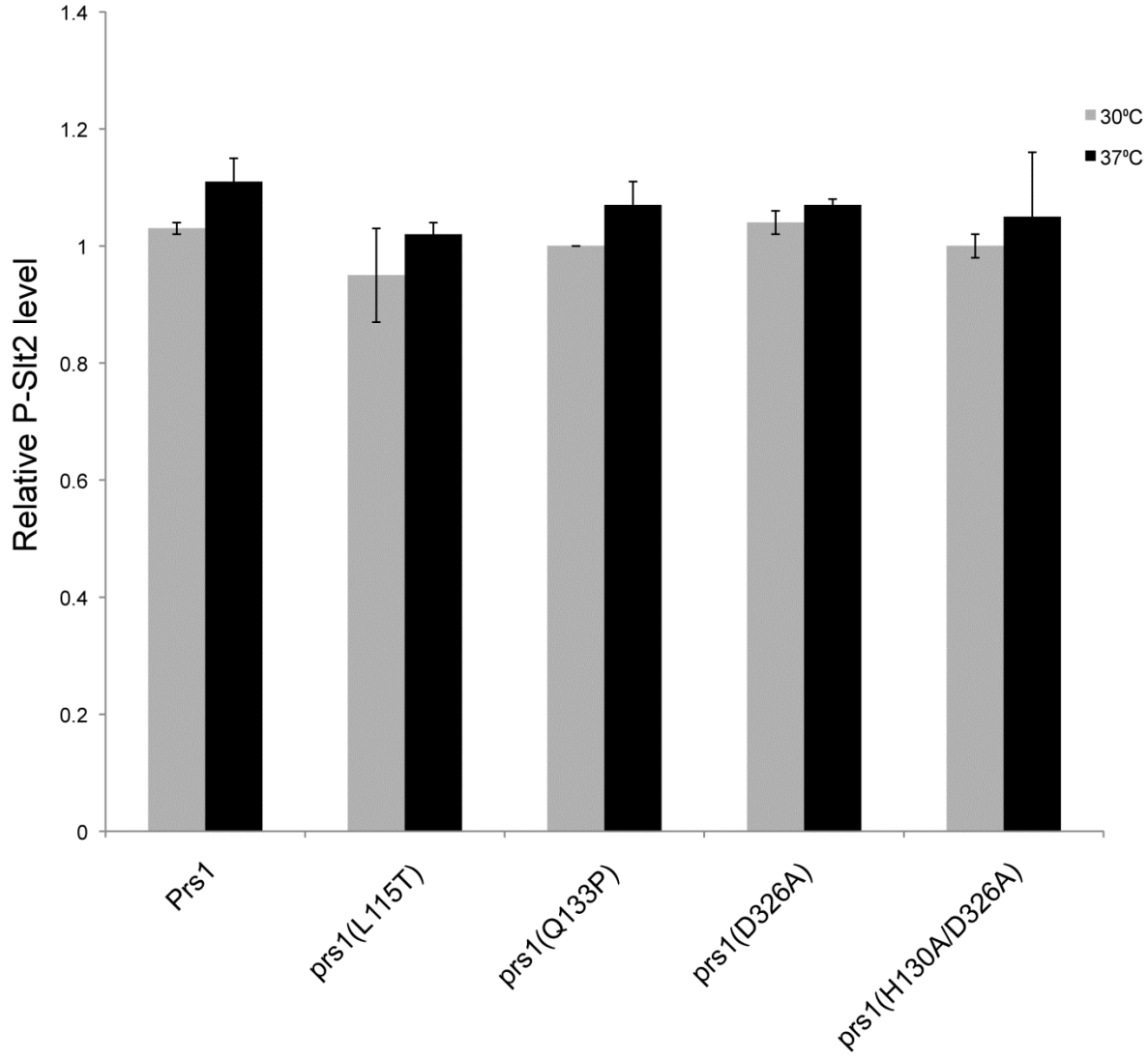

Figure 3.11: Quantification of P-Slt2 status in YN97-14 (*prs1Δprs5Δ*) rescued strains

The detected chemiluminesence signal from the Western blot in Figure 3.10 was quantified using ChemiDoc XRS+ imager (cf. Materials and Methods, section 2.12). The relative P-Slt2 level for each rescued strain was obtained by dividing the density of P-Slt2 signal by the density of the corresponding Slt2 signal. Each value represents the mean ± SEM for three biological replicates. The raw data are shown in Appendix, Table 5.2.

3.5 Mutation of postulated phosphorylation sites of Prs5 influences temperature-induced Rlm1 expression

Prs5 with a MW of 54 KDa, is the largest polypeptide encoded by any of the five *PRS* genes in *S. cerevisiae* (Carter *et al*., 1997, Hernando *et al*., 1999, Schneiter *et al*., 2000). The reason for this is that it contains two NHRs: NHR5-1 and NHR5-2. NHR5-1 consists of 70 aa and is located directly in front of the divalent cation-binding site whereas NHR5-2 consists of 116 aa and is located at a similar position to NHR1-1 of Prs1 (Hernando *et al*., 1998, Vavassori *et al*., 2005a). By phosphoproteome analysis it was shown that Prs5 is one of the 11 triply phosphorylated proteins in yeast (Ficarro *et al*. (2002)). The three aa residues of Prs5 found to be phosphorylated are to be found at the positions S_{364}, S_{367} and S_{369} and are located in the NHR5-2. The aa residues S_{364}, S_{367} and S_{369} were converted to non-phosphorylatable residues. In addition, other potential phosphorylation sites in close proximity to those postulated were also mutated (personal communication, Dr. Lilian Schweizer). All mutations were confirmed by sequencing and are documented in Table 3.1.

Table 3.1: Mutations of the triply phosphorylated aa residues of the Prs5 polypeptide

The three postulated phosphorylated sites, S_{364}, S_{367} and S_{369} and flanking theoretically phosphorylatable residues between aa 355 and 375, of the WT Prs5 Ficarro *et al*. (2002) were mutated by *in vitro* mutagenesis. Specifically, the hydrophilic serine residues at $S_{364,}$ S_{367} and S_{369} of the WT Prs5 were replaced by alanine (A) residues to generate prs5(479). Prs5(362.2) and prs5(365.1) were created by introducing additional mutations to prs5(479) at the positions indicated by the red lettering. The deleted region in prs5(365.5) (indicated by dashes) arose fortuitously during *in vitro* mutagenesis and the resulting frame-shift created a truncated Prs5 polypeptide. Single mutations for the postulated phosphorylation sites – S_{364}, S_{367} and S_{369} – were also created.

Prs5 WT	$_{355}$A	A	L	E	M	K	K	T_{362}	T_{363}	Sp_{364}	T_{365}	S	Sp_{367}	T	Sp_{369}	S	Q	S	S	N	S_{375}
prs5(479)	A	A	L	E	M	K	K	T_{362}	T_{363}	S_{364}A	T_{365}	S	S_{367}A	T	S_{369}A	S	Q	S	S	N	S_{375}
prs5(S364A)	A	A	L	E	M	K	K	T_{362}	T_{363}	S_{364}A	T_{365}	S	S_{367}	T	S_{369}	S	Q	S	S	N	S_{375}
prs5(S367A)	A	A	L	E	M	K	K	T_{362}	T_{363}	S_{364}	T_{365}	S	S_{367}A	T	S_{369}	S	Q	S	S	N	S_{375}
prs5(S369A)	A	A	L	E	M	K	K	T_{362}	T_{363}	S_{364}	T_{365}	S	S_{367}	T	S_{369}A	S	Q	S	S	N	S_{375}
prs5(362.2)	A	A	L	E	M	K	K	T_{362}A	T_{363}A	S_{364}A	T_{365}A	S	S_{367}A	T	S_{369}A	S	Q	S	S	N	S_{375}
prs5(365.1)	A	A	L	E	M	K	K	T_{362}	T_{363}	S_{364}A	T_{365}A	S_{366}A	S_{367}A	T_{368}A	S_{369}A	S	Q	S	S	N	S_{375}
prs5(365.5)	A	A	L	E	M	K	K	T_{362}	T_{363}	-	-	-	-	-	R	R	N	L	L	I	R

In order to determine what, if any, influence the mutations have on CWI, WT *PRS5* or the plasmid-borne mutated versions thereof listed in Table 3.1 were transformed, individually into YN96-68 (***prs5***Δ [pHPS100-Ura]) and Rlm1 expression was measured at 30^{o}C and 37^{o}C. The transformants were streaked out onto appropriate media and incubated at 30^{o}C for three days until well-defined colonies had developed. A single colony from each transformed strain was inoculated into 10 ml SC-Leu-Ura media, incubated o/n with shaking at 30^{o}C and processed for the measurement of Rlm1 expression as described in Materials and Methods, section 2.13. When an intact *PRS5* gene is present β-galactosidase activity increases approximately 2.5-fold following incubation at 37^{o}C (Figure 3.12). In the absence of *PRS5* Rlm1 expression at 30^{o}C is virtually identical to that of the WT but the increase in expression at 37^{o}C is less than 1.5-fold (vector). Of the four *in vitro*-mutated strains only prs5(365.1) showed a reduced Rlm1 expression at 30^{o}C which is capable of increasing 1.4-fold following incubation at 37^{o}C. Of the three remaining mutations the truncated version of Prs5, prs5(365.5), has an elevated Rlm1 expression at 30^{o}C which increases approximately 1.4-fold. Both prs5(479) and prs5(362.2) have elevated expression at 30^{o}C which in the latter increases only minimally following incubation at 37^{o}C. In summary the altered Rlm1 expression in the Prs5 mutants tested would suggest that interfering with Prs5 alters signalling through the CWI pathway.

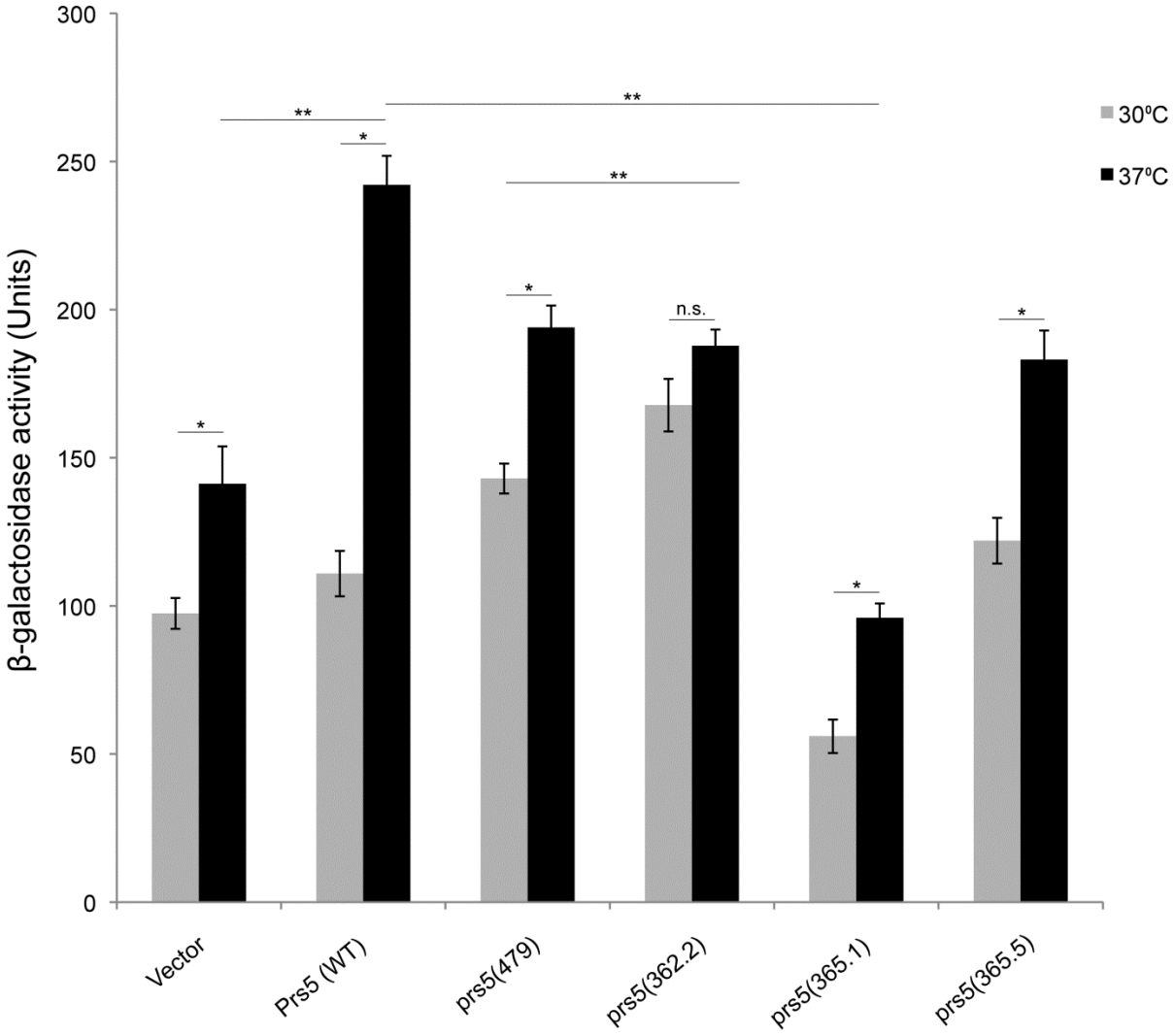

Figure 3.12: Influence of mutating the postulated phosphorylation sites in Prs5 on Rlm1 expression at 30°C and 37°C

In this experiment YN96-68 (*prs5*Δ) transformants containing the Rlm1 reporter plasmid (pHPS100-Ura) and individual plasmid-borne mutated versions of Prs5 (cf. Table 3.1) were used to evaluate Rlm1 expression following incubation at 30°C and 37°C. All strains were grown on SC-Leu-Ura media o/n at 30°C before incubation at 30°C or 37°C in 50 ml of the same culture media until an $OD_{660} \approx 1.0$ was obtained. Each value represents the mean ± s.d. for nine measurements for each of three independent transformants, **p*<0.05, ***p*<0.01 (TukeyHSD test), n.s., not statistically significant. The raw data are shown in Appendix, Table 5.3.

3.5.1 Influence of *in vitro* generated *PRS5* mutations on the phosphorylation status of Slt2

In addition to being assayed for Rlm1 expression (cf. Figure 3.12), the cultures grown at 30^{o}C and 37^{o}C were used to prepare crude extracts which were subjected to Western blotting (Material and Methods, section 2.10) to determine the phosphorylation status of Slt2. AS can be seen in Figure 3.13 in the WT *PRS5* strain, the signal obtained at 30^{o}C for P-Slt2 increased in intensity after incubation at 37^{o}C. All other transformants, with the exception of prs5(362.2), showed a temperature-dependent increase in the phosphorylation status of Slt2. The mutant prs5(362.2) was apparently phosphorylated to the same degree at 30^{o}C and 37^{o}C and correlates with the non-significant increase in Rlm1 expression at 37^{o}C (Figure 3.12). Signal strength was quantified and the data are presented in the Figure 3.14. The β-galactosidase activity as a measure of Rlm1 expression in the *in vitro* mutated versions of Prs5 correlates with the signal quantification of P-Slt2 relative to the anti-Slt2 signal with the exception of prs5(479) which had elevated Rlm1 expression at 30^{o}C. Furthermore, prs5(365.1) has reduced Rlm1 expression at both 30^{o}C and 37^{o}C which correlates with the reduced P-Slt2 signal.

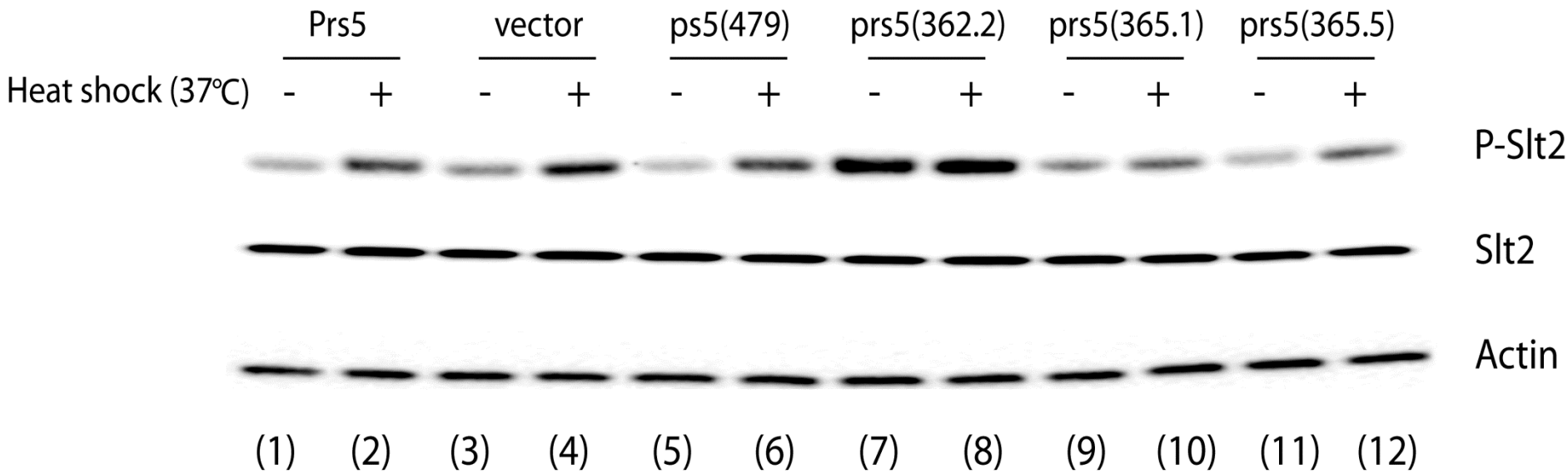

Figure 3.13: Elevated incubation temperature influences the phosphorylation status of Slt2 in *PRS5* mutants

For each strain crude extract equivalent to 15 µg protein per lane was separated on a 4-20% SDS-PAGE gel and transferred to a PVDF membrane. The membrane was cut horizontally into two sections: the upper section was probed with antibodies against P-Slt2 (anti-phospho-pThr^{202}/Tyr^{204}) as primary antibody (sc-16982-R, 1:1000 dilution) and anti-goat-rabbit secondary antibody (sc-2004, 1:5000 dilution). Slt2 was detected by stripping and re-probing the same membrane with anti-Slt2 primary antibody (sc-20168, 1:1000 dilution) and secondary antibody IgG-HRP (sc-2004, 1:5000 dilution). The lower section of the membrane was probed for actin (loading control) using anti-actin goat primary polyclonal IgG (sc-1615, 1:1000 dilution) and donkey anti-goat secondary IgG-HRP (sc-2020, 1:10000 dilution). The signals were detected by chemiluminescence. Western blots were performed on three biological replicates.

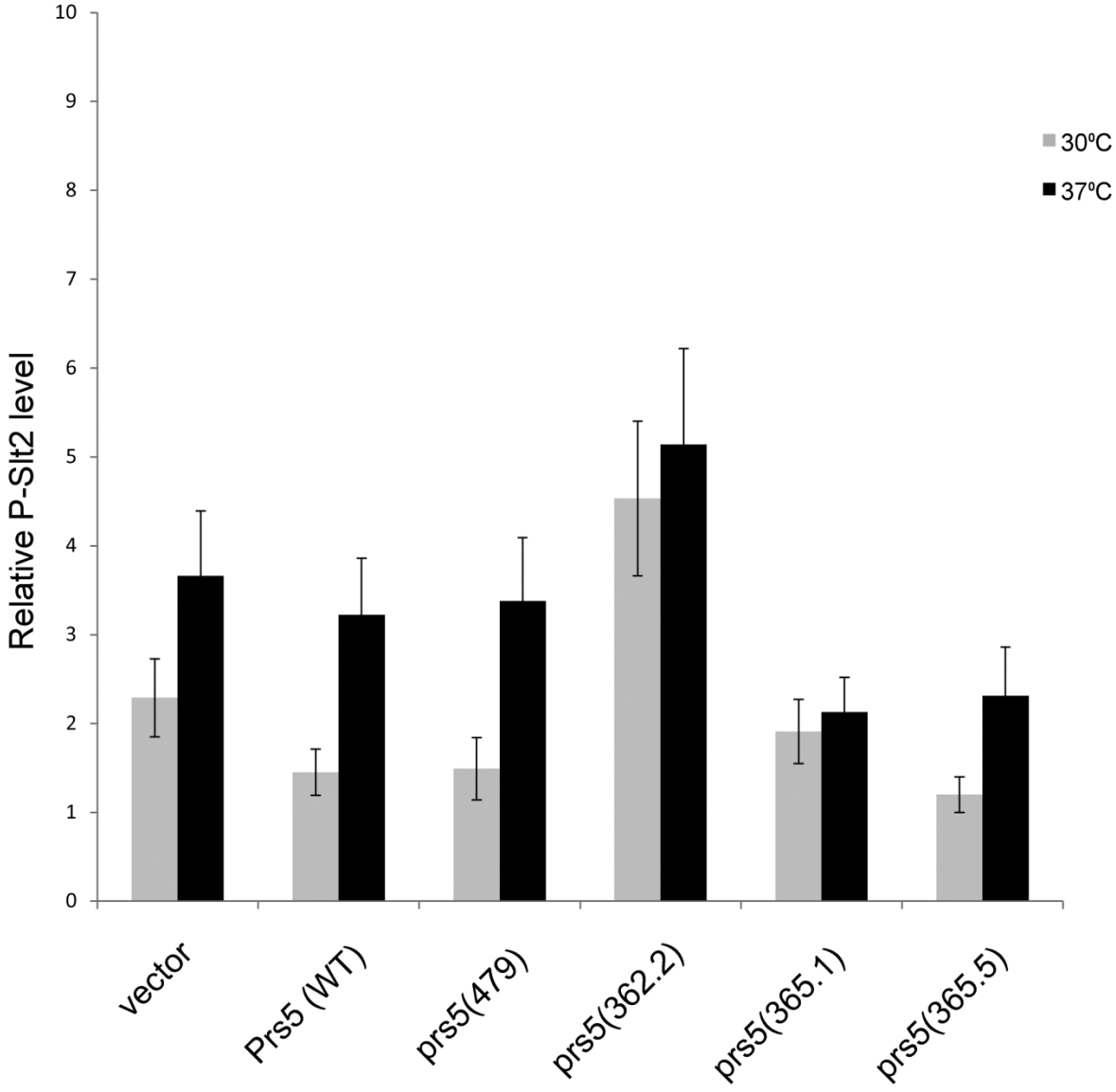

Figure 3.14: Quantification of P-Slt2 in strains carrying the *in vitro* mutated versions of Prs5

The detected chemiluminescence signals from the Western blots (Figure 3.13) were quantified using the ChemiDoc imager. The relative P-Slt2 level was obtained by dividing the density of the P-Slt2 signasl by the density of the actin signal. Each value represents the mean ± S.E.M. The raw data are shown in Appendix, Table 5.4.

3.5.2 What is the individual contribution of the three postulated phosphorylated serine residues mutated in prs5(479) to Rlm1 expression following growth at elevated temperature?

In an attempt to answer this question each of the serine residues at positions 364, 367 and 369 was mutated individually to alanine (Table 3.1). The mutations were confirmed by sequencing and the mutated plasmids were introduced into YN96-68 (*prs5*Δ [pHPS100-Ura]) to create the following strains: YN96-68 [pHPS100-Ura;prs5(S364A)], YN96-68 [pHPS100-Ura;prs5(S367A)] and YN96-68 [pHPS100-Ura;prs5(S369A)]. Each of the single mutants was capable of increased Rlm1 expression, approximately two-fold, following incubation at 37^{o}C (Figure 3.15). This is in comparison to prs5(479) which has an elevated Rlm1 expression relative to the WT at 30^{o}C and increases only 1.25-fold after incubation at 37^{o}C. It can be said that none of the individual mutants responded differently from the situation illustrated by the two independent transformants YN96-68 [Prs5;pHPS100-Ura] and YN96-68 [pHPS100-Ura;Prs5] recreating the WT genotype by inverting the order in which the plasmids were transformed into YN96-68. Nevertheless, none of the mutants displayed the elevated Rlm1 expression measured in prs5(479) at 30^{o}C, implying that when all three serine residues are mutated they have an additive effect on signalling in the CWI pathway.

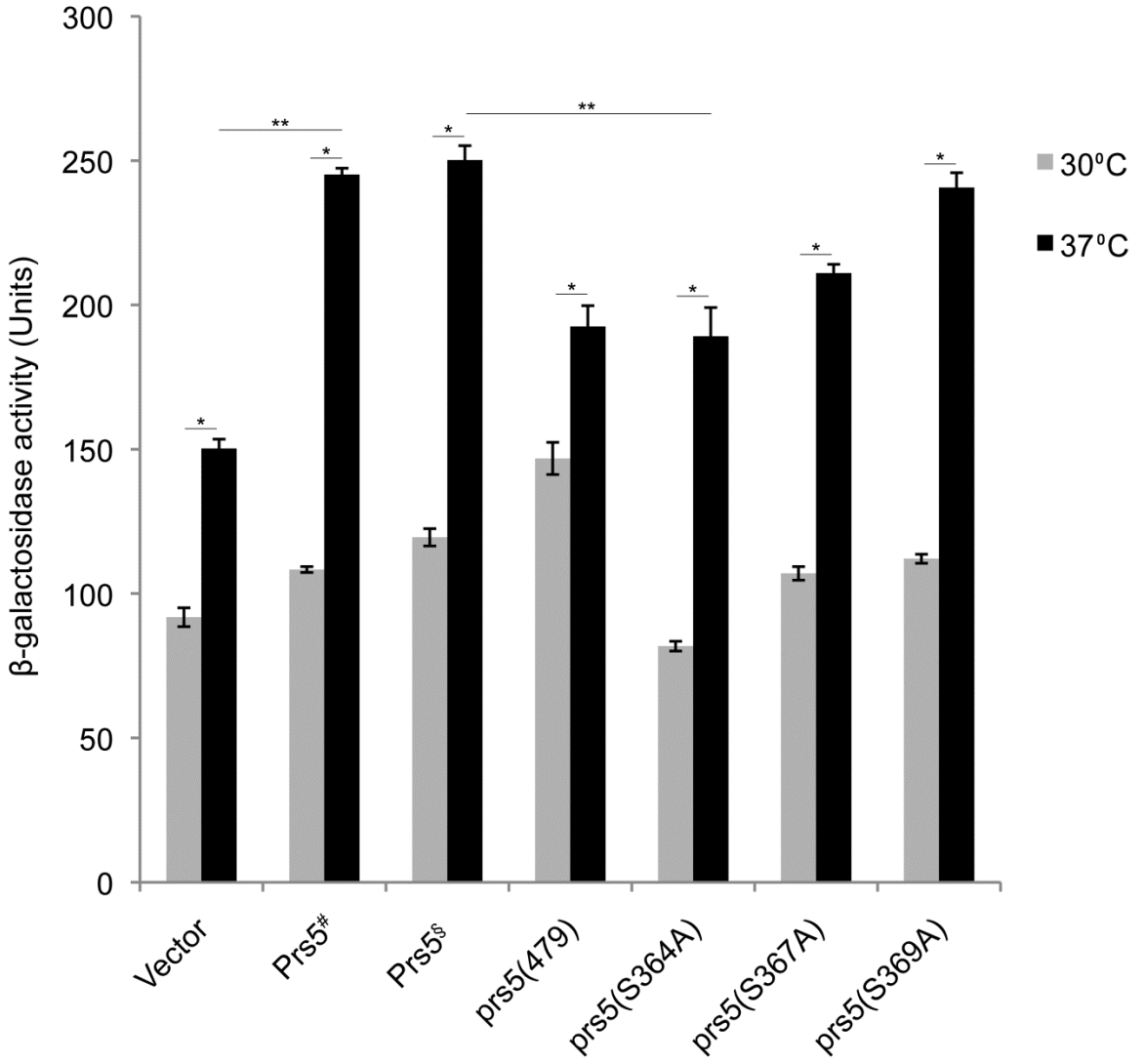

Figure 3.15: Rlm1 expression of single mutations of Prs5 in comparison with Prs5 (WT) and prs5(479)

In this series of experiments, the YN96-68 transformants containing the Rlm1 reporter plasmid (pHPS100-Ura) and plasmid-borne single mutation of phosphorylatable version of Prs5 and two independent WT strains created by changing the order in which the two plasmids were transformed as indicated by # and § were used to measure Rlm1 expression following incubation at 30°C and 37°C. All strains were grown on SC-Leu-Ura media o/n at 30°C before incubation at 30°C or 37°C in 50 ml of the same culture media until an OD_{660} ≈ 1.0 was obtained. Data: mean ± s.d. for three measurements for two independent transformants; *p<0.05, **p<0.01 (TukeyHSD test). The raw data are shown in Appendix, Table 5.5.

3.5.3 Phosphorylation status of Slt2 following mutation of S_{364}, S_{367} and S_{369} aa residues of Prs5

The involvement of the three phosphosites of Prs5 at aa residues S_{364}, S_{367} and S_{369} (Table 3.1) on the phosphorylation status of Slt2 was examined in response to mild heat shock at 37^{o}C. This was achieved by inoculating cultures grown at 30^{o}C into media pre-warmed to 37^{o}C and is a recognised means of achieving mild heat shock (Levin, 2005). The cultures used for Rlm1 expression (cf, Figure 3.14) were processed and subjected to Western blotting (Material and Methods, section 2.10). Each of the single mutants displayed a pattern of Slt2 phosphorylation comparable to that of the WT following incubation at 37^{o}C. This is in contrast to prs5(479) which has an elevated Rlm1 expression and a strong P-Slt2 signal at 30^{o}C. No changes in the Slt2 or actin signals were observed at either temperature or in response to the Prs5 variant present (Figure 3.16). Signal strength was quantified and the data are presented in the Figure 3.17.

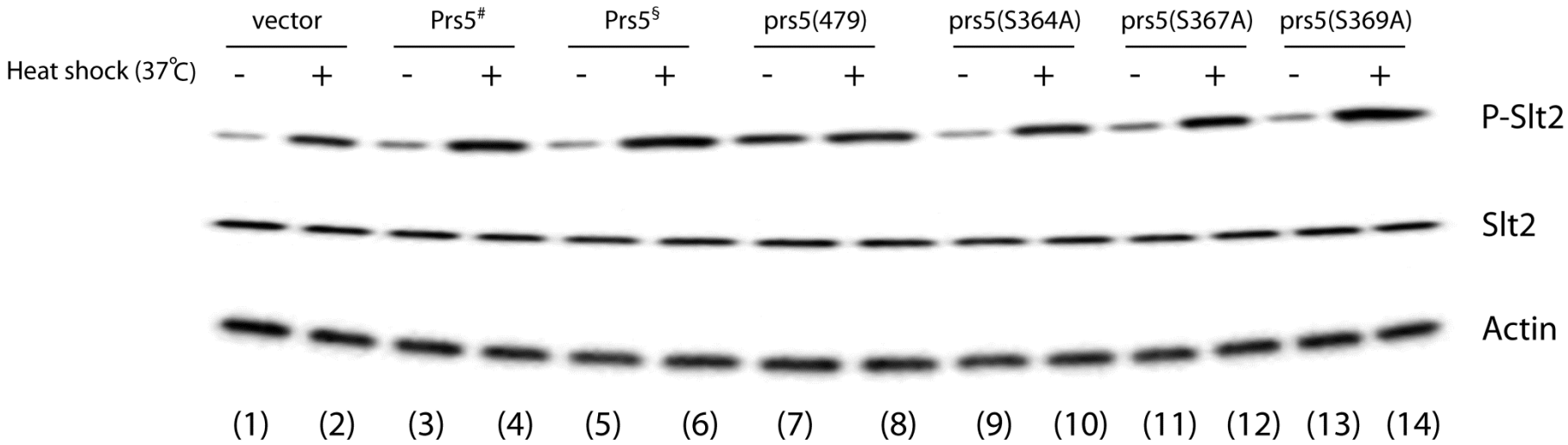

Figure 3.16: Slt2 phosphorylation status of single serine residues, S364, S367 and S369, mutated in prs5(479)

The cultures used for β-galactosidase activity were processed for Western blotting. The membrane was cut and challenged with the antibodies as described in the legend to Figure 3.13. The three signals were detected by chemiluminescence. Western blots were performed on three biological replicates.

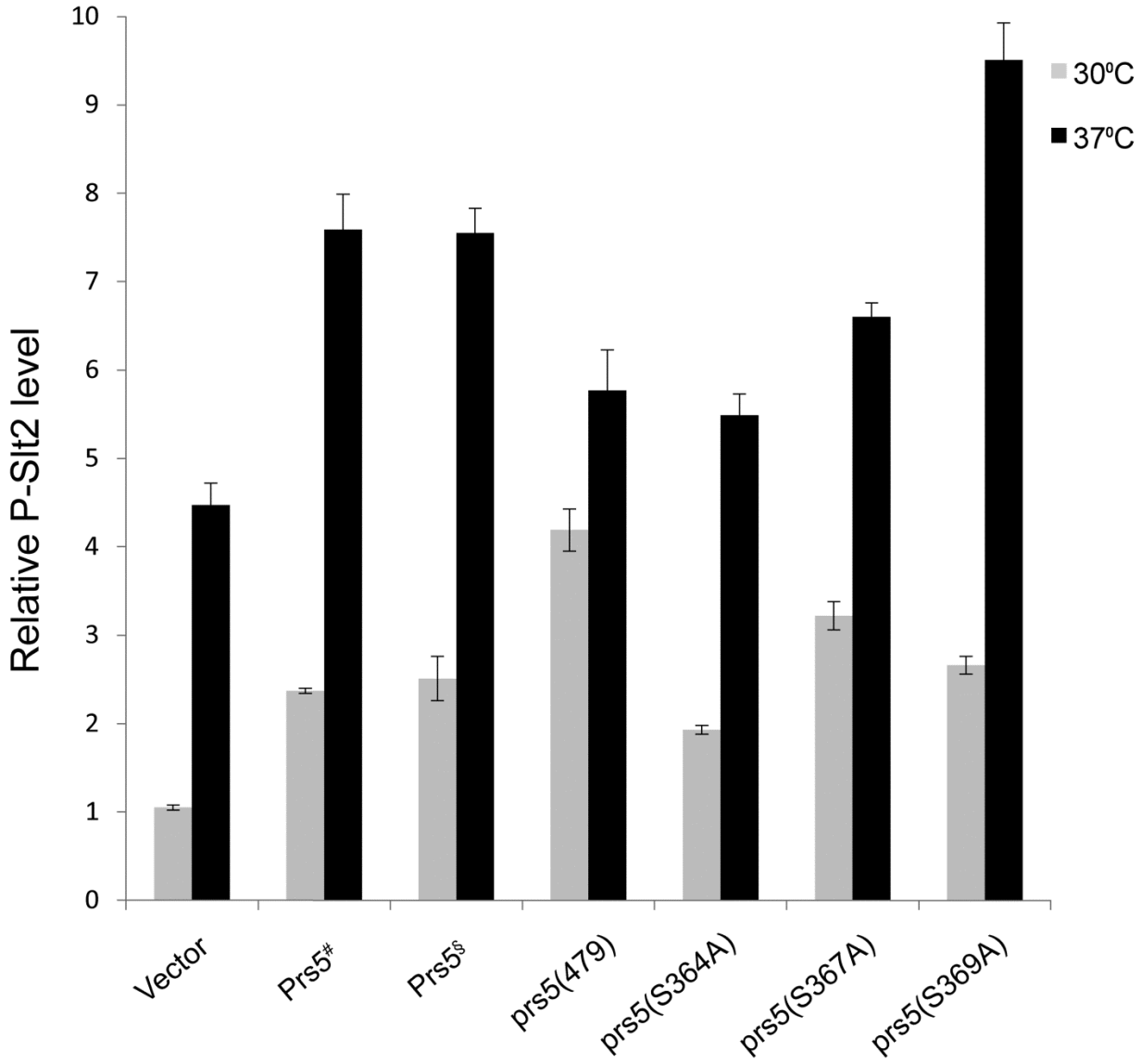

Figure 3.17: Quantification of P-Slt2 status of single serine residues mutated in prs5(479)

Chemiluminescence signals from the Western blot shown in Figure 3.16 were quantified. The relative P-Slt2 level was obtained by dividing the density of the P-Slt2 signal by the density of the corresponding actin signal. Two independent WT strains created by changing the order in which the two plasmids were transformed are indicated by # as well as §. Each value represents the mean ± SEM. WT was transformed in different orientation. The raw data are shown in Appendix, Table 5.6.

3.5.4 Evaluation of Fks2 expression in the single mutations $S_{364}A$, $S_{367}A$ and $S_{369}A$ of Prs5 in comparison to Prs5 (WT) and prs5(479)

FKS1 and FKS2, are a pair of closely related genes that encode alternative subunits of the glucan synthase (GS) complex, each capable of supporting GS activity or cell viability. Fks2 is responsible for synthesizing 1,3-β-glucan chains, a major structural component of the cell wall in *S. cerevisiae* (Zhao *et al*., 1998, Sobering *et al*., 2002).

The MAPK/Slt2 activation predominantly activates downstream transcription factors, which in turn activate the expression of cell wall-related proteins of which Fks2 is one (Zhao *et al*., 1998, de Nobel *et al*., 2000a). Mild heat shock activates *FKS2* expression *via* CWI signalling (Jung *et al*., 2002). Previous work has shown that *FKS2-lac*Z is one of the reliable reporters to examine CWI-induced transcription caused by heat shock and other toxic or cell wall-damaging agents, such as Congo red, CFW or caffeine (Kim *et al*., 2008, Levin, 2011).

Vavassori (2005) has demonstrated that deletion of *PRS5* abolishes the temperature-dependent increase in Fks2 expression. The influence of the *in vitro* mutations of *PRS5* on the expression of *FKS2*, was investigated as follows: YN96-68 containing the WT Prs5, the non-phosphorylatable mutants of Prs5 or the vector was transformed with the *FKS2-lac*Z reporter plasmid. β-galactosidase activity was then measured at 30^{o}C and 37^{o}C. It is obvious from Figure 3.18 that in the absence of *PRS5* Fks2 expression is considerably reduced following incubation at 37^{o}C in comparison to the WT, although Rlm1 expression is virtually identical to that of the two WT strains tested (cf. Figure 3.15). However, the levels of detectable Fks2 expression for the individual mutants grown at 30^{o}C are similar to those of Prs5 whereas prs5(479) has elevated Fks2 expression. After mild heat shock at 37^{o}C induction of Fks2 expression in the WT and the mutant $S_{369}A$ achieved a 2.5-fold increase whereas the mutations at $S_{364}A$ and $S_{367}A$ had similar Fks2 expression as prs5(479) under the same conditions, although this mutant had a level of Fks2 expression at 30^{o}C which is comparable with that of the *PRS5* deletant strain after heat shock. This result is in agreement with the observations reported for the same set of strains tested for Rlm1 expression (Figure 3.15), lending weight to the hypothesis that the Prs5 polypeptide plays at least a supporting role in the maintenance of CWI.

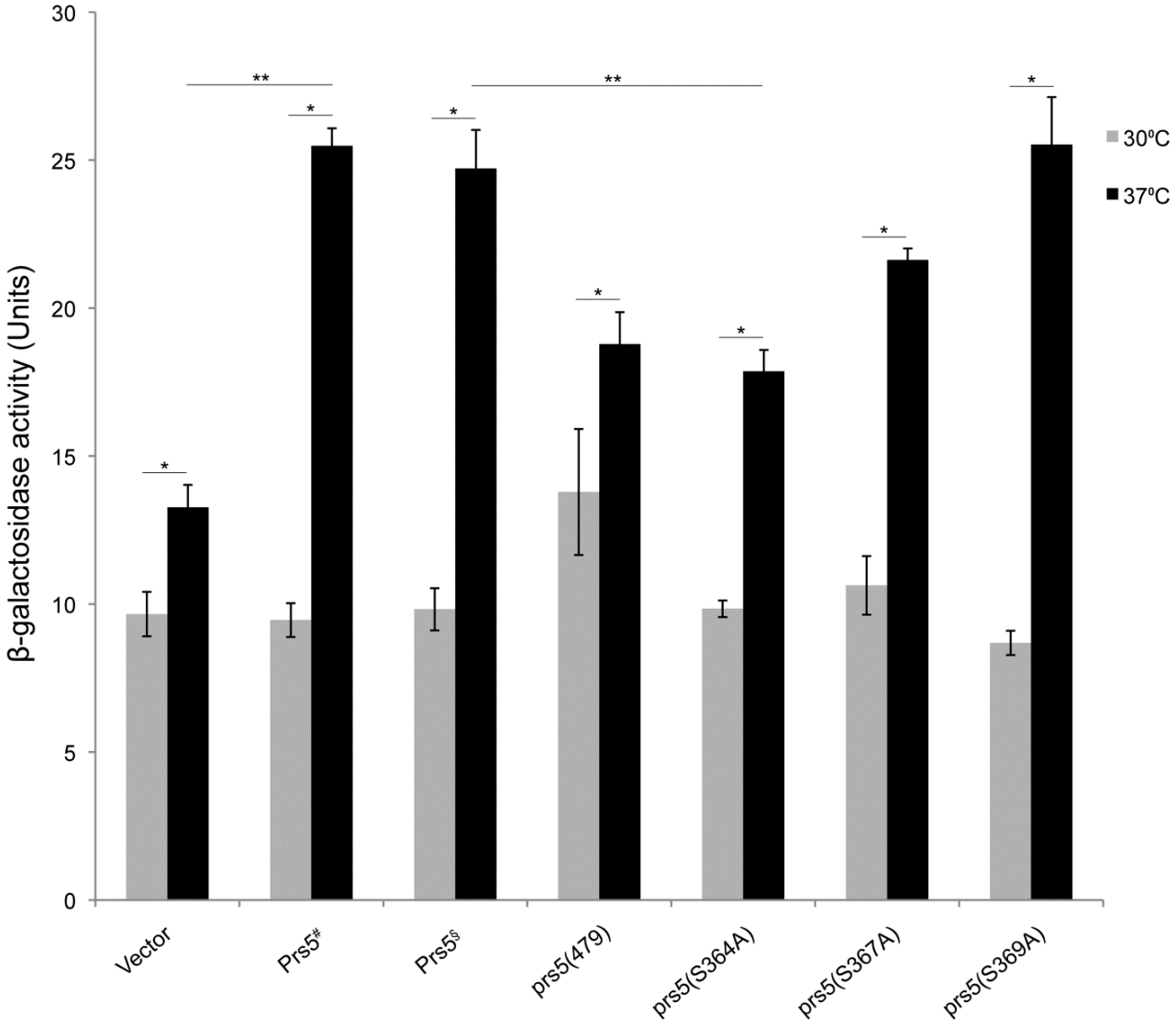

Figure 3.18: Fks2 activity of individual mutations of S364A, S367A and S369A of Prs5 in comparison to Prs5 (WT) and prs5(479)

The YN96-68 transformants were grown o/n in SC-Leu-Ura media and diluted into fresh SC-Leu-Ura media with a starting OD_{600}≈ 0.5 before incubating for 3 hr at 30°C or 37°C. Two independent WT strains created by changing the order in which the two plasmids were transformed are indicated by # and §, respectively. Each value plotted represents the mean ± s.d. of three measurements each for two independent transformants; *p<0.05, **p<0.01, (TukeyHSD test). The raw data are shown in Appendix, Table 5.7.

3.6 Introduction of Prs5 and *in vitro*-generated mutations thereof into YN97-14 rescued strains results in a synthetic growth defect and compromised CWI signalling

The importance of intact *PRS1* for the maintenance of CWI and cell viability in *S. cerevisiae* has been documented previously (Ugbogu *et al*., 2013). Plasmid versions of Prs5 [pGAD-Prs5] and mutated versions therof were transformed into YN97-14 containing pHPS100-Ura and pGBT-Prs1. This series of transformants was examined for their ability to grow at 30°C and 37°C and for their Rlm1 expression at both temperatures. As illustrated in Figure 3.19 all strains grew at 30°C but growth was completely abolished at 37°C unless the media contained 1 M sorbitol.

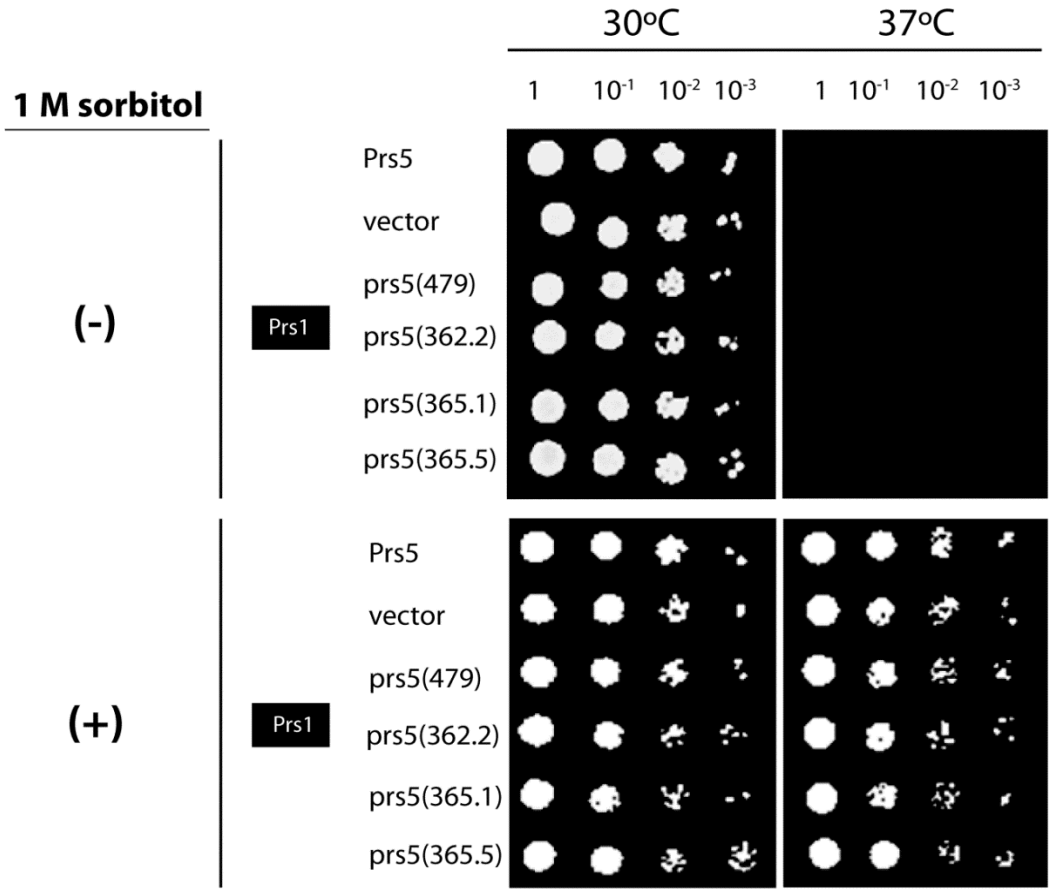

Figure 3.19: Temperature sensitivity of strains obtained by combining Prs1 and the *in vitro* mutations of Prs5 in YN97-14

YN97-14 containing the Prs1-and the Prs5-plasmids indicated were grown o/n at 30°C in SC-Ura-Trp-Leu and processed for spotting on the same media with or without 1 M sorbitol as described in Materials and Methods, section 2.5.1. The plates were incubated at 30°C and 37°C for three days and images were obtained on the third day by the ChemiDoc imager.

After spotting Rlm1 expression was tested in four biological replicates of each transformant by culturing single colonies from either the sorbitol-free plate incubated at 30^{o}C or from the sorbitol-containing plate incubated at 37^{o}C. As shown in Figure 3.20(**a**) following incubation at 30^{o}C the plasmid combination Prs1+prs5(365.1) had the highest Rlm1 expression followed by the combination Prs1+Prs5 and Prs1+prs5(365.5). However, the combination of Prs1 with either prs5(479) or prs5(362.2) resulted in Rlm1 expression at a level comparable to the combination Prs1+vector. On the other hand, Rlm1 expression in the cultures grown at 37^{o}C, in spite of being lower than the expression at 30^{o}C was higher in all combinations of Prs1 with Prs5 and the mutated versions thereof than in the combination Prs1+vector. This unexpected reduced level of Rlm1 expression following mild heat shock may be due to the presence of sorbitol in the culture medium and has been encountered previously (Alonso-Monge *et al*., 2001, Wojda *et al*., 2003).

In three of the four remaining rescued strains it was possible to measure Rlm1 expression following combination of prs1(L115T), prs1(D326A) and prs1(H130A/D326A) with Prs5 and *in vitro*-generated mutations thereof (Figure 3.20(**b**)-(**c)**).The combination of Prs5 WT with each of the Prs1 mutations did not result in Rlm1 expression at the level measured for Prs1+Prs5 (cf. Figure 3.20(**a**)). The elevated Rlm1 expression observed for the combination Prs1+prs5(365.1) was not observed in any of the combinations tested. When Prs5 was combined with prs1(H130A/D326A) Rlm1 expression was virtually abolished at 30^{o}C but increased 6-fold following incubation at 37^{o}C. The combination of prs1(H130A/D326A) with prs5(362.2) had elevated Rlm1 expression at 30^{o}C but the lowest at 37^{o}C of all combinations with this double mutant. Even taking into consideration the fact that the presence of sorbitol can interfere with CWI it is obvious that the combination of WT Prs1 and its various *in vitro*-generated mutations and WT Prs5 and its various *in vitro*-generated mutations has a profound effect on CWI signalling.

When prs1(Q133P) was combined with Prs5 and its derivative growth at 30^{o}C was reduced at 30^{o}C (cf. Figures 3.19 and 3.21) and was not corrected by the addition of sorbitol to the media. In common with the other combinations of Prs1 with Prs5 there was no growth at 37^{o}C and inclusion of 1 M sorbitol in the media corrected this

growth defect only partially. In spite of repeated attempts it proved impossible to measure Rlm1 expression in this context.

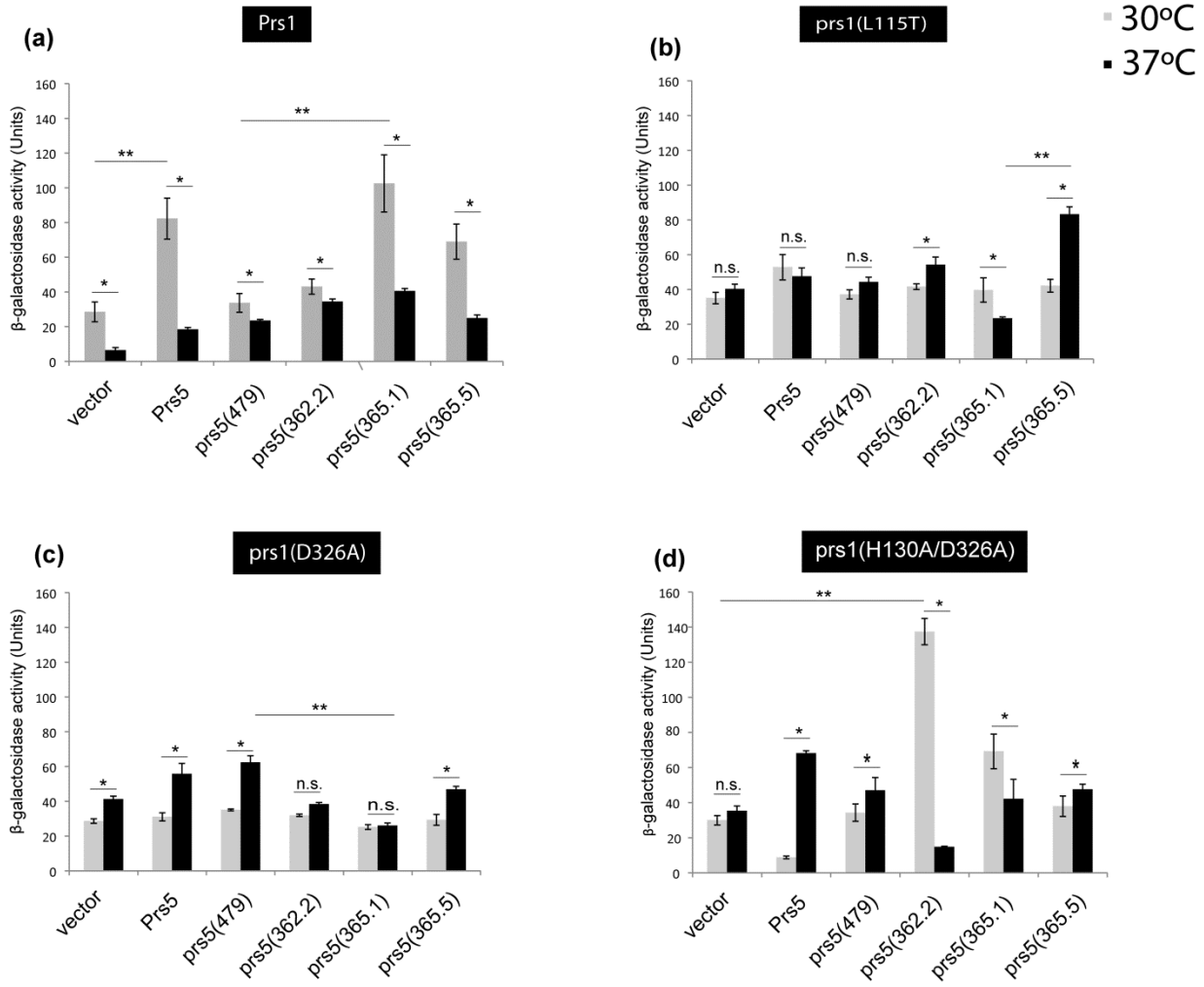

Figure 3.20: Influence of Prs5 *in vitro* mutations on Rlm1 expression in YN97-14 rescued strains

Rlm1 expression as a result of combining Prs5 or *in vitro* mutations thereof with YN97-14 WT Prs1 (**a**), YN97-14 prs1(L115T) (**b**), YN97-14 prs1(D326A) (**c**) and YN97-14 prs1(H130A/D326A) (**d**). Four biological replicates of each of the tested transformants were cultured at 30°C without or at 37°C with 1 M sorbitol and tested for Rlm1 expression. Data: mean ± sd. of three measurements each for two independent transformants; *p<0.05, **p<0.01, n.s., not significant (TukeyHSD test). The raw data are presented in Appendix, Tables 5.8-5.12.

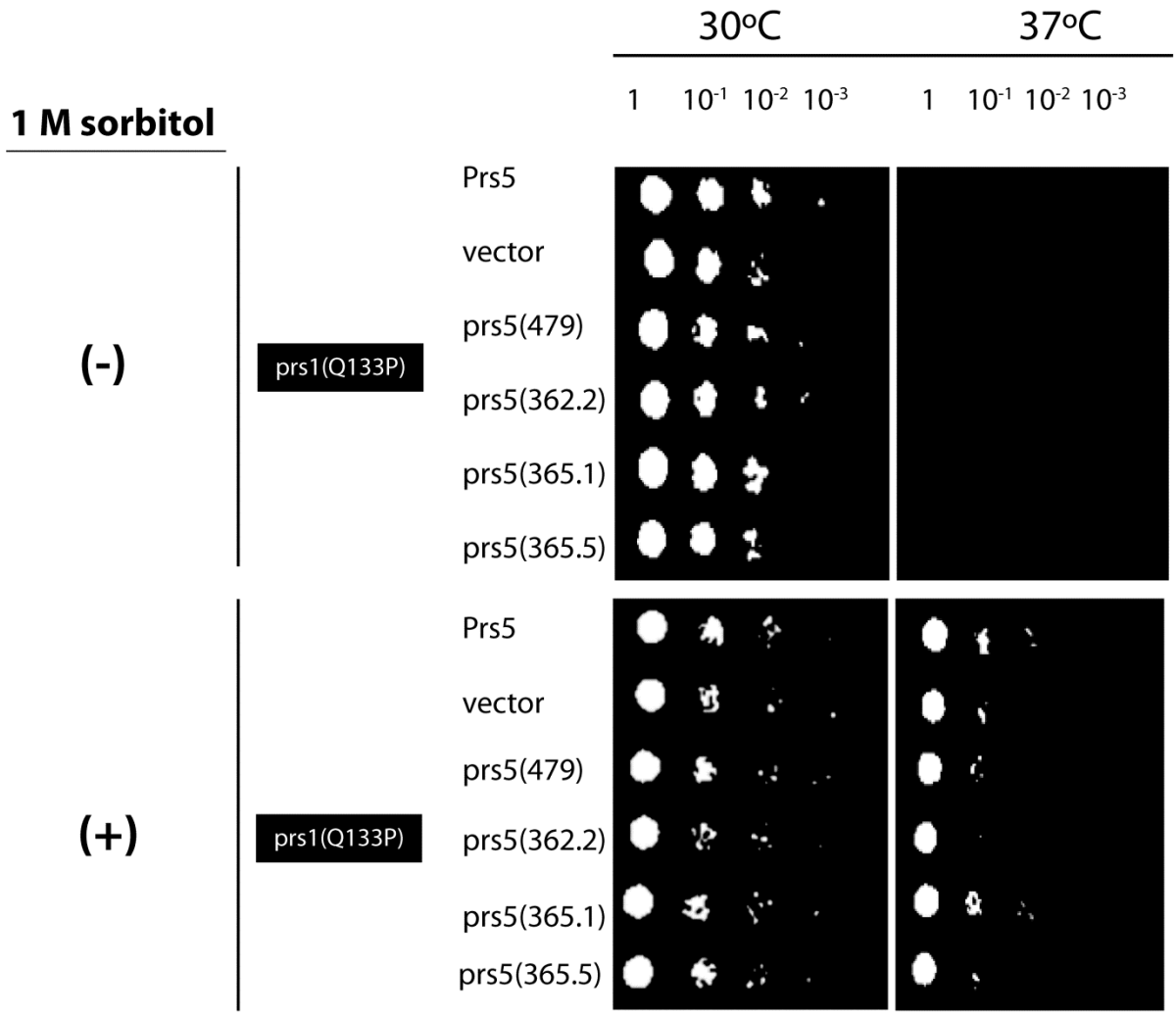

Figure 3.21: Temperature sensitivity of prs1(Q133P) in combination with Prs5 WT and its derivatives

Temperature sensitivity of the transformants generated from combination of prs1(Q133P) with WT Prs5 or *in vitro*-generated mutations thereof in YN97-14 was tested. Further details, see legend to Figure 3.19.

3.7 Detection of His-tagged Prs5 by Western blot analysis

Recombinant DNA technology enables the modification, expression, identification and isolation of proteins of interest from host cells (Young *et al*., 2012). Isolation and purification of proteins have been simplified by fusing tags to create recombinant proteins (Terpe, 2003). One of the most commonly used tags is the His-tag which is composed of six consecutive histidine residues (6×His). Histidine residues are known to interact specifically with divalent metals, such as Ni^{2+} (Yip *et al*., 1989). This is the basis for the specific interaction which allows the purification of His-tagged proteins. Ni^{2+}-ions are immobilized on a chromatographic support (Yip *et al*., 1989). The cell lysate is applied under low salt conditions to a column containing the immobilized Ni^{2+}-ions and non-specifically bound proteins are eluted under the same conditions. The His-tagged protein is then selectively eluted by applying an increasing concentration of imidazole. Imidazole mimics histidine and binds to the Ni^{2+}-coordination centre of the affinity column and displaces the His-tagged protein. Specifically, crude extracts prepared from the strain YN11-01 as described in Materials & Methods, section 2.17 were subjected to affinity chromatography.

Prior to the isolation of His-tagged Prs5 a time course experiment was carried out to verify the galactose induction of His-tagged Prs5 encoded by the plasmid, pYESDEST52-*PRS5*-His6X-V5::URA3 (Fasolo *et al*., 2011). In Figure 3.22, the Western blot shows the presence of the band that corresponds to the His-tagged Prs5. In addition, since YN11-01 contains an integrated copy of GFP-Prs1 (Schneiter *et al*., 2000) at the *PRS1* locus the membrane was also probed with GFP antibodies. The signal corresponding to GFP-Prs1 is visible under all growth conditions. The lower bands visible in lanes (2)-(5) are the result of the growth in the presence of galactose. No band was visible in lane (1) which contains the crude extract of YN11-01 grown in SC-Ura+2% raffinose for 6 hr. This confirms that YN11-01 contains a galactose-inducible His-tagged protein. This protein has a MW of 57 KDa consisting of the Prs5 polypeptide with a MW of 53.5 KDa (http://www.yeastgenome.org/) and 4 KDa contributed by the C-terminal peptide containing the V5-epitope and the polyhistidine tag.

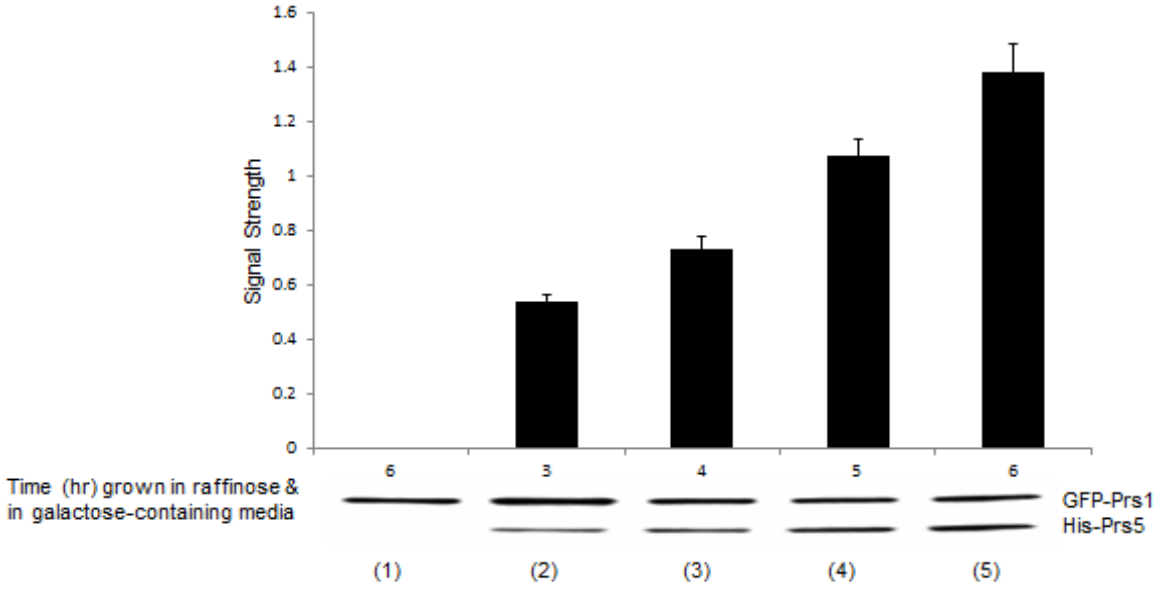

Figure 3.22: His-tagged Prs5 and GFP-Prs1 detection by Western blotting analysis of crude protein extracts of raffinose-grown and galactose-induced cultures of YN11-01

Lane (1): Crude extract corresponding to 25 ug of protein from YN11-01 grown in SC-Ura+2% raffinose for 6 hr. Lanes (2)-(5): Crude extracts corresponding to 25 ug of protein from YN11-01 shifted from SC-Ura+2% raffinose to SC-Ura+2% galactose media for 3, 4, 5 and 6 hr, respectively. Following electrophoresis on a 4-20% SDS-PAGE gel the products were transferred to a PVDF membrane. The membrane was blocked by incubating in 5% non-fat dried milk in TBS-T for 1 hr and subsequently incubated with either anti-His antibodies (sc-8036) or anti-GFP antibodies (sc-73556) diluted 1:1000 for 1 hr and a 1:5,000 dilution of goat anti-mouse IgG-HRP (sc-2060) for 1 hr. The membrane was treated with Bio-Rad detection reagent and exposed to X-ray film for 15 min. There was no visible signal in the raffinose-grown YN11-01 crude extract (lane (1)) and there is a visible signal after 3 hr of galactose induction which increases slightly with respect to time (lanes (3)-(5)). As expected, the strength of the GFP-Prs1 signal remained constant in lanes (1-5). The values are expressed as signal strength +/- S.D. The experiment was done on three biological replicates. The raw data are shown in Appendix 5.12.

3.7.1 Partial purification of His-tagged Prs5 proteins

The crude extract from the 6 hr galactose-induced YN11-01 culture (Figure 3.22) was applied to a $(Ni^{2+})_6$ fast flow Sepharose™ column (1 ml HisTrap FF, GE Healthcare) connected to the ÄKTA Avant 250 as described in Materials and Methods, section 2.16.1. The elution profile of the His-tagged Prs5 protein is shown in Figure 3. 23. Fractions corresponding to the protein peak eluting with 200 mM imidazole were collected and subjected to Western blotting. The Western blot in Figure 3.24 shows that both the crude extract and the purified sample contain a

distinct band corresponding to a protein with an apparent MW of 57 KDa. The relative intensity of the signals obtained in the crude and affinity-purified extracts is consistent with a purification factor of at least 5-fold since the amount of protein loaded in lane (2) was 20% of that loaded in lane (1).

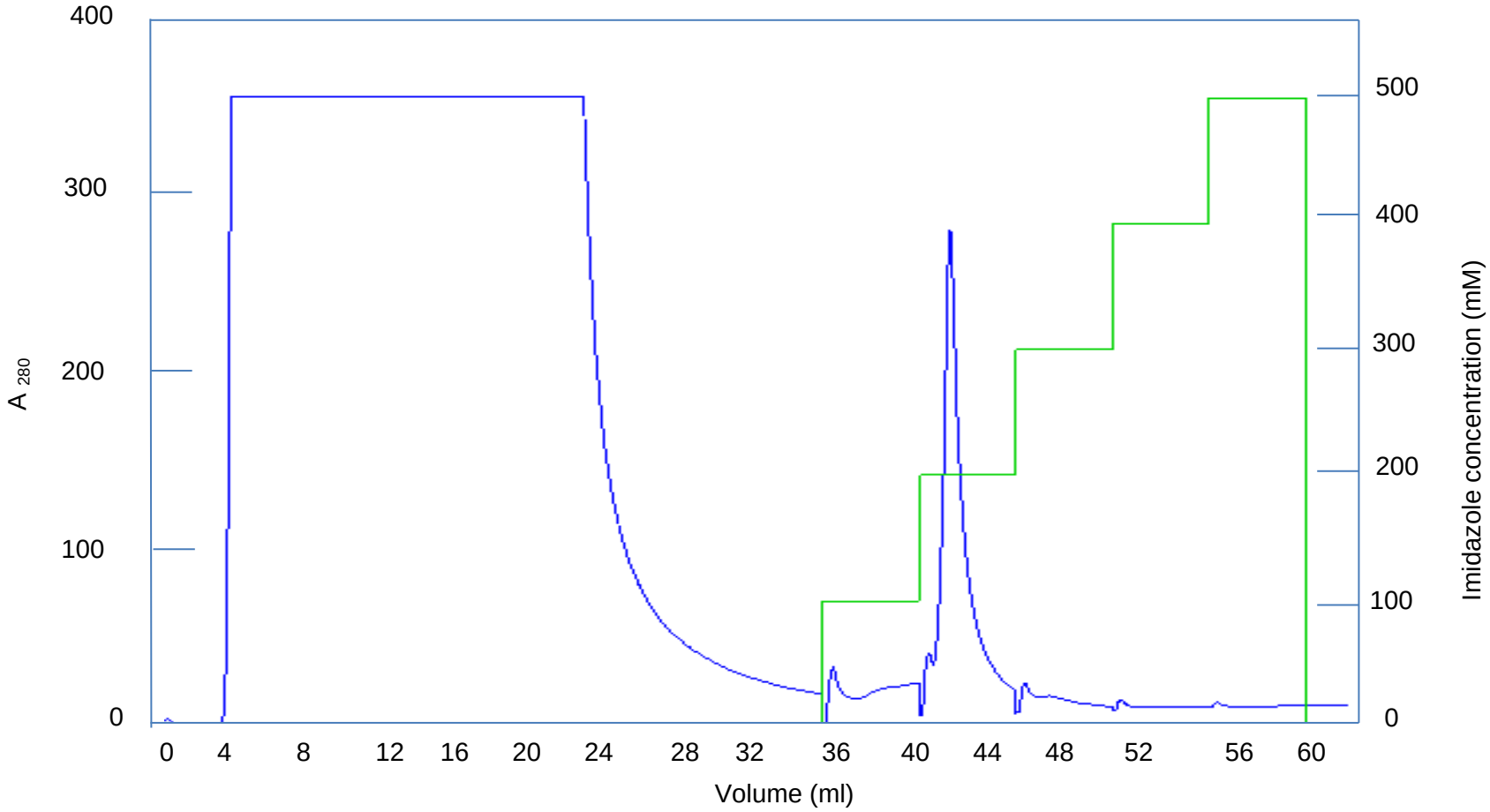

Figure 3.23: Purification profile of His-tagged Prs5 obtained from a 6 hr galactose-induced extract of YN11-01

His-tagged Prs5 was isolated from YN11-01 galactose-induced cells using ÄKTA Avant 250 as described in Materials and Methods, section 2.16.1. The right hand y-axis shows the concentration of imidazole in the step gradient used for elution. Crude extract corresponding to 10 mg/ml protein was supplied to the column at a flow rate of 1 ml/min. Once the A280nm absorption had reached a minimum, the elution of the His-tagged Prs5 protein was initiated by increasing the concentration of imidazole from zero to 500 mM (green trace). Fractions containing the protein peak (Volume 40-44 (ml)) eluting at 200 mM imidazole were collected and subjected to Western blotting.

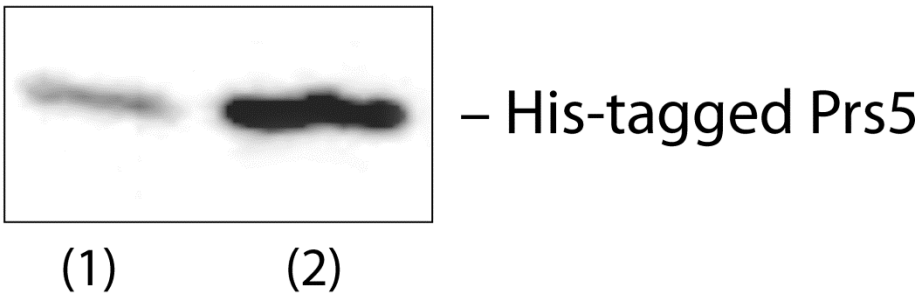

Figure 3.24: Western blot analysis of YN11-01 crude extract of YN11-01 and the peak fractions eluted with 200 mM imidazole

Lane (1): 25 µg crude extract of galactose-induced YN11-01 culture for 6 hr. Lane (2): 5 µg of the combined fractions eluted from the Ni^{2+}-column with 200 mM imidazole as shown in Figure 3.23) were separated on a 4-20 % SDS-PAGE and transferred to a PVDF membrane. After transfer and blocking, the membrane was treated as described in the legend to Figure 3.22.

3.7.2 Mass spectrometry (MS) analysis of His-tagged Prs5

MS analysis was carried out on material obtained from a His SpinTrap™ column. The reason for using His SpinTrap technology was to obtain a more concentrated protein suspension by reducing the elution volume to 300 µl rather than the 10-fold larger elution volume obtained with the ÄKTA purifier Avant 250, thereby allowing the visualization of protein bands in a stained gel. A further reason was to reduce the purification time. Using the His SpinTrap column takes approximately 10 min whereas the automated ÄKTA purification requires at least 1 hr. 10 mg/ml crude extract of the YN11-01 [*prs5Δ::kanMX4-loxP* [pYES-DEST52-*PRS5*-His6X-V5::URA3]] prepared as described in Materials and Methods, section 2.15, was applied to a 1 ml His SpinTrap™ column, after which the column was washed and protein eluted with either 200 mM or 300 mM imidazole-containing buffer (Materials and Methods, section 2.16.2). 25 µg of the crude extract and 2.5 µg of the eluted fractions were separated on 4-20% SDS-PAGE and subsequently stained with Coomassie Blue R250 (Materials & Methods, section 2.9.3), followed by Western blotting. Comparison of the stained gel and the corresponding Western blot (Figures 3.25 (**a**) and (**b**)) revealed that the His-tagged Prs5 protein was detectable in the crude extract (lane (1)), in the flow through (lane (2)) and in the eluted fractions (lanes (5)-(7)). No bands corresponding to His-tagged Prs5 were detectable in lanes

(3)-(4). The strength of the signal of the purified samples eluted with 200 mM or 300 mM imidazole was 10 times stronger than that of the crude extract (cf. lanes (1)-(2) and (6)-(7)). The amount of protein applied to lanes (6) and (7) was only 1/10th of that applied to lane (1). Taking into consideration the relative signal strengths this is consistent with an approximately 100-fold increase in the concentration of His-tagged Prs5 following His SpinTrap purification.

Interestingly, distinct bands in lanes (4) and (5) of the stained gel (Figure 3.25 **(a)**) did not cross-react with the His-tag antibody, but may represent polypeptides associated with Prs5. In order to identify these polypeptides the bands corresponding to Prs5 in lane (6) and the two non-cross-reacting bands with an apparent MW of 42,000 and 36,000 in lane (4) and (5) were excised from the gel and analysed by MS/MS after in-gel trypsin digestion. The MALDI TOF MS analysis was carried out by Dr. Catherine Botting and her colleagues at the BMS Mass Spectrometry and Proteomics Facility, University of St Andrews. The peptide fingerprints detected by the MASCOT search engine (https://bsrcmascot.st-andrews.ac.uk/mascot/x-cgi/ms-review.exe) were used to interrogate the NCBI (http://www.ncbi.nlm.nih.gov/pubmed) and the Saccharomyces Genome Database (SGD, http://www.yeastgenome.org) databases. Matches were obtained for Prs5 with the gel slice from lane (6). Peptides recovered matched 68% of the *S. cerevisiae* (S288c) Prs5 polypeptide. The MS/MS spectrum illustrated in Figure 3.26 corresponds to aa residues 445-456 of Prs5 with the sequence LIISNTVPQDR (Dujon *et al*., 1997) and a monoisotopic mass (Mr), of 1254.7.

The best matches for the lower (lane (4)) and upper (lane (5)) bands corresponded to GAPDH (36 KDa) and elongation factor 1-α (TDH2) (42 KDa), respectively (data not shown).

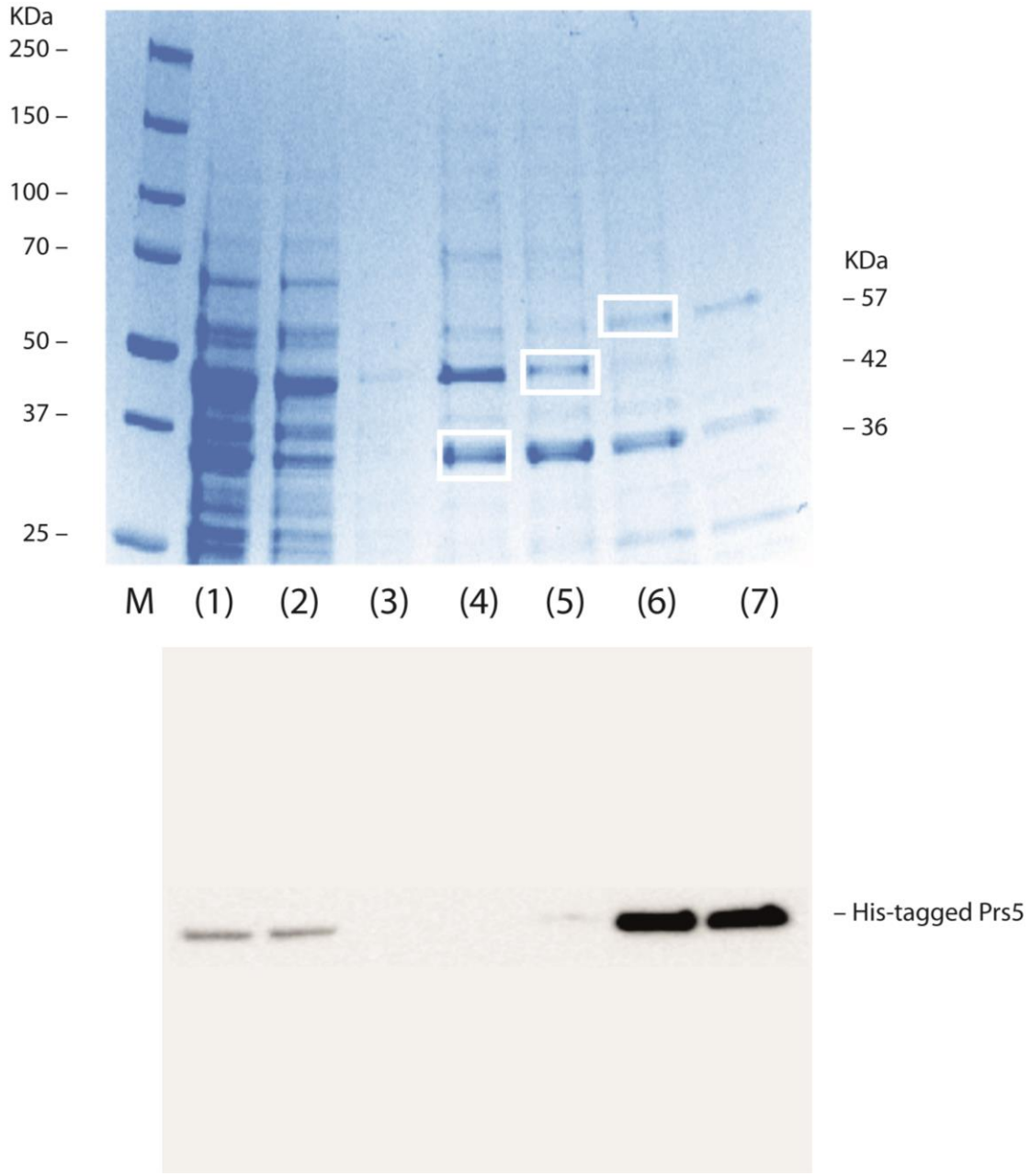

Figure 3.25: SDS-PAGE and Western blot analysis of His-tagged Prs5

25 µg crude extract of YN11-01 and 2.5 µg partially purified His-tagged Prs5 (Materials and Methods section 2.16.2) were separated on a 4-20% SDS-PAGE and stained with Coomassie Brilliant Blue R250 (**a**) and subjected to Western blotting (**b**). The membrane was blocked by incubating in 5% non-fat dried milk in TBS-T for 1 hr and subsequent incubation with anti-His antibodies (sc-8036) diluted 1:1000 for 1 hr and a 1:5,000 dilution of goat anti-mouse IgG-HRP (sc-2060) for 1 hr. The membrane was treated with Bio-Rad detection reagent and and images obtained using Chemdoc imager.

Lane M: Marker (PageRuler^{TM} prestained protein ladder, Bio-Rad);
Lane (1): Crude extract
Lane (2): Flow through
Lanes (3)-(4)): Washes with binding buffer containing 20 mM and 50 mM imidazole, respectively
Lanes (5)-(7): Elution with 100 mM, 200 mM and 300 mM imidazole, respectively.

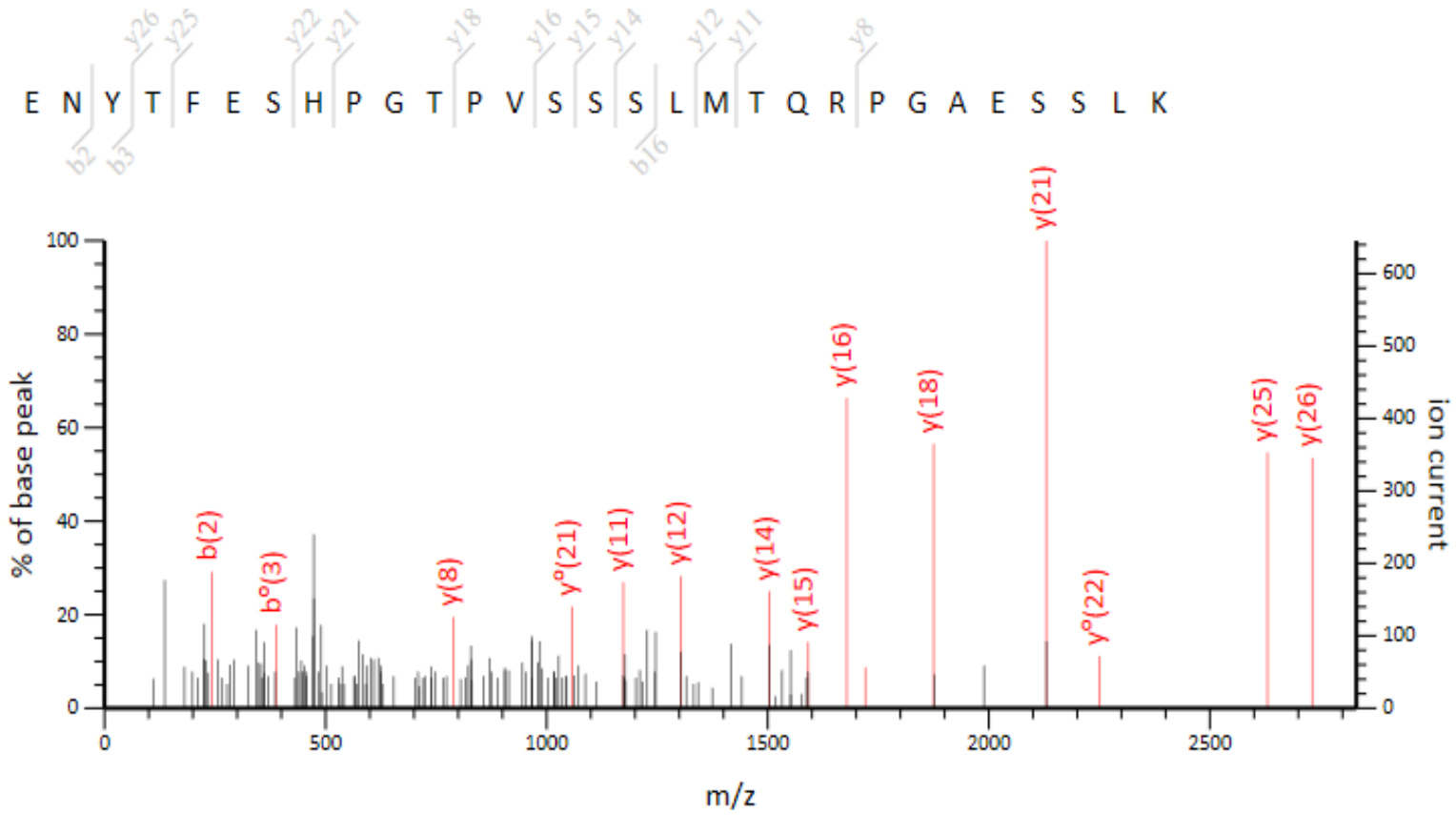

Figure 3.26: CID spectrum of the Prs5 peptide fragment, $_{117}$ENYTFESHPGTPVSSSLMTQRPGAESSLK$_{145}$ (gi: 6324511)

The eluted His-tagged Prs5 was subjected to SDS-PAGE. After staining and Western blotting the band highlighted in Figure 3.25 (a), lane (6) was subjected to MS/MS fragmentation after in-gel trypsin digestion. The b-series ion mass is the charge retained on the N-terminal fragment), the y-series ion mass is the charge retained on the C-terminal fragment resulting from the breakage of the C-N bond and the y*-series ion mass are products of further fragmentation of the y-series. The calculated monoisotopic mass of the peptide is 3136.4771.

To further investigate if His-tagged Prs5 co-purifies with other proteins, in addition to YN11-01 (*prs5Δ::kanMX4-loxP*) [pYES-DEST52-PRS5-His6X-V5::URA3]], YN97-91 (*prs2*Δ *prs4*Δ *prs5*Δ*::kanMX4-loxP*) [pYES-DEST52-PRS5-His6X-V5::URA3] which expresses only the Prs1 and Prs3 polypeptides and His-tagged Prs5, were purified on His SpinTrap columns. The purified extracts were subjected to SDS-PAGE and a section of the gel containing material with a MW in the range of 30-100 KDa was excised for each extract (data not shown). Prior to MS/MS analysis on ESI-QUAD-TOF the prominent band from each extract was excised and analysed separately, otherwise it would have dominated the spectrum completely. Using the Mascot software and interrogating the NCBI *S. cerevisiae* database 29 proteins including Prs5 and Prs3 were identified in YN11-01. The same search criteria identified 29 proteins in the prominent band of YN97-91, however, only Prs5, but not Prs3, was found. Analysis of the remainder of the gel slices identified 275 hits for YN11-01 and 254 for YN97-91 of which 92 were common to both strains. In the YN11-01 sample, in addition to Prs3 and Prs5, Prs1 was also identified. The Prs1 peptide identified is located in the NHR1-1 region of the protein, thus providing corroborative evidence that NHR1-1 is an integral part of the mature Prs1 protein (Figure 3.27).

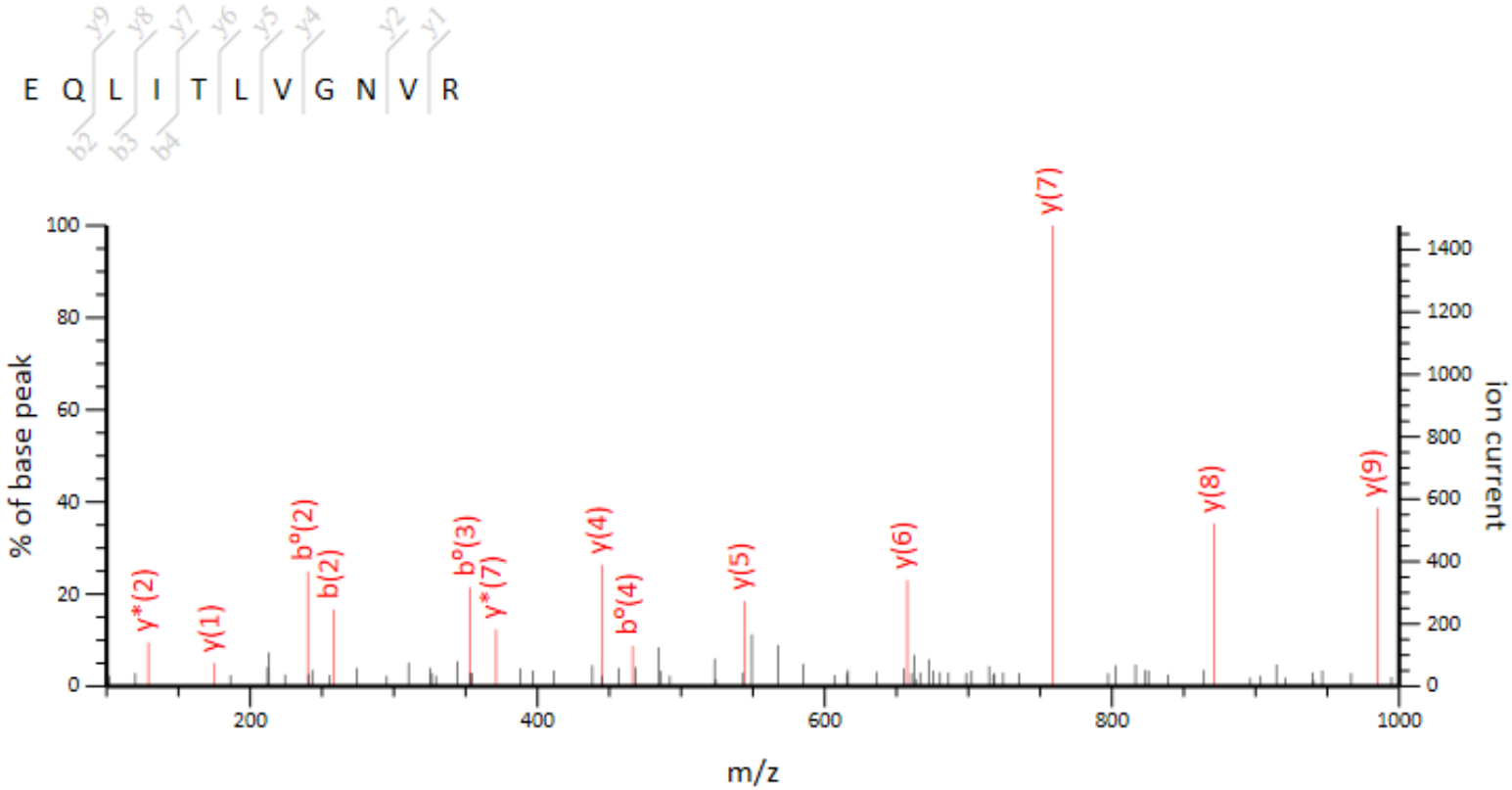

Figure 3.27: CID spectrum of the Prs1 peptide, $_{307}$EQLITLVGNVR$_{317}$ (gi: 6322667)

A gel 'chunk' was digested with trypsin and subjected to MS/MS fragmentation. The NCBI Yeast Database was interrogated by the fragmentation fragments and the Prs1 peptide (gi: 6322667) identified which together with four others identified corresponded to a 17% coverage of the Prs1 polypeptide. The b-, y- and y*--series ion masses of the peptide are illustrated. The calculated mass of the peptide is 1240.7139. The peptide coincides with the C-terminal junction of NHR1-1.

The proteins listed in Table 3.2 are a selection of those identified by MS/MS. Prs5, elongation factor 1α and TDH2 (GAPDH isozyme 2) identified in the first experiment were again identified in the second experiment in addition to other proteins. In the second experiment Prs1, Prs3, Prs5, Rho1 and other associated proteins were identified for YN11-01. With the exception of Pet9, Rpt4, Prs1, Sfh1, Zuo1 and Rho1 the same sets of proteins were identified for YN97-91 as shown in Table 3.2. Many of the identified proteins are involved in protein synthesis, transcription and heat shock response.

Table 3.2: Proteins and peptides identified by ESI-MS/MS analysis of YN11-01 and YN97-91

Protein	Peptide sequence	Known function	aa location	MW (KDa)	YN11-01	YN97-91
Prs5	K.LIISNTVPQDR.T	PRPP synthesis, histidine & tryptophan	445-457	54	+	+
Prs3	R.ITAIIPNFPYAR.Q		87-100	35	+	+
Prs1	R.EQLITLVGNVR.G		306-318	47	+	-
Hsp26	R.LLGEGGLR.G	Heat shock protein	23-32	24	+	+
Gal1	R.DYLTTSPVR.F	Galactose metabolism	375-385	59	+	+
RPL17B	K.YLDQVLDHQR.A	Protein synthesis	46-57	21	+	+
Vma2	K.ILDEFYDR.A	Contains nucleotide binding sites	479-488	57	+	+
Pet9	K.SDGVAGLYR.G	Major ADP/ATP translocator	182-192	35	+	-
Mir1	K.FLVFER.A	Regulation of calcium-mediated signaling	187-194	33	+	+
Rpt4	R.ASTPMFLLSR.K	H3 methylation	343-354	65	+	-
Ser1	K.DLINFNDIGLGIGEISHR.S	Required for serine and glycine biosynthesis	28-47	44	+	+
G4p1	K.EQSAQAAQWESVLK.S	tRNA aminoacylation	22-37	42	+	+
Yck2	R.GQLPWQGLK.A	morphogenesis and glucose sensing	277-287	62	+	+
Pho88	K.APSLFGGMGQTGPK	Inorganic phosphate transportation	154-168	21	+	+
Sfh1	R.FATSIVQDLGLTR.E	Essential for viability.	309-323	49	+	-
Vma13	K.ATQAIIGYTFK	Coupling ATP hydrolysis to proton translocation	288-299	55	+	+
Bmh1	K.ISDDILSVLDSHLIPSATTGESK.V	Regulation of exocytosis & MAPK signalling	74-98	30	+	+
Hog1	K.ICDFGLAR.I	Regulates stress responses & morphogenesis	152-161	47	+	+
Zuo1	K.TIVDSGKLPSSLLSYFV	A member of HSP70 family	416-433	49	+	-
Rho1	R.NDPQTIEQLR.Q	Cell wall synthesis & regulates Pkc1	127-138	24	+	-
Mkt1	R.SNTESVLLQR.S	Forms cytoplasmic foci upon DNA replication stress	120-131	95	-	+
TDH2 (GAPDH isozyme 2)	M.VRVAINGFGR.I	Involves in glycolysis & gluconeogenesis	1-12	36	+	+

The list of proteins shown is a selection of the proteins identified in the most prominent band in the gel chunk for MS analysis: aa-amino acid; + detected; - not detected; MW, molecular weight. Protein abbreviations and functions were taken from Saccharomyces Genome Database (SGD, http://www.yeastgenome.org).

Discussion

4 Discussion

One means of gaining insight into the machinery of a cell is to isolate the individual components thereof. If the isolation of the individual components is carried out under non-denaturing conditions it may be possible to pull out other molecules associated with the component being investigated. By exploiting the advantages of protein tagging (Lichty *et al*., 2005), a technique which permits the attachment of a specific label to a selected protein, it is possible to gain information about interacting partners of the tagged protein within a complex. This provides information on whether or not different centres of metabolism are associated with each other in the living cell and if so, do specific conditions have to prevail. The associations identified may provide an explanation of the unexpected consequences observed when an alteration in the cell's primary metabolism affects an apparently unrelated cell component by revealing hitherto undiscovered links in cellular metabolism.

Data obtained can be used to create a map of how different nodes of metabolism interact with each other in the cell. It would also be possible to define both spatial and temporal interactions between metabolic nodes. Temporal interactions are likely to take place at different times during the cell cycle and/or possibly as a response to perturbations in the cell's metabolism whereas spatial interactions ensure the smooth running of the cell's metabolism. The perturbation investigated in this study exists in the different yeast strains created which lack one or more of the component polypeptides of the Prs enzyme. Information gained on the connectivity of apparently unrelated metabolic nodes will help to confirm known metabolic connectivity and has the potential to identify hitherto unknown interactions.

Extensive genetic studies have shown that *S. cerevisiae* cells are viable if they contain at least one of the following three minimal functional units – Prs1/Prs3, Prs2/Prs5 or Prs4/Prs5 (Hernando *et al*., 1999). Interestingly, Prs1 and Prs5 polypeptides contain insertions, termed non-homologous regions (NHRs), because at the time of their discovery the NHRs shared no similarity to any known sequences available in the databases. In the meantime sequence similarity of 77% has been found for Prs1 polypeptides of *S. cerevisiae* and *A. gossypii* (Ashbya Genome Database, AER083c). The sequence similarity is maintained in the N-terminal portion

of NHR1-1 for both species but drops off in the region of the *Bam*HI restriction site located centrally in the NHR1-1 of *S. cerevisiae*. Interestingly, sequences upstream of the *Bam*HI restriction site seem to be of importance for the connection of Prs1 and Mpk1/Slt2 in *S. cerevisiae* ((Ugbogu *et al*., 2013), Figure 5). Overall there is approximately 60% sequence identity in the *PRS5* genes from *S. cerevisiae* (YOL061w) and *A. gossypii* (ADR314c). However, there is a loss of sequence similarity at the locations of NHR5-1 and NHR5-2. Interestingly, one of the three postulated phosphosites of NHR5-2, S_{367}, is conserved in both species. The locations of NHR1-1 and NHR5-2 mean that the Mg^{2+}/ATP- and the PRPP-binding sites in *S. cerevisiae* Prs1 and Prs5 are more widely separated than in Prs2, Prs3 or Prs4. This could well be an explanation for the requirement of heterodimers as the minimal functional unit and correlates with the finding that it proved impossible to delete more than three of the five *PRS* genes and maintain viability (Hernando *et al*., 1999). Given the importance of Prs it is not surprising that mutations in any of the three human *PRPS* genes, two of which are X-linked and the third is located on chromosome 7 (Becker and Ahmed, 2000), have a serious impact on human metabolism. For instance, superactivity of Prs is associated with gouty arthritis whereas reduced Prs activity is associated with human neuropathies, such as Arts syndrome (de Brouwer *et al*., 2007) and Charcot-Marie-Tooth (CMTX5) disease (Synofzik *et al*., 2014). By means of *in vitro* mutagenesis we have introduced mutations into the *PRS1* gene of *S. cerevisiae so* that it contained either the mutation corresponding to Arts syndrome or CMTX5. Other mutations created in *PRS1* altered the Mg^{2+}/ATP- and/or the PRPP-binding sites. These mutated versions of *PRS1* have been used to investigate synthetic lethality caused by simultaneous deletion of the *PRS1* and *PRS5* ORFs. Synthetic lethality of *PRS* null mutations is also encountered when the *PRS3* and *PRS5* ORFs are deleted simultaneously and in the combinations *prs1*Δ*prs2*Δ*prs4*Δ and *prs2*Δ*prs3*Δ*prs4*Δ (Hernando *et al*., 1999). The synthetic lethality observed for the null mutations of the *PRS* genes is consistent with the hypothesis that these genes act in parallel pathways– metabolism and CWI– as represented by the two interacting sub-complexes, Prs1/Pr3 and Prs2/Prs4/Prs5 (Tucker and Fields, 2003, Ye *et al*., 2005, Ooi *et al*., 2006). All synthetic lethal interactions of *PRS* deletions encountered disturb both sub-complexes. To a certain extent these two parallel pathways are compensatory; if *PRS1* and *PRS3* are

deleted the strain is temperature-sensitive and grows more slowly (Wang *et al*., 2004) whereas deletion of *PRS2 PRS4 and PRS5* does not affect doubling time but has a significant impact on the enzyme activity, reducing it to 20% of that of the WT which is still sufficient to maintain viability.

The published data by (Ugbogu *et al*., 2013), obtained during the course of this PhD point to the requirement of NHR1-1 of Prs1 for the rescue of synthetic lethality but rules out the necessity of the PRPP-binding site at D326 of Prs1. Previously published data (Wang *et al*., 2004) has shown that Prs1 interacts with Slt2/Mpk1, the MAPK of the CWI pathway, only when NHR1-1 is present. This is a strong argument for the synthetic lethality of a *prs1*Δ*prs5*Δ strain being the result of a break-down of CWI in combination with impaired Prs activity. The interaction of Prs1 with the CWI pathway provides physical evidence for the phenotypes – caffeine sensitivity, Calcofluor White resistance and release of alkaline phosphatase – all of which are associated with *PRS1* deletant strains and diagnostic of impaired CWI signalling (Schneiter *et al*., 2000). Interestingly, when the Mg^{2+}/ATP-binding site, H130, is mutated there is no rescue but simultaneous mutation of H130 and D326 allows a certain degree of rescue. Both the Charcot-Marie-Tooth mutation at L115 and the Arts syndrome mutation at Q133 in *S. cerevisiae PRS1* are capable of rescuing synthetic lethality (Ugbogu *et al*., 2013).

In spite of their ability to rescue synthetic lethality it has been shown that in a *prs1*Δ background each of the *in vitro*-generated *PRS1* mutations influenced the temperature-dependent expression of Rlm1, a transcription factor belonging to the MADS box family (Watanabe *et al*., 1997) and an endpoint of the CWI pathway, following mild heat shock. Each of the mutants caused an increase in Rlm1 expression at 30°C, albeit not to the extent of a total *PRS1* deletion (Ugbogu *et al*., 2013).

Investigation of Rlm1 expression in the rescued strains (Figure 3.9) proved interesting and raised further questions. In order to measure Rlm1 expression it is necessary to introduce a second plasmid, one of the pHPS100 series of Rlm1 reporter plasmids (Kirchrath *et al*., 2000), in this case pHPS100-Leu, into the rescued strains. It would be reasonable to expect that the strain YN97-14

(*prs1*Δ*prs5*Δ) rescued with *PRS1* would show the same temperature-dependent Rlm1 response as a *prs5*Δ strain. At first glance this is the case. However, closer inspection revealed that the rescued strain, in spite of a modest temperature-dependent increase in Rlm1 expression, had less than 1/3rd of the Rlm1 transcriptional readout of a *prs5*Δ strain (Figure 3.9, inset). The only significant temperature response was observed in the strains rescued with Q133P or H130A/D326A. However, the basal expression of Rlm1 in the strain containing Q133P was reduced with respect to the other strains. If there was no interdependence of Prs1 and Prs5 the temperature-dependent Rlm1 response should have been comparable with that obtained when the same plasmid constructs were tested in a *prs1*Δ strain. When *PRS5* is present Q133P increased three-fold, D326A and H130A/D326A both increased four-fold whereas L115T increased 10-fold (Ugbogu *et al*., 2013). When *PRS5* is absent, it was possible to measure Rlm1 expression in liquid culture after a heat shock over a period of 2-3 doubling times (Figure 3.9). However, none of the rescued strains survived incubation at 37°C when grown on plates unless the media contained 1 M sorbitol (Figures 3.7). This is a clear indication that the rescued strains have impaired CWI although each of the mutated Prs1-plasmids which rescued synthetic lethality contains an intact NHR1-1 (Figure 1.2) and there is a modest increase in Phospho-Slt2 following exposure to mild heat shock in liquid culture over an extended period of time – up to 8 hr (Figure 3.10).

One outstanding question concerns the temperature sensitivity of the strains rescued with *PRS1* and *in vitro* mutants thereof in pGBT9 vectors. This is in contrast to the original YN97-14 strain which contains pVT1 (Hernando *et al*., 1999). Not only in pGAD-based plasmids but also in pGBT9-based plasmids is the expression from the *ADH1* promoter constitutive, but low (Bartel *et al*., 1993). A possible explanation is that the constitutive *ADH1* promoter in the pGBT9 plasmid backbone has a low level of expression resulting in *PRS1* expression at a level capable of maintaining viability at 30^{o}C but is insufficient to cope with temperature stress.

Rescue with Q133P resulted in a lower Rlm1 expression than in any of the other rescued strains. The Q133P mutation is located 60 aa residues upstream of NHR1-1 and three aa residues C-terminal to the cation-binding site. Theoretically, the

exchange of P (proline) for Q (glutamine) results in a disturbance of an α-helical section of *B. subtilis* Prs and *hPRPS1*, both of which have been crystallized (Eriksen *et al*., 2000, Li *et al*., 2007) and is termed “helix breakage”. The sequence of this region is conserved in the *S. cerevisiae PRS1* gene and it is therefore a reasonable assumption that the Q133P mutation alters the structure of Prs1. When tested for their caffeine sensitivity the rescued strain containing Q133P was more sensitive than the others (Figure 3.8). The addition of 1 M sorbitol in the presence of caffeine did relieve the caffeine sensitivity of Q133P but to a lesser extent than that of the other strains at 30°C. The combined stresses of caffeine and mild heat shock were not counteracted in the presence of 1 M sorbitol to the same degree in Q133P as in the other rescued strains. These observations are of interest because the rescued strain (YN97-14 (*prs1*Δ*prs5*Δ [prs1(Q133P)]) is more sensitive to caffeine with growth being inhibited at 3 mM whereas YN96-65 (*prs1*Δ [prs1(Q133P)]) (YN96-65) is capable of growth in the presence of 4 mM caffeine (Figures 3.8 and ((Ugbogu *et al*., 2013), Figure 4). Furthermore, the increased caffeine sensitivity of the rescued strains would suggest that the absence of *PRS5* has a negative impact on the maintenance of CWI.

Rlm1 expression is dependent on Slt2 phosphorylation (Watanabe *et al*., 1997). However, when the degree of Slt2 phosphorylation was examined by Western blotting the reduced expression of Rlm1 in Q133P at 30°C was not associated with a reduced phosphorylation level of Slt2 (cf. Figures 3.9 and 3.10). Surprisingly, the strength of the P-Slt2 signal in the Western blot varied across the strains tested with a temperature-dependent increase being most obvious in L115T, D326A and H130A/D326A. However, there was little difference in the relative P-Slt2 signal between all five strains at either 30°C or 37°C (Figure 3.11). Astonishingly, there was apparent variation in the strength of the Slt2 signal in response to mild heat shock, most notably in L115T and D326A. Such a temperature-dependent increase in Slt2 has been reported previously for an HA-tagged version of Slt2 (Hahn and Thiele, 2002), although it is generally accepted that Slt2 expression is not temperature-dependent (Kamada *et al*., 1995).

There is cumulative evidence that Prs5 contributes to CWI maintenance, possibly *via* Rlm1 expression. When CWI is examined in YN96-68 (*prs5*Δ) using the WT and the

collection of plasmids (Table 3.1) carrying *in vitro*-generated mutations of the aa residues of Prs5 postulated to be phosphorylated and located in the NHR5-2 region there were obvious plasmid-dependent differences in Rlm1 expression (Figure 3.12). It is stated in the literature (Ficarro *et al*., 2002) that of 216 phosphopeptides investigated only 11 were triply phosphorylated, one of which is Prs5. The three potentially phosphorylatable residues of Prs5 at positions S_{364}, S_{367} and S_{369} were simultaneously mutated in the plasmid prs5(479). When this plasmid was introduced into YN96-68 (*prs5*Δ) Rlm1 expression was increased at 30°C to approximately the same level as Rlm1 expression in the *prs5*Δ strain at 37°C implying that one or more of these three phosphosites may play a supporting role in the maintenance of CWI *via* Rlm1 expression. Additional mutations in the neighbouring phosphorylatable aa residues also influenced Rlm1 expression, albeit to different extents: mutation of residues N-terminal to those in prs5(479) (plasmid prs5(362.2)) caused a further increase in Rlm1 expression at 30°C whereas mutation of residues C-terminal to those in prs5(479) (plasmid prs5(365.1)) caused a reduction in Rlm1 expression at both 30°C and 37°C. Rlm1 expression was elevated at 37°C in the presence of all mutated Prs5 plasmids but never to the extent measured when Prs5 WT was present. The importance of this region for maintaining CWI is also demonstrated by elevated Rlm1 expression at 30°C in the presence of the truncated version of Prs5 (plasmid prs5(365.5)) which arose spontaneously during *in vitro* mutagenesis and contains a deletion of all three phosphosites and terminates prematurely 19 aa residues beyond them (Table 3.1).

The importance of Prs1 in the maintenance of CWI of *S. cerevisiae* has been previously reported (Ugbogu *et al*., 2013) and further investigated here. With the intention of re-creating the WT scenario the YN97-14 strains rescued from synthetic lethality by Prs1 or mutated versions thereof were transformed with Prs5 (WT) and its *in vitro*-mutated versions. However, the inclusion of the additional plasmid, even one containing WT Prs5, failed to correct the temperature sensitivity of the original rescued strains. This temperature sensitivity is associated with impaired CWI since as shown in Figure 3.19 when Prs1 WT is combined with Prs5 WT, prs5(479), prs5(362.2), prs5(365.1) or prs5(365.5), it is possible to rescue the temperature-sensitive phenotype only by the inclusion of 1 M sorbitol in the media. When Rlm1 expression was measured only the rescued strains containing Prs5 (WT) or

prs5(365.1) (Figure 3.20 (a)) were capable of expressing Rlm1 at 30°C at a level comparable with that of a WT strain. In the rescued strains containing prs1(L115T) together with Prs5 WT or its mutants no combination had a WT level of Rlm1 expression. In fact, Rlm1 expression remained at the level measured in the original rescued strain with the exception of the combination of prs1(L115T) and the truncated version of Prs5 (prs5(365.5)) which achieved a two-fold increase in Rlm1 expression at 37°C (Figure 3.20(b)). On the other hand, mutation of the the PRPP-binding site of Prs1, D326A in combination with Prs5 (WT) and prs5(479) led to a 1.5-fold increase of Rlm1 expression at the elevated temperature (Figure 3.20(c)). However, of all the strains created with H130A/D326A in combination with Prs5 (WT) and *in vitro* mutations thereof only in the presence of Prs5 (WT) was an increase measured in Rlm1 expression at 37^{o}C (Figure 3.20(d)) which is close to that reported for H130A/D326A in a *PRS1* deletant strain ((Ugbogu *et al*., 2013), Figure 6). Surprisingly, prs5(365.2) in this context results in a four-fold increase in Rlm1 expression at 30°C while at 37°C it is almost completely abolished.

On combining the helix breaker mutation prs1(Q133P) with Prs5 WT and *in vitro* mutations thereof, it was obvious from the temperature sensitivity test that growth was severely impaired at both temperatures and furthermore, the temperature-sensitive phenotype was not corrected by the inclusion of 1 M sorbitol in the media (Figure 3.21). It proved impossible to measure Rlm1 expression even after repeated attempts. This is not surprising since Q133P was the one mutant which was least successful in rescuing the synthetic lethality of YN97-14 (Figure 3.9) ((Ugbogu *et al*., 2013), Figure 3(a)). The inability of all the strains tested to grow at elevated temperature is a strong indication that alteration in either *PRS1* or *PRS5* has a significant effect on *S. cerevisiae* viability and the CWI pathway. It is therefore concluded that in addition to providing PRPP to the cell, two of the five Prs polypeptides, Prs1 and Prs5, have evolved in such a way that they are required for maintenance of CWI.

Mutation of the three phosphosites individually (Figure 3.15) and examination of their influence on Rlm1 expression at 30°C and 37°C, revealed that only when all three residues were mutated simultaneously was there a temperature-dependent effect on Rlm1 expression. However, in each of the three individual mutations the level of

Rlm1 expression was lower at 30°C than in either the WT or prs5(479). Western blot analysis of the strains carrying plasmid-borne versions of the *in vitro* mutations of Prs5 tested for Rlm1 expression was performed to examine the effect of mild heat shock on the phosphorylation status of Slt2 (Figures 3.13 and 3.16). Interestingly, when the intensity of the protein bands was quantified, the same fold effect was observed for all the strains except for the strain carrying prs5(362.2) which had the highest degree of phosphorylation at 30°C and increases slightly at 37°C (Figure 3.14). The elevated P-Slt2 signal at 30°C is in agreement with the elevated Rlm1 expression of the strain at the same temperature (Figure 3.12). The phosphorylation status of Slt2 in the strains carrying the individually mutated postulated phosphosites at aa residues 364, 367 and 369 is virtually the same as in the WT at 30°C and 37°C but lower than in prs5(479). Of the three individual mutants the P-Slt2 signal reaches the highest level in prs5(S369A) following incubation at 37°C (Figures 3.16 and 3.17).

To extend the investigation of Prs5's role in CWI we tested the influence of the mutations on Fks2 expression, which is a second endpoint of the CWI pathway (Zhao *et al*., 1998, de Nobel *et al*., 2000a) and provides a measure of cell wall damage (Jung and Levin, 1999, de Nobel *et al*., 2000a, Truman *et al*., 2009, Kim and Levin, 2010). It was previously shown (Vavassori, 2005, Wang, 2005) that in the absence of *PRS5*, in comparison to the WT, Fks2 expression was not increased following mild heat shock. When the combined and individual versions of the three phosphorylation sites, 364, 367 and 369, were tested for Fks2 expression following heat shock, none of the individual mutants responded differently to heat shock from the WT. However, simultaneous mutation of the three residues in question resulted in increased Fks2 expression at 30°C and a reduction in the increase of the expression at 37°C (Figure 3.18).

In summary it can be said that mutation of the three postulated phosphosites in Prs5 and the neighbouring region influences both Rlm1 and Fks2 transcriptional readouts as well as Slt2 phosphorylation. However, it cannot be said whether the influence of Fks2 is mediated directly *via* the influence of Mpk1/Slt2 on SBF or *via* Rlm1 acting on Mlp1 which in turn influences Swi4/Swi6 or a combination of both (Figure. 7) (Kim *et al*., 2008, Levin, 2011).

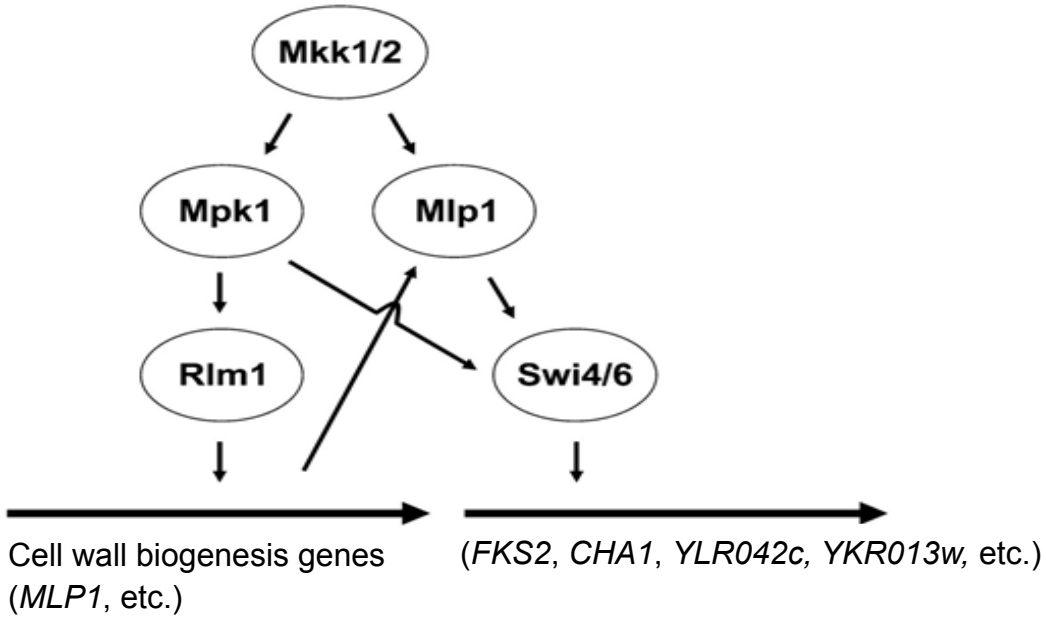

Figure 4.1: Model for activation of transcription by CWI signalling.

Mpk1/Slt2 phosphorylates Rlm1 under cell wall stress. Among the genes activated is *MLP1*, an orthologue of *MPK1*. Mlp1 is phosphorylated at T192 by Mkk1/2 and is an alternative activator for the Swi4/Swi6 transcription factor stimulating *FKS2* expression (modified after Levin, 2011).

An interesting connection between Fks2 and Prs1 occurs during transcription initiation of the *FKS2* gene. *FKS2* is one of the genes transcribed by the Paf1 complex (Chang *et al*., 1999, Truman *et al*., 2009, Kim and Levin, 2011). It has been demonstrated recently that there is an interaction between Mpk1/Swi4/Swi6 and the Paf1 complex at the promoter of *FKS2*. When the *FKS2* promoter is occupied by these two complexes, Mpk1/Slt2 is recruited to the Paf1 complex and *FKS2* is transcribed. An initial investigation showed that in the absence of *PAF1 PRS1* transcription was reduced by approximately 50% (Chang *et al*., 1999). It is therefore possible to speculate that in the absence of *PAF1 FKS2* transcription would be impaired as would *PRS1* transcription, thus creating a scenario of compromised CWI which is consistent with the phenotypes associated with perturbation of the Prs complexes. Furthermore, disruption of Paf1 has a negative impact on the induction of galactose-regulated genes (Shi *et al*., 1996). Deletion of *either PRS1* or *PRS3* abolishes growth on 2% galactose as the sole carbon source (Figure 3.2) whereas deletion of *PRS2*, *PRS4* or *PRS5* had no effect, further evidence that the two sub-complexes of Prs contribute differentially to certain aspects of yeast metabolism.

4.1 Interdependence of Prs1 and Prs3

Further insight into the interaction between the five Prs polypeptides has been gained by examining yeast strains which contain an integrated version of *GFP-PRS1* at the cognate locus. The results corroborate the genetic evidence for the existence of the Prs1/Prs3 complex since in the strain lacking *PRS3* the GFP-Prs1 signal is lost (Figure 3.1). Restoration of the GFP-Prs1 signal was achieved by introducing a plasmid-borne version of Prs3 into the strain. Admittedly, the strength of the GFP-Prs1 signal in the presence of a plasmid-borne copy of Prs3 is less than that of the WT (Figure 3.1, lanes (3), (8) and (9)). A possible explanation for this is that Prs3 expressed from the plasmid pGAD-Prs3 is under the control of the *ADH1* promoter which in the pGAD background has a constitutive, but low, expression (Bartel *et al*., 1993). Interestingly, the presence of the *GAL4* activation domain located between the *ADH1* promoter and the *PRS3* ORF does not interfere with the ability of Prs3 to stabilize Prs1. The Western blotting experiment also provides a possible explanation for the synthetic lethality caused by simultaneous deletion of *PRS3* and *PRS5* since in the absence of *PRS3*, Prs1 is unstable; therefore, such a strain is effectively *prs1*Δ *prs3*Δ*prs5*Δ.

4.2 Interaction of Prs1 with the CWI pathway

To verify the Y2H interaction of Prs1 with Slt2, as described in Wang *et al*. (2004), co-immunoprecipitation was performed using crude extracts of a yeast strain which contains an N-terminal GFP-tagged version of Prs1 at the *PRS1* locus (Schneiter *et al*., 2000) and episomal, plasmid-borne copies of C-terminally FLAG-tagged WT Slt2 and two mutated constructs thereof. One mutated plasmid was altered at the aa residues T190 and Y192 of Mkp1/Slt2. T190 and Y192 were converted to alanine (A) and phenylalanine (F), respectively and resulted in the loss of the two phosphorylation sites within the activation loop of Slt2 that are phosphorylated by Mkk1/2 (Figure 1.2) following activation of the CWI pathway. The other mutation in Slt2 converted lysine (K) at aa residue 54 to arginine (R), thereby blocking the kinase activity of Slt2 and preventing the activation of the transcription factor Rlm1 (Kim *et al*., 2007, Kim *et al*., 2008). The co-immunoprecipitation revealed that both the WT and the kinase-negative species of Slt2 interacted with Prs1; however, the non-

phosphorylatable version of Slt2 did not. Furthermore, the faint GFP signal observed following interaction of WT Slt2 was not visible with either of the two mutant forms at 30°C (Figure 3.4, lanes (3), (9) and (15)). Nevertheless, both WT Slt2 and the kinase inactive mutant slt2(K54R) interacted with Prs1 following the mild heat shock induced by shifting the incubation temperature from 30^{o}C to 37^{o}C (lanes (4) and (16)).

Confirmation of the results of the co-immunoprecipitation was obtained by using a plasmid-borne, galactose-inducible C-terminally His-tagged version of Prs1 instead of the N-terminally GFP-labelled Prs1 chromosomally integrated at the *PRS1* locus in combination with the FLAG-tagged WT and mutated versions of Slt2. The strain YN96-65 from which the entire coding region of *PRS1* has been deleted, was the host strain for the plasmids (Figure 3.5). In the absence of galactose there was no interaction with any of the three Slt2 species tested (lanes (1), (4) and (7)). However, following growth in galactose His-tagged Prs1 interacted with both the WT and the kinase-inactive species of Slt2 and the signal strength increased in response to mild heat shock (lanes (2), (3), (8) and (9)). Galactose induction of Prs1 produced no signal at either 30^{o}C or 37^{o}C in the presence of the non-phosphorylatable version of Slt2 (lanes (5) and (6)).

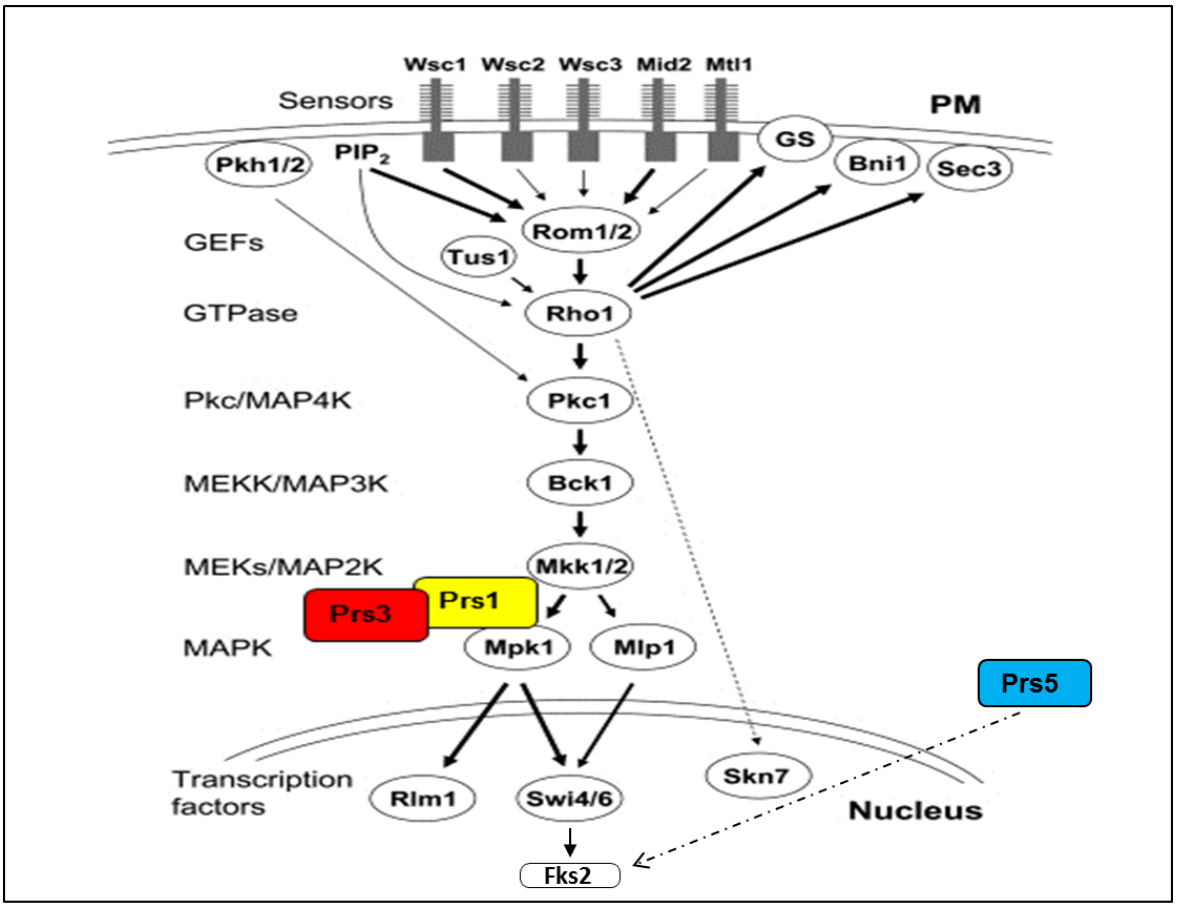

Figure 4.2: Interaction of Prs1 with Mpk1/Slt2

This figure illustrates the interaction of the Prs1/Prs3 subcomplex with Mpk1/Slt2 as demonstrated by Y2H (Wang *et al*., 2004) and co-immunoprecipitation. The dashed line (-·-·->) linking Prs5 to Fks2 is suggested by the results obtained when the mutations S_{364}A, S_{367}A and S_{369}A in Prs5 were tested for their influence on the expression of Fks2 (cf. 3.5.4). For further details of nomenclature, see legend of Figures 1.3 (modified after Levin, 2011).

Taking the results of the two independent co-immunoprecipitation approaches and previous Y2H data (Wang *et al*., 2004) into consideration, there is now sufficient evidence to state that Prs1 and Slt2 interact with each other, most likely *via* NHR1-1 of Prs1, when Slt2 is phosphorylated in its activation loop by MKK1/2 at T190 and Y192 with the signal increasing in strength following a mild heat shock. Therefore, Slt2 must be phosphorylated, i.e. the CWI pathway must be activated at least to this point, in order to associate with Prs1. This result is reminiscent of the finding by Kim *et al*. (2008) that the catalytic activity of Slt2 is not necessary for the association of Slt2 and Swi4; the latter is a component of the SBF dimeric complex (Swi4/Swi6) which in addition to being necessary for regulation of G_1-specific transcription,

synthesis and repair of DNA (Harrington and Andrews, 1996), is also an endpoint of the CWI pathway (Kim *et al*., 2008, Truman *et al*., 2009).

A co-immunoprecipitation experiment in which the NHR1-1 has been deleted from the labelled version of Prs1 would be the final proof that the interaction between Prs1 and Slt2 is dependent on the presence of NHR1-1. One would predict that there would be no interaction with any version, including the WT, of Slt2. Taking into account the data reported in section 3.1 and in (Ugbogu *et al*., 2013) it is highly likely it is the Prs1/Prs3 subcomplex which is associated with Mpk1/Slt2 since in the absence of *PRS3* Prs1 appears to be unstable (Figure 3.1), an example of "guilt-by-association" (Oliver, 2000)

4.3 Isolation of the Prs5 polypeptide and associated proteins

The data acquired and discussed so far, are compatible with Prs5 contributing to the maintenance of CWI. Exploitation of the tagged version of Prs5 expressed in either a WT background YN11-01 (*prs5*Δ) or in the strain YN97-91 which is devoid of the Prs2/Prs4/Prs5 complex could be expected to throw some light on interacting partners of Prs5. It has been previously shown by Y2H that the yeast homologue of GSK3, Rim11, interacts with Prs3 and Prs5 (Vavassori, 2005, Wang, 2005, Kleineidam *et al*., 2009). Affinity purification of the His-tagged Prs5 followed by separation on SDS-PAGE revealed that elution with increasing concentration of imidazole gave rise to distinct protein bands which did not cross-react with the antibody against the His-tag. The band corresponding to the His-tagged Prs5 (Figure 3.25, lane (6)) as well as the two non-crossreacting bands highlighted in lanes (4) and (5) were subjected to MALDI-TOF analysis (Domon and Aebersold, 2006, Bensimon *et al*., 2012). Using correlative yeast database searching seven peptides matched with Prs5 (S288c) and covered 36% of the 496 aa residues of this polypeptide. In agreement with the specificity of trypsin which cleaves specifically at the C-terminal side of the basic aa residues lysine and arginine (R/K) when they are not followed by proline (P) each of the seven peptides had either an arginine (R) or lysine (K) residue at its C-terminus with the aa residue immediately N-terminal to the first aa residue of the peptide was also either arginine or lysine. The longest peptide

identified extended from position 117-145 of Prs5 (ENYTFESHPGTPVSSSLMTQRPGAESSLK; gi: 6324511) and coincides with the N-terminal region of the NHR5-1 of Prs5 (Figure 1.4). A second peptide from position 273-291 (IPDYQDAVIVSPDAGGAKR) matched a region of ribose-phosphate pyro-phosphokinase from *Wickerhamomyces ciferrii* (GenBank: CCH46852.1, gi: 406601506). One other match corresponded to a synthetic histidine-tagged glucoamylase construct (gi: 46398247) and the remaining four matches were with unknown proteins of fungal origin (Mascot database). The sample was also treated with alkaline phosphatase but no coverage of the Prs5 peptide reported to be phosphorylated was obtained, in agreement with the strain having been grown at 30^{o}C (Dr Catherine Botting, personal communication). According to MS/MS analysis the 42 KDa non-crossreacting band corresponded to Tef2 *of S. cerevisiae* (S288c) and the remaining 44 peptides recognized the translation elongation factor 1α from a variety of fungi (Mascot database).

The material in the three excised bands (Figure 3.25, lanes (4), (5) and (6)) was subjected to electrospray ionization (ESI) which is suited to the analysis of complex peptide mixtures (Gygi and Aebersold, 2000). As was to be expected the highest number of matches, 119, was achieved for Prs5 from *S. cerevisiae* (S288c) with 55% coverage of the polypeptide. The MS/MS profile for Prs5 peptide (LIISNTVPQDR) extending from position 446-456 is shown in Figure 3.26. The additional 35 peptides did not match any other Prs polypeptides from *S. cerevisiae*. ESI of the 42 KDa band identified again Tef2 from *S. cerevisiae* (S288c) and other translational elongation factors of fungal origin. The 36 KDa band was analyzed by ESI and consisted mostly of peptide mixtures falling in the category of GAPDH proteins, e.g. Tdh1, Tdh2 and Tdh3 from *S. cerevisiae* (S288c) which are involved in the synthesis of 1,3-bisphosphoglycerate found in the cytoplasm and the yeast cell wall (http://www.yeastgenome.org).

An isolation of the His-tagged Prs5 polypeptide from the same two strains was repeated using His SpinTrap^{TM} technology. The material eluted with 200 mM imidazole was separated by SDS-PAGE and a section of the gel-containing proteins with a MW in the range of 30-100 KDa was excised for each strain (data not shown). The material from the gel was divided into two aliquots for each strain, an intensely

stained band in the middle of the chunk. 29 proteins could be identified in the intense band of YN11-01 and included Prs3 and Prs5. The corresponding intense band from YN97-91 also identified 29 proteins, *inter alia* only Prs5 (Mascot database). Following ESI-QUAD-TOF the peptides obtained from the YN11-01 chunk could be matched to 488 proteins in the entire NCBI protein database (http://www.ncbi.nlm.nih.gov/pubmed) including Prs1, Prs3 and Prs5 from *S. cerevisiae*. Interestingly, the identified Prs1 peptide ($_{229}$QGDHPNEEENIILSNGIQTAR$_{249}$, gi: 6322667) is located in the NHR1-1 region of the Prs1 polypeptide. A further Prs1 peptide extending from 307-317 spanned the C-terminal junction of NHR1-1 (Figure 3.27). This is further evidence that NHR1-1 is an integral part of the Prs1 polypeptide which links the Prs1/Prs3 complex to Mkp1/Slt2 of the CWI pathway. 588 hits were found for the YN97-91 chunk, two of which corresponded to Prs3 and Prs5. Upon closer inspection of the data it was found that there were 11 proteins, including Prs3 and Prs5, from *S. cerevisiae*, common to both strains. Other proteins co-migrating with Prs5 are stress response proteins (Hog1, Bmh1), morphogenesis and glucose sensing regulators, transcription, protein synthesis and heat shock proteins (Yck2, Vma2, YJL177w, Hsp26, Zuo1) are included in Table 3.2. However, further investigation is required since there is a possibility that weak or transient protein interactions may not be detected. One approach would be to use Blue Native-PAGE or size exclusion chromatography, both of which separate components of protein complexes according to size. It is possible that as a result of the interaction between Prs1 and a component of the CWI pathway that Prs1 or the Prs1/Prs3 complex shuttles between the cytoplasm and the nucleus to accomplish the activation of the genes whose products are involved in the re-modelling of the cell wall. One approach would be to create GFP-tagged versions of Prs1 and Prs3 in centromeric vectors in order to detect any change in the location of the tagged proteins by confocal microscopy when the cells are exposed to conditions in which the CWI pathway is switched on.

Summary and perspective

The results of this study presented here provide further evidence for dual functionality of the two Prs complexes Prs1/Prs3 and Prs2/Prs4/Prs5. The reason for the dual functionality may be related to the presence of the non-homologous regions (NHRs) in Prs1 and Prs5. Interestingly, NHR1-1 and NHR5-2, albeit to a lesser extent, both contribute to the maintenance of CWI. Co-immunoprecipitation has confirmed the interaction of Prs1 with activated, but catalytically inactive, Mpk1/Slt2, although the site of interaction has not been localized to the NHR1-1 as shown by Y2H analysis. The three neighbouring phosphosites in NHR5-2 have also been shown to play a role in the expression of Fks2, the alternative subunit of 1,3-β-GS, which is predominantly expressed under stress conditions and is an endpoint of the CWI pathway. On account of the existence of the NHRs one can describe Prs1 and Prs5 as moonlighting proteins (Jeffery, 1999). When complexed in the minimal functional units – Prs1/Prs3, Prs2/Prs5, Prs4/Prs5 – or in the two interacting sub-complexes of Prs1/Prs3 and Prs2/Prs4/Prs5 they ensure that the essential metabolite, PRPP, required for metabolism is linked to the signalling pathway responsible for maintaining CWI. Data available in the PhosphoPep database (Bodenmiller *et al*., 2008) is consistent with the first aa of NHR1-1, S_{199} being phosphorylated by Torc1 and Mkk1, both of which are components of the CWI pathway. Knockouts of either of these two kinases resulted in a 1.9 and 1.6-fold increase, respectively, in the expression of *PRS1*. It is intriguing to speculate that these two kinases may influence Prs1 expression in concert with the activation of the CWI pathway.

A potential kinase candidate for the three phosphosites in Prs5 NHR5-2 is Rim11 (Bianchi *et al*., 1993, Hirata *et al*., 2003, Griffioen *et al*., 2003, Yabuki *et al*., 2014) which has been shown in a high-throughput assay to interact with Prs2, Prs3 and Prs5 (Ho *et al*., 2002) and confirmed by us in Y2H analysis (Kleineidam *et al*., 2009). Preliminary Y2H analysis indicates that mutation of the three phosphosites interferes with the interaction of Prs5/Prs4 and Prs5/Rim11 (Young, 2012) (E. Young, unpublished data).

One aspect of PRPP metabolism, not addressed in this study, is the impact of mutating *PRS* genes on nucleotide pools. An interrogation of SGD has shown that

Ixr1 which regulates the expression of the ribonucleotide reductase, Rnr1 is involved in the maintenance of dNTP pools (Yao *et al*., 2003, An *et al*., 2006) and also regulates Prs1 and Prs3 in opposite ways. Interestingly Ixr1 is implicated in the regulation of Prs1, Prs3, Rim11, and Rlm1 (Tsaponina *et al*., 2011).

The synthetic lethality of a *prs1*Δ*prs5*Δ strain can be rescued by a WT copy of *PRS1* as well as by versions of *PRS1* mutated in the Mg^{2+}/ATP and the PRPP-binding sites or in conserved residues corresponding to missense mutations associated with human neuropathies. However, the presence of NHR1-1 is essential for the rescue of the synthetic lethality, as was also demonstrated by the inability of h*PRPS1* which does not contain an equivalent of NHR1-1, to rescue synthetic lethality (Ugbogu *et al*., 2013).

The results obtained will also prove useful in the international project aimed at constructing a 'designer' yeast containing synthetic chromosomes (Annaluru *et al*., 2014, Pennisi, 2014). It would appear that at the very least *S. cerevisiae* has a requirement for the product of the *PRS1* gene on account of its role in the maintenance of CWI and for the *PRS3* gene since, when this is absent, Prs1 is unstable.

Although the investigations have been performed in yeast the reaction carried out by Prs is found in all organisms with the exception of parasites which rely on the host's metabolism. . This would offer the opportunity of exploiting Prs as a drug target. Information gained from the yeast *PRS* genes could identify region(s) in the unique bacterial *PRS* gene which could be targeted for drug therapy. A further example relevant to the broader biomedical application of this work is provided by the considerable sequence similarity of the *S. cerevisiae* and *Candida albicans* Prs polypeptides (CGD, http://www.candidagenome.org/). Such information may be beneficial in identifying potential drug targets against candidiasis (Maubon *et al*., 2014), the most common deep-seated human fungal infection that endanger the life of the patient.

In humans increased Prs activity is associated with gouty arthritis whereas reduced Prs activity is associated with human neuropathies. In the long time it might be possible to find a way of interacting with the *h*PRPS complex, such that Prs activity

could be modulated to reduce the superactivity associated with gouty arthritis. Another, more speculative approach would to investigate the PRPS-associated polypeptides (PAPs) which are thought to exert a regulatory function on Prs (Tatibana *et al*., 1995). Such an approach might, in the long term, lead to a means of regulating Prs activity in humans to counteract the reduce activity associated with human neuropathies.

References

References

Addinall, S. G., Downey, M., Yu, M., Zubko, M. K., Dewar, J., Leake, A., Hallinan, J., Shaw, O., James, K., Wilkinson, D. J., Wipat, A., Durocher, D. & Lydall, D. (2008). A genomewide suppressor and enhancer analysis of cdc13-1 reveals varied cellular processes influencing telomere capping in *Saccharomyces cerevisiae*. *Genetics* **180,** 2251-2266.

Addinall, S. G., Holstein, E. M., Lawless, C., Yu, M., Chapman, K., Banks, A. P., Ngo, H. P., Maringele, L.,Taschuk, M., Young, A., Ciesiolka, A., Lister, A. L., Wipat, A., Wilkinson, D. J. & Lydall, D. (2011). Quantitative fitness analysis shows that NMD proteins and many other protein complexes suppress or enhance distinct telomere cap defects. *PLoS Genet.* **7**, e1001362.

Aguilar-Uscanga, B. & François, J. M. (2003). A study of the yeast cell wall composition and structure in response to growth conditions and mode of cultivation. *Lett. Appl. Microbiol.* **37**, 268-274.

Ahmed, M., Taylor, W., Smith, P. R. & Becker, M. A. (1999). Accelerated transcription of *PRPS1* in X-linked overactivity of normal human phosphoribosylpyrophosphate synthetase. *J. Biol. Chem.* **274**, 7482-7488.

Akella, R., Moon, T. M. & Goldsmith, E. J. (2008). Unique MAP Kinase binding sites. *Biochim. Biophys. Acta* **1784**, 48-55.

Alderwick, L. J., Lloyd, G. S., Lloyd, A. J., Lovering, A. L., Eggeling, L. & Besra, G. S. (2011). Biochemical characterization of the *Mycobacterium tuberculosis* phosphoribosyl-1-pyrophosphate synthetase. *Glycobiology* **21**, 410-425.

Alonso-Monge, R., Real, E., Wojda, I., Bebelman, J.-P., Mager, W. H. & Siderius, M. (2001). Hyperosmotic stress response and regulation of cell wall integrity in *Saccharomyces cerevisiae* share common functional aspects. *Mol. Microbiol.* **41**, 717-730.

An, X., Zhang, Z., Yang, K. & Huang, M. (2006). Cotransport of the heterodimeric small subunit of the *Saccharomyces cerevisiae* ribonucleotide reductase between the nucleus and the cytoplasm. *Genetics* **173**, 63-73.

Annaluru, N., Muller, H., Mitchell, L. A., Ramalingam, S., Stracquadanio, G., Richardson, S. M., Dymond, J. S., Kuang, Z., Scheifele, L. Z., Cooper, E. M., Cai, Y., Zeller, K., Agmon, N., Han, J. S., Hadjithomas, M., Tullman, J., Caravelli, K., Cirelli, K., Guo, Z., London, V., Yeluru, A., Murugan, S., Kandavelou, K., Agier, N., Fischer, G., Yang, K., Martin, J. A., Bilgel, M., Bohutski, P., Boulier, K. M., Capaldo, B. J., Chang, J., Charoen, K., Choi, W. J., Deng, P., Dicarlo, J. E., Doong, J., Dunn, J., Feinberg, J. I., Fernandez, C., Floria, C. E., Gladowski, D., Hadidi, P., Ishizuka, I., Jabbari, J., Lau, C. Y., Lee, P. A., Li, S., Lin, D., Linder, M. E., Ling, J., Liu, J., Liu, J., London, M., Ma, H., Mao, J., Mcdade, J. E., McMillan, A., Moore, A. M., Oh, W. C., Ouyang, Y., Patel, R., Paul, M., Paulsen, L. C., Qiu, J., Rhee, A., Rubashkin, M. G., Soh, I. Y., Sotuyo, N. E., Srinivas, V., Suarez, A., Wong, A., Wong, R., Xie, W. R., Xu, Y., Yu, A. T., Koszul, R., Bader, J. S., Boeke, J. D. & Chandrasegaran, S. (2014). Total synthesis of a functional designer eukaryotic chromosome. *Science* **344,** 55-58.

Arts, W. F., Loonen, M. C., Sengers, R. C. & Slooff, J. L. (1993). X-linked ataxia, weakness, deafness, and loss of vision in early childhood with a fatal course. *Annu. Neurol.* **33**, 535-539.

Ausubel, F.M., Brent, R., Kingston, R.E., Moore, D.D., Seidman, J.G., Smith, J.A. & Struhl, K. (1995). Current Protocols in Molecular biology. Greene Publishing Associates and Wiley-Interscience, New York.

Baetz, K., Moffat, J., Haynes, J., Chang, M. & Andrews, B. (2001). Transcriptional coregulation by the cell integrity mitogen-activated protein kinase Slt2 and the cell cycle regulator Swi4. *Mol. Cell. Biol.* **21**, 6515 - 6528.

Bartel, P. L., Chien, C.-T., Sternglanz, R. & Fields, S. (1993). Using the two-hybrid system to detect protein-protein interactions: In *Cellular Interactions in Development: A Practical Approach*, pp. 153-179. Edited by D. A. Hartley. Oxford: Oxford University Press.

Becker, M. A., Losman, M. J., Wilson, J. & Simmonds, H. A. (1986). Superactivity of human phosphoribosyl pyrophosphate synthetase due to altered regulation by nucleotide inhibitors and inorganic phosphate. *Biochim. Biophys. Acta* **882**, 168-176.

Becker, M. A., Puig, J. G., Mateos, F. A., Jimenez, M. L., Kim, M. & Simmonds, H. A. (1988). Inherited superactivity of phosphoribosylpyrophosphate synthetase: Association of uric acid overproduction and sensorineural deafness. *Am. J. Med.* **85**, 383-390.

Becker, M. A., Kim, M. & Husain, K. (1989). PRPP and purine nucleotide metabolism in human lymphoblasts with both PRPP synthetase superactivity and HGPRT deficiency. *Adv. Exp. Med. Biol.* **253**, 13-20.

Becker, M. A., Taylor, W., Smith, P. R. & Ahmed, M. (1996). Overexpression of the normal phosphoribosylpyrophosphate synthetase 1 isoform underlies catalytic superactivity of human phosphoribosylpyrophosphate synthetase. *J. Biol. Chem.* **271**, 19894-19899.

Becker, M. A. & Ahmed, M. (2000). Cell type-specific differential expression of human PRPP synthetase (PRPS) genes. *Adv. Exp. Med. Biol.* **486**, 5-10.

Becker, M. A. (2001). Phosphoribosylpyrophosphate synthetase and the regulation of phosphoribosylpyrophosphate production in human cells. *Prog. Nucleic Acid Res. Mol. Biol.* **69**, 115-148.

Bensimon, A., Heck, A. J. & Aebersold, R. (2012). Mass spectrometry-based proteomics and network biology. *Annu. Rev. Biochem.* **81**, 379-405.

Bianchi, M. W., Plyte, S. E., Kreis, M. & Woodgett, J. R. (1993). A *Saccharomyces cerevisiae* protein-serine kinase related to mammalian glycogen synthase kinase-3 and the *Drosophila melanogaster* gene *shaggy* product. *Gene* **134**, 51-56.

Binley, K. M., Radcliffe, P. A., Trevethick, J., Duffy, K. A. & Sudbery, P. E. (1999). The yeast *PRS3* gene is required for cell integrity, cell cycle arrest

upon nutrient deprivation, ion homeostasis and the proper organization of the actin cytoskeleton. *Yeast* **15**, 1459-1469.

Bodenmiller, B., Campbell, D., Gerrits, B., Lam, H., Jovanovic, M., Picotti, P., Schlapbach, R. & Aebersold, R. (2008). PhosphoPep – a database of protein phosphorylation sites in model organisms. *Nature Biotech.* **26**, 1339-1340.

Boeke, J. D., LaCroute, F. & Fink, G. R. (1984). A positive selection for mutants lacking orotidine-5'-phosphate decarboxylase activity in yeast: 5-fluoro-orotic acid resistance. *Mol. Gen. Genet.* **197**, 345-346.

Bradford, M. M. (1976). A rapid and sensitive method for the quantitation of microgram quantities of protein utilizing the principle of protein-dye binding. *Anal. Biochem.* **72**, 248-254.

Breda, A., Martinelli, L. K., Bizarro, C. V., Rosado, L. A., Borges, C. B., Santos, D. S. & Basso, L. A. (2012). Wild-type phosphoribosylpyrophosphate synthase (PRS) from *Mycobacterium tuberculosis*: a bacterial class II PRS? *Plos One* **7**, e39245.

Bruckner, A., Polge, C., Lentze, N., Auerbach, D. & Schlattner, U. (2009). Yeast two-hybrid, a powerful tool for systems biology. *Int. J. Mol. Sci.* **10**, 2763-2788.

Buehrer, B. M. & Errede, B. (1997). Coordination of the mating and cell integrity mitogen-activated protein kinase pathways in *Saccharomyces cerevisiae*. *Mol. Cell. Biol.* **17**, 6517-6525.

Carter, A. T., Narbad, A., Pearson, B. M., Beck, K. F., Logghe, M., Contreras, R. & Schweizer, M. (1994). Phosphoribosylpyrophosphate synthetase (PRS): a new gene family in *Saccharomyces cerevisiae*. *Yeast* **10**, 1031-1044.

Carter, A. T., Beiche, F., Hove-Jensen, B., Narbad, A., Barker, P. J., Schweizer, L. M. & Schweizer, M. (1997). *PRS1* is a key member of the gene family encoding phosphoribosylpyrophosphate synthetase in *Saccharomyces cerevisiae*. *Mol. Gen. Genet.* **254**, 148-156.

Chang, M., French-Cornay, D., Fan, H. Y., Klein, H., Denis, C. L. & Jaehning, J. A. (1999). A complex containing RNA polymerase II, Paf1p, Cdc73p, Hpr1p, and Ccr4p plays a role in protein kinase C signaling. *Mol. Cell. Biol.* **19**, 1056-1067.

Chen, R. E. & Thorner, J. (2007). Function and regulation in MAPK signaling pathways: Lessons learned from the yeast *Saccharomyces cerevisiae*. *Biochim. Biophys. Acta* **1773**, 1311-1340.

Cherney, M. M., Cherney, L. T., Garen, C. R. & James, M. N. (2011). The structures of *Thermoplasma volcanium* phosphoribosyl pyrophosphate synthetase bound to ribose-5-phosphate and ATP analogs. *J. Mol. Biol.* **413**, 844-856.

Cid, V. J., Duran, A., del Rey, F., Snyder, M. P., Nombela, C. & Sánchez, M. (1995). Molecular basis of cell integrity and morphogenesis in *Saccharomyces cerevisiae*. *Microbiol. Rev.* **59**, 345-386.

de Brouwer, A. P., van Bokhoven, H., Nabuurs, S. B., Arts, W. F., Christodoulou, J. & Duley, J. (2010). *PRPS1* mutations: Four distinct syndromes and potential treatment. *Am. J. Hum. Genet.* **86**, 506-518.

de Brouwer, A. P. M., Williams, K. L., Duley, J. A., Van Kuilenburg, A. B. P., Nabuurs, S. B., Egmont-Petersen, M., Lugtenberg, D., Zoetekouw, L., Banning, M. J. G., Roeffen, M., Hamel, B. C. J., Weaving, L., Ouvrier, R. A., Donald, J. A., Wevers, R. A., Christodoulou, J. & Van Bokhoven, H. (2007). Arts syndrome is caused by loss-of-function mutations in PRPS1. *Am. J. Hum. Genet.* **81**, 507-518.

de Nobel, H., Ruiz, C., Martin, H., Morris, W., Brul, S., Molina, M. & Klis, F. M. (2000a). Cell wall perturbation in yeast results in dual phosphorylation of the Slt2/Mpk1 MAP kinase and in an Slt2-mediated increase in *FKS2-lac*Z expression, glucanase resistance and thermotolerance. *Microbiology* **146**, 2121-2132.

de Nobel, H., van Den Ende, H. & Klis, F. M. (2000b). Cell wall maintenance in fungi. *Trends Microbiol.* **8**, 344-345.

Delley, P. A. & Hall, M. N. (1999). Cell wall stress depolarizes cell growth *via* hyperactivation of RHO1. *J. Cell Biol.* **147**, 163-174.

Denis, V. & Cyert, M. S. (2005). Molecular analysis reveals localization of *Saccharomyces cerevisiae* protein kinase C to sites of polarized growth and Pkc1p targeting to the nucleus and mitotic spindle. *Eukaryotic Cell* **4**, 36-45.

Domon, B. & Aebersold, R. (2006). Mass spectrometry and protein analysis. *Science* **312**, 212-217.

Douglas, C. M., Foor, F., Marrinan, J. A., Morin, N., Nielsen, J. B., Dahl, A. M., Mazur, P., Baginsky, W., Li, W., El-Sherbeini, M. Clemas, J.A., Mandala, S. M., Frommer, B. R. and Kurtz, M. B. (1994). The *Saccharomyces cerevisiae FKS1 (ETG1)* gene encodes an integral membrane protein which is a subunit of 1,3-β-D-glucan synthase. *Proc. Natl. Acad. Sci. USA.* **91**, 12907-12911.

Dujon, B., Boyer, J., Fairhead, C., Gaillon, L., Galisson, F., Michaux, G., Perrin, A., Tettelin, H., Thierry, A., Albermann, K., Hani, J., Heumann, K., Mewes, H. W., Zollner, A., Kleine, K., Aldea, M., Casas, C., Herrero, E., Alexandraki, D., Katsoulou, C., Tzermia, M., Ansorge, W., Benes, V., Rechmann, S., Schwager, C., Teodoru, C., Voss, H., Wiemann, S., Arino, J., Casamayor, A., Bohn, C., Bolotin-Fukuhara, M., Daignan-Fornier, B., Dang, D. V., Kalogeropoulos, A., Valens, M., Bordonné, R., Camasses, A., Madania, A., Martin, R. P., Poch, O., Tarassov, I. A., Winsor, B., Chéret, G., Sor, F., Cziepluch, C., Jauniaux, J. C., Kordes, E., Poirey, R., Pujol, A., Tobiasch, E., de Haan, M., Grivell, L. A., Maarse, A. C., Delius, H., Hebling, U., Hofmann, B., Durand, P., Hilger, F., Portetelle, D., Vandenbol, M., Feldmann, H., Mannhaupt, G., Vetter, I., Gamo, F. J., Gancedo, C., Lafuente, M. J., Goffeau, A., Purnelle, B., Goulding, S. E., Hand, N. J., Parle-mcdermott, A. G., Wolfe, K. H., Habbig, B., Hattenhorst, U., Hollenberg, C. P., Ramezani Rad, M., Hernando, Y., Pearson, B. M., Schweizer, M., Zumstein, E., Hiesel, R., Unseld, M., Hughes, B., Pohl, T. M., Landt, O., Louis, E. J., Marck, C.,

Paces, V., Vlcek, C., Pettersson, B., Sterky, F., Uhlen, M., Voet, M., Volckaert, G., Wambutt, R. & Wedler, H. (1997). The nucleotide sequence of *Saccharomyces cerevisiae* chromosome XV. *Nature* (6632 Suppl.)*,* **387,** 98-102.

Duttler, S., Pechmann, S. & Frydman, J. (2013). Principles of cotranslational ubiquitination and quality control at the ribosome. *Mol. Cell* **50**, 379-393.

Dwane, S. & Kiely, P. A. (2011). Tools used to study how protein complexes are assembled in signaling cascades. *Bioengineered* **2**, 247-259.

Edmunds, J. W. & Mahadevan, L. C. (2004). MAP kinases as structural adaptors and enzymatic activators in transcription complexes. *J. Cell Sci.* **117**, 3715-3723.

Elble, R. (1992). A simple and efficient procedure for transformation of yeasts. *BioTechniques* **13**, 18-20.

Eriksen, T. A., Kadziola, A., Bentsen, A. K., Harlow, K. W. & Larsen, S. (2000). Structural basis for the function of *Bacillus subtilis* phosphoribosyl-pyrophosphate synthetase. *Nat Struct. Biol.* **7**, 303-308.

Evangelista, M., Blundell, K., Longtine, M. S., Chow, C. J., Adames, N., Pringle, J. R., Peter, M. & Boone, C. (1997). Bni1p, a yeast formin linking Cdc42p and the actin cytoskeleton during polarized morphogenesis. *Science* **276**, 118-122.

Fasolo, J., Sboner, A., Sun, M. G., Yu, H., Chen, R., Sharon, D., Kim, P. M., Gerstein, M. & Snyder, M. (2011). Diverse protein kinase interactions identified by protein microarrays reveal novel connections between cellular processes. *Genes Develop.* **25**, 767-778.

Ficarro, S. B., McCleland, M. L., Stukenberg, P. T., Burke, D. J., Ross, M. M., Shabanowitz, J., Hunt, D. F. & White, F. M. (2002). Phosphoproteome analysis by mass spectrometry and its application to *Saccharomyces cerevisiae*. *Nature Biotech.* **20**, 301-305.

Fiedler, D., Braberg, H., Mehta, M., Chechik, G., Cagney, G., Mukherjee, P., Silva, A. C., Shales, M., Collins, S. R., Van Wageningen, S., Kemmeren, P., Holstege, F. C., Weissman, J. S., Keogh, M. C., Koller, D., Shokat, K. M. & Krogan, N. J. (2009). Functional organization of the *S. cerevisiae* phosphorylation network. *Cell* **136**, 952-963.

Flandéz, M., Cosano, I. C., Nombela, C., Martin, H. & Molina, M. (2004). Reciprocal regulation between Slt2 MAPK and isoforms of Msg5 dual-specificity protein phosphatase modulates the yeast cell integrity pathway. *J. Biol. Chem.* **279**, 11027-11034.

Free, S. J. (2013). Fungal cell wall organization and biosynthesis. *Adv. Genet.* **81**, 33-82.

Friant, S., Lombardi, R., Schmelzle, T., Hall, M. N. & Riezman, H. (2001). Sphingoid base signaling *via* Pkh kinases is required for endocytosis in yeast. *EMBO J.* **20**, 6783-6792.

Fuchs, B. B. & Mylonakis, E. (2009). Our paths might cross: The role of the fungal cell wall integrity pathway in stress response and cross talk with other stress response pathways. *Eukaryotic Cell* **8**, 1616-1625.

Furukawa, K. & Hohmann, S. (2013). Synthetic biology: Lessons from engineering yeast MAPK signalling pathways. *Mol. Microbiol.* **88**, 5-19.

Gallacher, L. (2014). The role of three phosphorylated residues in Prs5 NHR5-2 on Rlm1 expression. *BSc Honours project*: School of Life Sciences, Heriot-Watt Univesity, Edinburgh.

Garcia-Pavia, P., Torres, R. J., Rivero, M., Ahmed, M., Garcia-Puig, J. & Becker, M. A. (2003). Phosphoribosylpyrophosphate synthetase overactivity as a cause of uric acid overproduction in a young woman. *Arthritis Rheum* **48**, **2036-2041.**

Garcia, R., Bermejo, C., Grau, C., Pérez, R., Rodriguez-Peña, J., Francois, J., Nombela, C. & Arroyo, J. (2004). The global transcriptional response to

transient cell wall damage in *Saccharomyces cerevisiae* and its regulation by the cell integrity signaling pathway. *J. Biol. Chem.* **279**, 15183 - 15195.

Gavin, A. C., Aloy, P., Grandi, P., Krause, R., Boesche, M., Marzioch, M., Rau, C., Jensen, L. J., Bastuck, S., Dumpelfeld, B., Edelmann, A., Heurtier, M. A., Hoffman, V., Hoefert, C., Klein, K., Hudak, M., Michon, A. M., Schelder, M., Schirle, M., Remor, M., Rudi, T., Hooper, S., Bauer, A., Bouwmeester, T., Casari, G., Drewes, G., Neubauer, G., Rick, J. M., Kuster, B., Bork, P., Russell, R. B. & Superti-Furga, G. (2006). Proteome survey reveals modularity of the yeast cell machinery. *Nature* **440**, 631-636.

Griffioen, G., Swinnen, S. & Thevelein, J. M. (2003). Feedback inhibition on cell wall integrity signaling by Zds1 involves Gsk3 phosphorylation of a cAMP-dependent protein kinase regulatory subunit. *J. Biol. Chem.* **278**, 23460-23471.

Groves, J. D., Falson, P., LE Maire, M. & Tanner, M. J. (1996). Functional cell surface expression of the anion transport domain of human red cell band 3 (AE1) in the yeast *Saccharomyces cerevisiae*. *Proc. Natl. Acad. Sci. U S A.* **93,** 12245-50.

Guo, S., Shen, X., Yan, G., Ma, D., Bai, X., Li, S. & Jiang, Y. (2009). A MAP kinase dependent feedback mechanism controls Rho1 GTPase and actin distribution in yeast. *Plos One* **4**, e6089.

Guthrie, C. & Fink, G. R. (1991). Guide to Yeast Genetics and Molecular Biology: Methods in Enzymology (Academic Press, San Diego, CA) **194**,1–932.

Gygi, S. P. & Aebersold, R. (2000). Mass spectrometry and proteomics. *Curr. Opin. Chem. Biol.* **4**, 489-494.

Haarer, B., Viggiano, S., Hibbs, M. A., Troyanskaya, O. G. & Amberg, D. C. (2007). Modeling complex genetic interactions in a simple eukaryotic genome: actin displays a rich spectrum of complex haploinsufficiencies. *Genes Develop.* **21**, 148-159.

Hahn, J.-S. & Thiele, D. J. (2002). Regulation of the S*accharomyces cerevisiae* Slt2 kinase pathway by the stress-inducible Sdp1 dual specificity phosphatase. *J. Biol. Chem.* **277**, 21278-21284.

Hampsey, M. (1997). A review of phenotypes in *Saccharomyces cerevisiae*. *Yeast* **13**, 1099-1133.

Hang, M. & Smith, M. M. (2011). Genetic analysis implicates the Set3/Hos2 histone deacetylase in the deposition and remodeling of nucleosomes containing H2A.Z. *Genetics* **187**, 1053-1066.

Harrington, L. A. & Andrews, B. J. (1996). Binding to the yeast Swi4,6-dependent cell cycle Box, CACGAAA, is cell cycle regulated *in vivo*. *Nucleic Acids Res.* **24**, 558-565.

Harrison, J., Bardes, E., Ohya, Y. & Lew, D. (2001). A role for the Pkc1p/Mpk1p kinase cascade in the morphogenesis checkpoint. *Nat. Cell Biol.* **3**, 417 - 420.

Heinisch, J. (2005). Baker's yeast as a tool for the development of antifungal kinase inhibitors--targeting protein kinase C and the cell integrity pathway. *Biochim. Biophys. Acta* **1754**, 171 - 182.

Heinisch, J. J. & Dufrêne, Y. F. (2010). Is there anyone out there? – Single-molecule atomic force microscopy meets yeast genetics to study sensor functions. *Integrative Biol.* **2**, 408-415.

Hernando, Y., Parr, A. & Schweizer, M. (1998). *PRS5*, the fifth member of the phosphoribosyl pyrophosphate synthetase gene family in *Saccharomyces cerevisiae*, is essential for cell viability in the absence of either *PRS1* or *PRS3*. *J. Bacteriol.* **180**, 6404-6407.

Hernando, Y., Carter, A. T., Parr, A., Hove-Jensen, B. & Schweizer, M. (1999). Genetic analysis and enzyme activity suggest the existence of more than one minimal functional unit capable of synthesizing phosphoribosyl pyrophosphate in *Saccharomyces cerevisiae*. *J. Biol. Chem.* **274**, 12480-12487.

Hilden, I., Hove-Jensen, B. & Harlow, K. W. (1995). Inactivation of *Escherichia coli* phosphoribosylpyrophosphate synthetase by the 2',3'-dialdehyde derivative of ATP. Identification of active site lysines. *J. Biol. Chem.* **270**, 20730-20736.

Hirata, Y., Andoh, T., Asahara, T. & Kikuchi, A. (2003). Yeast glycogen synthase kinase-3 activates Msn2p-dependent transcription of stress responsive genes. *Mol. Biol. Cell* **14**, 302-312.

Ho, Y., Gruhler, A., Heilbut, A., Bader, G. D., Moore, L., Adams, S. L., Millar, A., Taylor, P., Bennett, K., Boutilier, K., Yang, L., Wolting, C., Donaldson, I., Schandorff, S., Shewnarane, J., Vo, M., Taggart, J., Goudreault, M., Muskat, B., Alfarano, C., Dewar, D., Lin, Z., Michalickova, K., Willems, A. R., Sassi, H., Nielsen, P. A., Rasmussen, K. J., Andersen, J. R., Johansen, L. E., Hansen, L. H., Jespersen, H., Podtelejnikov, A., Nielsen, E., Crawford, J., Poulsen, V., Sorensen, B. D., Matthiesen, J., Hendrickson, R. C., Gleeson, F., Pawson, T., Moran, M. F., Durocher, D., Mann, M., Hogue, C. W., Figeys, D. & Tyers, M. (2002). Systematic identification of protein complexes in *Saccharomyces cerevisiae* by mass spectrometry. *Nature* **415**, 180-183.

Hove-Jensen, B., Harlow, K. W., King, C. J. & Switzer, R. L. (1986). Phosphoribosylpyrophosphate synthetase of *Escherichia coli.* Properties of the purified enzyme and primary structure of the prs gene. *J. Biol. Chem.* **261**, 6765-6771.

Hove-Jensen, B. (1989). Phosphoribosylpyrophosphate (PRPP)-less mutants of *Escherichia coli*. *Mol. Microbiol.* **3**, 1487-1492.

Iizasa, T., Taira, M., Shimada, H., Ishijima, S. & Tatibana, M. (1989). Molecular cloning and sequencing of human cDNA for phosphoribosyl pyrophosphate synthetase subunit II. *FEBS Lett.* **244**, 47-50.

Inagaki, M., Schmelzle, T., Yamaguchi, K., Irie, K., Hall, M. N. & Matsumoto, K. (1999). PDK1 homologs activate the Pkc1-mitogen-activated protein kinase pathway in yeast. *Mol. Cell. Biol.* **19**, 8344-8352.

Ito, T., Chiba, T., Ozawa, R., Yoshida, M., Hattori, M. & Sakaki, Y. (2001). A comprehensive two-hybrid analysis to explore the yeast protein interactome. *Proc. Natl. Acad. Sci. USA.* **98**, 4569-4574.

Jaehning, J. A. (2010). The Paf1 complex: Platform or player in RNA polymerase II transcription? *Biochim. Biophys. Acta* **1799**, 379-388.

Jarolim, S., Ayer, A., Pillay, B., Gee, A. C., Phrakaysone, A., Perrone, G. G., Breitenbach, M. & Dawes, I. W. (2013). *Saccharomyces cerevisiae* genes involved in survival of heat shock. *Genes Genomes Genet.* **3**, 2321-2333.

Jeffery, C. J. (1999). Moonlighting proteins. *Trends Biochem. Sci.* **24**, 8-11.

Jensen, K., Dandanell, G., Hove-Jensen, B. & WillemoËs, M. (2008). Nucleotides, Nucleosides, and Nucleobases. *EcoSal Plus, (doi:101128/ecosalplus362)*.

Jiménez-Sánchez, M., Cid, V. J. & Molina, M. (2007). Retrophosphorylation of Mkk1 and Mkk2 MAPKKs by the Slt2 MAPK in the yeast cell integrity pathway. *J. Biol. Chem.* **282**, 31174-31185.

Jiménez, A., Santos, M. A. & Revuelta, J. L. (2008). Phosphoribosyl pyrophosphate synthetase activity affects growth and riboflavin production in *Ashbya gossypii*. *BMC Biotechnol.* **8**, 67. (doi:10.1186/1472-6750-867).

Jung, U., Sobering, A., Romeo, M. & Levin, D. (2002). Regulation of the yeast Rlm1 transcription factor by the Mpk1 cell wall integrity MAP kinase. *Mol. Microbiol.* **46**, 781 - 789.

Jung, U. S. & Levin, D. E. (1999). Genome-wide analysis of gene expression regulated by the yeast cell wall integrity signalling pathway. *Mol Microbiol.* **34**, 1049-1057.

Kadziola, A., Jepsen, C. H., Johansson, E., McGuire, J., Larsen, S. & Hove-Jensen, B. (2005). Novel class III phosphoribosyl diphosphate synthase: structure and properties of the tetrameric, phosphate-activated, non-allosterically inhibited enzyme from *Methanocaldococcus jannaschii*. *J. Mol. Biol.* **354**, 815-828.

Kamada, Y., Jung, U. S., Piotrowski, J. & Levin, D. E. (1995). The protein kinase C-activated MAP kinase pathway of *Saccharomyces cerevisiae* mediates a novel aspect of the heat shock response. *Genes Develop.* **9**, 1559-1571.

Katashima, R., Iwahana, H., Fujimura, M., Yamaoka, T., Ishizuka, T., Tatibana, M. & Itakura, M. (1998). Molecular cloning of a human cDNA for the 41-kDa phosphoribosylpyrophosphate synthetase-associated protein. *Biochim. Biophys. Acta* **1396**, 245-250.

Keyse, S. M. (2000). Protein phosphatases and the regulation of mitogen-activated protein kinase signalling. *Curr. Opin. Cell. Biol.* **12**, 186-192.

Khorana, H. G. (1960). Synthesis of nucleotides, nucleotide coenzymes and polynucleotides. *Federation Proc.* **19**, 931-941.

Kim, H. J., Sohn, K. M., Shy, M. E., Krajewski, K. M., Hwang, M., Park, J. H., Jang, S. Y., Won, H. H., Choi, B. O., Hong, S. H., Kim, B. J., Suh, Y. L., Ki, C. S., Lee, S.Y., Kim, S. H. & Kim, J. W. (2007). Mutations in PRPS1, which encodes the phosphoribosyl pyrophosphate synthetase enzyme critical for nucleotide biosynthesis, cause hereditary peripheral neuropathy with hearing loss and optic neuropathy (CMTX5). *Am. J. Hum. Genet.* **81**, 552-558.

Kim, K. Y. & Levin, D. E. (2010). Transcriptional reporters for genes activated by cell wall stress through a non-catalytic mechanism involving Mpk1 and SBF. *Yeast* **27**, 541-548.

Kim, K. Y. & Levin, David E. (2011). Mpk1 MAPK association with the Paf1 complex blocks Sen1-mediated premature transcription termination. *Cell* **144**, 745-756.

Kim, K. Y., Cosano, I. C., Levin, D. E., Molina, M. & Martín, H. (2007). Dissecting the transcriptional activation function of the cell wall integrity MAP kinase. *Yeast* **24**, 335-342.

Kim, K. Y., Truman, A. W. & Levin, D. E. (2008). Yeast Mpk1 mitogen-activated protein kinase activates transcription through Swi4/Swi6 by a noncatalytic mechanism that requires upstream signal. *Mol Cell. Biol.* **28**, 2579-2589.

Kirchrath, L., Lorberg, A., Schmitz, H. P., Gengenbacher, U. & Heinisch, J. J. (2000). Comparative genetic and physiological studies of the MAP kinase Mpk1p from *Kluyveromyces lactis* and *Saccharomyces cerevisiae*. *J. Mol. Biol.* **300**, 743-758.

Kita, K., Otsuki, T., Ishizuka, T., Ishijima, S. & Tatibana, M. (1989). Rat liver phosphoribosylpyrophosphate synthetase: Existence as heterogeneous aggregates and identification of the catalytic subunit. *Adv. Exp. Med. Biol.* **253**, 1-6.

Kleineidam, A., Vavassori, S., Wang, K., Schweizer, L. M., Griac, P. & Schweizer, M. (2009). Valproic acid- and lithium-sensitivity in *PRS* mutants of *Saccharomyces cerevisiae*. *Biochem. Soc. Trans.* **37**, 1115-1120.

Klis, F. M., Mol, P., Hellingwerf, K. & Brul, S. (2002). Dynamics of cell wall structure in *Saccharomyces cerevisiae*. *FEMS Microbiol. Rev.* **26**, 239-256.

Klis, F. M., Boorsma, A. & De Groot, P. W. J. (2006). Cell wall construction in *Saccharomyces cerevisiae*. *Yeast* **23**, 185-202.

Kolawa, N., Sweredoski, M. J., Graham, R. L., Oania, R., Hess, S. & Deshaies, R. J. (2013). Perturbations to the ubiquitin conjugate proteome in yeast Δ*ubx* mutants identify Ubx2 as a regulator of membrane lipid composition. *Mol. Cell. Proteomics* **12**, 2791-2803.

Kono, K., Nogami, S., Abe, M., Nishizawa, M., Morishita, S., Pellman, D. & Ohya, Y. (2008). G1/S cyclin-dependent kinase regulates small GTPase Rho1p through phosphorylation of RhoGEF Tus1p in *Saccharomyces cerevisiae*. *Mol Biol. Cell* **19**, 1763-1771.

Krasley, E., Cooper, K., Mallory, M., Dunbrack, R. & Strich, R. (2006). Regulation of the oxidative stress response through Slt2p-dependent destruction of cyclin C in *Saccharomyces cerevisiae*. *Genetics* **172**, 1477 - 1486.

Krath, B. N., Eriksen, T. A., Poulsen, T. S. & Hove-Jensen, B. (1999). Cloning and sequencing of cDNAs specifying a novel class of phosphoribosyl diphosphate synthase in *Arabidopsis thaliana*. *Biochim. Biophys. Acta* **1430**, 403-408.

Krath, B. N. & Hove-Jensen, B. (2001). Implications of secondary structure prediction and amino acid sequence comparison of class I and class II phosphoribosyl diphosphate synthases on catalysis, regulation, and quaternary structure. *Protein Sci.* **10**, 2317-2324.

Krause, S. A., Cundell, M. J., Poon, P. P., McGhie, J., Johnston, G. C., Price, C. & Gray, J. V. (2012). Functional specialisation of yeast Rho1 GTP exchange factors. *J. Cell Sci.* **125**, 2721-2731.

Kuranda, K., Leberre, V., Sokol, S., Palamarczyk, G. & Francois, J. (2006). Investigating the caffeine effects in the yeast *Saccharomyces cerevisiae* brings new insights into the connection between TOR, PKC and Ras/cAMP signalling pathways. *Mol. Microbiol.* **61**, 1147-1166.

Laemmli, U. K. (1970). Cleavage of Structural proteins during the assembly of the head of bacteriophage T4. *Nature* **227**, 680-685.

Lee, M. E., Singh, K., Snider, J., Shenoy, A., Paumi, C. M., Stagljar, I. & Park, H. O. (2011). The Rho1 GTPase acts together with a vacuolar glutathione S-conjugate transporter to protect yeast cells from oxidative stress. *Genetics* **188**, 859-870.

León Ortiz, A. M., Reid, R. J. D., Dittmar, J. C., Rothstein, R. & Nicolas, A. (2011). Srs2 overexpression reveals a helicase-independent role at replication forks that requires diverse cell functions. *DNA Repair* **10**, 506-517.

Levin, D., Bowers, B., Chen, C., Kamada, Y. & Watanabe, M. (1994). Dissecting the protein kinase C/MAP kinase signalling pathway of *Saccharomyces cerevisiae*. *Cell. Mol. Biol. Res.* **40**, 229 - 239.

Levin, D. E. (2005). Cell wall integrity signaling in *Saccharomyces cerevisiae*. *Microbiol. Mol. Biol. Rev.* **69**, 262-291.

Levin, D. E. (2011). Regulation of cell wall biogenesis in *Saccharomyces cerevisiae*: The cell wall integrity signaling pathway. *Genetics* **189**, 1145-1175.

Li, S., Lu, Y., Peng, B. & Ding, J. (2007). Crystal structure of human phosphoribosylpyrophosphate synthetase 1 reveals a novel allosteric site. *Biochem. J.* **401**, 39-47.

Li, X., Ferro-Novick, S. & Novick, P. (2013). Different polarisome components play distinct roles in Slt2p-regulated cortical ER inheritance in *Saccharomyces cerevisiae*. *Mol. Biol. Cell* **24**, 3145-3154.

Lichty, J. J., Malecki, J. L., Agnew, H. D., Michelson-Horowitz, D. J. & Tan, S. (2005). Comparison of affinity tags for protein purification. *Protein Exp. Purif.* **41**, 98-105.

Lin, Y. Y., Lu, J. Y., Zhang, J., Walter, W., Dang, W., Wan, J., Tao, S. C., Qian, J., Zhao, Y., Boeke, J. D., Berger, S. L. & Zhu, H. (2009). Protein acetylation microarray reveals that NuA4 controls key metabolic target regulating gluconeogenesis. *Cell* **136**, 1073-1084.

Liu, X., Han, D., Li, J., Han, B., Ouyang, X., Cheng, J., Li, X., Jin, Z., Wang, Y., Bitner-Glindzicz, M., Kong, X., Xu, H., Kantardzhieva, A., Eavey, R. D., Seidman, C. E., Seidman, J. G., Du, L. L., Chen, Z. Y., Dai, P., Teng, M., Yan, D. & Yuan, H. (2010). Loss-of-function mutations in the PRPS1 gene cause a type of nonsyndromic X-linked sensorineural deafness, DFN2. *Am. J. Hum. Genet.* **86**, 65-71.

Loewith, R. & Hall, M. N. (2011). Target of rapamycin *(TOR)* in nutrient signaling and growth control. *Genetics* **189,** 1177-201.

Lucarelli, A. P., Buroni, S., Pasca, M. R., Rizzi, M., Cavagnino, A., Valentini, G., Riccardi, G. & Chiarelli, L. R. (2010). *Mycobacterium tuberculosis* phosphoribosylpyrophosphate synthetase: biochemical features of a crucial enzyme for mycobacterial cell wall biosynthesis. *Plos One* **5**, e15494.

Madden, K., Sheu, Y. J., Baetz, K., Andrews, B. & Snyder, M. (1997). SBF cell cycle regulator as a target of the yeast PKC-MAP kinase pathway. *Science* **275**, 1781-1784.

Madden, K. & Snyder, M. (1998). Cell polarity and morphogenesis in budding yeast. *Annu. Rev. Microbiol.* **52**, 687-744.

Manning, B. D., Padmanabha, R. & Snyder, M. (1997). The Rho-GEF Rom2p localizes to sites of polarized cell growth and participates in cytoskeletal functions in *Saccharomyces cerevisiae*. *Mol. Biol. Cell* **8**, 1829-1844.

Manning, G., Plowman, G. D., Hunter, T. & Sudarsanam, S. (2002). Evolution of protein kinase signaling from yeast to man. *Trends Biochem. Sci.* **27**, 514-520.

Marín, M., Flandéz, M., Bermejo, C., Arroyo, J., Martín, H. & Molina, M. (2009). Different modulation of the outputs of yeast MAPK-mediated pathways by distinct stimuli and isoforms of the dual-specificity phosphatase Msg5. *Mol Genet. Genomics* **281**, 345 - 359.

Martín, H., Rodríguez-Pachón, J. M., Ruiz, C., Nombela, C. & Molina, M. (2000). Regulatory mechanisms for modulation of signaling through the cell Integrity Slt2-mediated pathway in *Saccharomyces cerevisiae*. *J. Biol. Chem.* **275**, 1511-1519.

Martín, H., Flandéz, M., Nombela, C. & Molina, M. (2005). Protein phosphatases in MAPK signalling: We keep learning from yeast. *Mol. Microbiol.* **58**, 6-16.

Mascaraque, V., Hernaez, M. L., Jiménez-Sánchez, M., Hansen, R., Gil, C., Martín, H., Cid, V. J. & Molina, M. (2013). Phosphoproteomic analysis of protein kinase C signaling in *Saccharomyces cerevisiae* reveals Slt2 mitogen-activated protein kinase (MAPK)-dependent phosphorylation of eisosome core components. *Mol. Cell. Proteomics* **12**, 557-574.

Maubon, D., Garnaud, C., Calandra, T., Sanglard, D. & Cornet, M. (2014). Resistance of *Candida* spp. to antifungal drugs in the ICU: where are we now? *Intensive Care Med.* **40,** 1241-1255.

Mazur, P., Morin, N., Baginsky, W., el-Sherbeini, M., Clemas, J. A., Nielsen, J. B. & Foor, F. (1995). Differential expression and function of two homologous subunits of yeast 1,3-β-D-glucan synthase. *Mol. Cell. Biol.* **15**, 5671-5681.

McClellan, A. J., Xia, Y., Deutschbauer, A. M., Davis, R. W., Gerstein, M. & Frydman, J. (2007). Diverse cellular functions of the Hsp90 molecular chaperone uncovered using systems approaches. *Cell* **131,** 121-35.

Miller, G. A., Rosenzweig, S. & Switzer, R. L. (1975). Oxygen-18 studies of the mechanism of pyrophosphoryl group transfer catalyzed by phosphoribosylpyrophosphate synthetase. *Arch. Biochem. Biophys.* **171**, 732-736.

Moehle, E. A., Ryan, C. J., Krogan, N. J., Kress, T. L. & Guthrie, C. (2012). The yeast SR-like protein Npl3 links chromatin modification to mRNA processing. *PLoS Genet.* **8**, e1003101.

Molina, M., Gil, C., Pla, J., Arroyo, J. & Nombela, C. (2000). Protein localisation approaches for understanding yeast cell wall biogenesis. *Microscopy Res. Technique* **51**, 601-612.

Molina, M., Cid, V. J. & Martín, H. (2010). Fine regulation of *Saccharomyces cerevisiae* MAPK pathways by post-translational modifications. *Yeast* **27**, 503-511.

Monnier, T. (2010). Creation in *Saccharomyces cerevisiae* of a missense mutation, Prs1[L115T], corresponding to the Prs1[M115] mutation associated with Charcot-Marie Tooth neuropathy and its characterisation. B*Sc Honours project*: School of Life Sciences, Heriot-Watt Univesity, Edinburgh.

Nonaka, H., Tanaka, K., Hirano, H., Fujiwara, T., Kohno, H., Umikawa, M., Mino, A. & Takai, Y. (1995). A downstream target of RHO1 small GTP-binding protein is PKC1, a homolog of protein kinase C, which leads to activation of the MAP kinase cascade in *Saccharomyces cerevisiae*. *EMBO J.* **14**, 5931-5938.

Nyhan, W. L., James, J. A., Teberg, A. J., Sweetman, L. & Nelson, L. G. (1969). A new disorder of purine metabolism with behavioral manifestations. *J. Pediatr.* **74**, 20-27.

Oliver, S. (2000). Guilt-by-association goes global. *Nature* **403**, 601-603.

Olszowy, J. & Switzer, R. L. (1972). Specific repression of phosphoribosylpyrophosphate synthetase by uridine compounds in *Salmonella typhimurium*. *J. Bacteriol.* **110**, 450-451.

Ooi, S. L., Pan, X., Peyser, B. D., Ye, P., Meluh, P. B., Yuan, D. S., Irizarry, R. A., Bader, J. S., Spencer, F. A. & Boeke, J. D. (2006). Global synthetic-lethality analysis and yeast functional profiling. *Trends Genet.* **22**, 56-63.

Ossareh-Nazari, B., Bonizec, M., Cohen, M., Dokudovskaya, S., Delalande, F., Schaeffer, C., Van Dorsselaer, A. & Dargemont, C. (2010). Cdc48 and Ufd3, new partners of the ubiquitin protease Ubp3, are required for ribophagy. *EMBO reports* **11**, 548-554.

Pan, X., Ye, P., Yuan, D. S., Wang, X., Bader, J. S. & Boeke, J. D. (2006). A DNA integrity network in the yeast *Saccharomyces cerevisiae*. *Cell* **124**, 1069-1081.

Pennisi, E. (2014). Building the ultimate yeast genome. *Science* **343,** 1426-1429.

Perkins, D. N., Pappin, D. J., Creasy, D. M. & Cottrell, J. S. (1999). Probability-based protein identification by searching sequence databases using mass spectrometry data. *Electrophoresis* **20**, 3551-3567.

Philip, B. & Levin, D. E. (2001). Wsc1 and Mid2 are cell surface sensors for cell wall integrity signaling that act through Rom2, a guanine nucleotide exchange factor for Rho1. *Mol. Cell. Biol.* **21**, 271-280.

Phizicky, E. M. & Fields, S. (1995). Protein-protein interactions: Methods for detection and analysis. *Microbiol. Rev.* **59**, 94-123.

Piper, P. W., Truman, A. W., Millson, S. H. & Nuttall, J. (2006). Hsp90 chaperone control over transcriptional regulation by the yeast Slt2(Mpk1)p and human

ERK5 mitogen-activated protein kinases (MAPKs). *Biochem. Soc. Trans.* **34**, 783-785.

Ptacek, J., Devgan, G., Michaud, G., Zhu, H., Zhu, X., Fasolo, J., Guo, H., Jona, G., Breitkreutz, A., Sopko, R., Mccartney, R. R., Schmidt, M. C., Rachidi, N., Lee, S. J., Mah, A. S., Meng, L., Stark, M. J., Stern, D. F., de Virgilio, C., Tyers, M., Andrews, B., Gerstein, M., Schweitzer, B., Predki, P. F. & Snyder, M. (2005). Global analysis of protein phosphorylation in yeast. *Nature* **438**, 679-684.

Qi, M. & Elion, E. A. (2005). MAP kinase pathways. *J. Cell Sci.* **118**, 3569-3572.

Queralt, E. & Igual, J. C. (2005). Functional connection between the Clb5 cyclin, the protein kinase C pathway and the Swi4 transcription factor in *Saccharomyces cerevisiae*. *Genetics* **171**, 1485-1498.

Ram, A. F., Brekelmans, S. S., Oehlen, L. J. & Klis, F. M. (1995). Identification of two cell cycle regulated genes affecting the β-1,3-glucan content of cell walls in *Saccharomyces cerevisiae*. *FEBS Lett.* **358**, 165-170.

Ray, A., Hector, R. E., Roy, N., Song, J. H., Berkner, K. L. & Runge, K. W. (2003). Sir3p phosphorylation by the Slt2p pathway effects redistribution of silencing function and shortened lifespan. *Nature Genet.* **33**, 522-526.

Richter, K., Haslbeck, M. & Buchner, J. (2010). The heat shock response: life on the verge of death. *Mol. Cell* **40**, 253-266.

Rikhvanov, E., Fedoseeva, I., Varakina, N., Rusaleva, T. & Fedyaeva, A. (2014). Mechanism of *Saccharomyces cerevisiae* yeast cell death induced by heat shock. Effect of cycloheximide on thermotolerance. *Biochemistry* **79**, 16-24.

Rodicio, R. & Heinisch, J. J. (2010). Together we are strong – cell wall integrity sensors in yeasts. *Yeast* **27**, 531-540.

Roessler, B. J., Nosal, J. M., Smith, P. R., Heidler, S. A., Palella, T. D., Switzer, R. L. & Becker, M. A. (1993). Human X-linked phosphoribosylpyrophosphate synthetase superactivity is associated with

distinct point mutations in the PRPS1 gene. *J. Biol Chem.* **268**, 26476-26481.

Schenk, L., Meinel, D. M., Strasser, K. & Gerber, A. P. (2012). La-motif-dependent mRNA association with Slf1 promotes copper detoxification in yeast. *RNA* **18**, 449-461.

Schmidt, A., Schmelzle, T. & Hall, M. N. (2002). The RHO1-GAPs SAC7, BEM2 and BAG7 control distinct RHO1 functions in *Saccharomyces cerevisiae*. *Mol. Microbiol.* **45**, 1433-1441.

Schneiter, R., Carter, A. T., Hernando, Y., Zellnig, G., Schweizer, L. M. & Schweizer, M. (2000). The importance of the five phosphoribosyl-pyrophosphate synthetase (Prs) gene products of *Saccharomyces cerevisiae* in the maintenance of cell integrity and the subcellular localization of Prs1p. *Microbiology* **146**, 3269-3278.

Shi, X., Finkelstein, A., Wolf, A. J., Wade, P. A., Burton, Z. F. & Jaehning, J. A. (1996). Paf1p, an RNA polymerase II-associated factor in *Saccharomyces cerevisiae*, may have both positive and negative roles in transcription. *Mol. Cell. Biol.* **16**, 669-676.

Sikorski, R. S. & Boeke, J. D. (1991). *In vitro* mutagenesis and plasmid shuffling: from cloned gene to mutant yeast. *Methods Enzymol.* **194**, 302-318.

Sobering, A. K., Jung, U. S., Lee, K. S. & Levin, D. E. (2002). Yeast Rpi1 is a putative transcriptional regulator that contributes to preparation for stationary phase. *Eukaryotic Cell* **1**, 56-65.

Sonoda, T., Taira, M., Ishijima, S., Ishizuka, T., Iizasa, T. & Tatibana, M. (1991). Complete nucleotide sequence of human phosphoribosyl pyrophosphate synthetase subunit I *(PRS I)* cDNA and a comparison with human and rat PRPS gene families. *J. Biochem.* **109**, 361-364.

Soriano-Carot, M., Ba*ñó*, M. C. & Igual, J. C. (2012). The yeast mitogen-activated protein kinase Slt2 is involved in the cellular response to genotoxic stress. *Cell Div.* **7**, 1-14.

Sperling, O., Boer, P., Persky-Brosh, S., Kanarek, E. & De Vries, A. (1972). Altered kinetic property of erythrocyte phosphoribosylpsyrophosphate synthetase in excessive purine production. *Rev. Eur. Etud. Clin. Biol.* **17**, 703-706.

Stark, C., Su, T. C., Breitkreutz, A., Lourenco, P., Dahabieh, M., Breitkreutz, B. J., Tyers, M. & Sadowski, I. (2010). PhosphoGRID: a database of experimentally verified *in vivo* protein phosphorylation sites from the budding yeast *Saccharomyces cerevisiae*. *Database* (Oxford)*, 2010*, bap026 (dio:10.1093/database/bap026).

Stark, M. J. R. (2004). Protein phoshorylation and dephosphorylation. In *The Metabolism and Molecular Physiology of Saccharomyces cerevisiae,* pp. 284-375. Edited by J. R. Dickinson & M. Schweizer. London, New York: CRC Press.

Swaney, D. L., Beltrao, P., Starita, L., Guo, A., Rush, J., Fields, S., Krogan, N. J. & Villen, J. (2013). Global analysis of phosphorylation and ubiquitylation cross-talk in protein degradation. *Nature Methods* **10**, 676-682.

Switzer, R. L. (1969). Regulation and mechanism of phosphoribosylpyrophosphate synthetase. I. Purification and properties of the enzyme from *Salmonella typhimurium*. *J. Biol. Chem.* **244**, 2854-2863.

Synofzik, M., Muller vom Hagen, J., Haack, T. B., Wilhelm, C., Lindig, T., Beck-Wodl, S., Nabuurs, S. B., Van Kuilenburg, A. B., de Brouwer, A. P. & Schols, L. (2014). X-linked Charcot-Marie-Tooth disease, Arts syndrome, and prelingual non-syndromic deafness form a disease continuum: evidence from a family with a novel PRPS1 mutation. *Orphanet. J. Rare Dis.* **9**, 24.

Szappanos, B., Kovacs, K., Szamecz, B., Honti, F., Costanzo, M., Baryshnikova, A., Gelius-Dietrich, G., Lercher, M. J., Jelasity, M., Myers, C. L., Andrews, B. J., Boone, C., Oliver, S. G., Pal, C. & Papp, B. (2011). An integrated approach to characterize genetic interaction networks in yeast metabolism. *Nature Genet.* **43**, 656-662.

Taira, M., Ishijima, S., Kita, K., Yamada, K., Iizasa, T. & Tatibana, M. (1987). Nucleotide and deduced amino acid sequences of two distinct cDNAs for rat phosphoribosylpyrophosphate synthetase. *J. Biol. Chem.* **262**, 14867-14870.

Taira, M., Iizasa, T., Yamada, K., Shimada, H. & Tatibana, M. (1989). Tissue-differential expression of two distinct genes for phosphoribosyl pyrophosphate synthetase and existence of the testis-specific transcript. *Biochim. Biophys. Acta* **1007**, 203-208.

Taira, M., Iizasa, T., Shimada, H., Kudoh, J., Shimizu, N. & Tatibana, M. (1990). A human testis-specific mRNA for phosphoribosylpyrophosphate synthetase that initiates from a non-AUG codon. *J. Biol. Chem.* **265**, 16491-16497.

Tang, W., Li, X., Zhu, Z., Tong, S., Zhang, X., Teng, M. & Niu, L. (2006). Expression, purification, crystallization and preliminary X-ray diffraction analysis of human phosphoribosyl pyrophosphate synthetase 1 (PRS1). *Acta Crystallogr. F. Sect. Struct. Biol. Cryst. Commun.* **62**, 432-434.

Tarassov, K., Messier, V., Landry, C. R., Radinovic, S., Serna Molina, M. M., Shames, I., Malitskaya, Y., Vogel, J., Bussey, H. & Michnick, S. W. (2008). An *in vivo* map of the yeast protein interactome. *Science* **320**, 1465-1470.

Tatibana, M., Kita, K., Taira, M., Ishijima, S., Sonoda, T., Ishizuka, T., Iizasa, T. & Ahmad, I. (1995). Mammalian phosphoribosyl-pyrophosphate synthetase. *Adv. Enzyme Regul.* **35**, 229-249.

Terpe, K. (2003). Overview of tag protein fusions: from molecular and biochemical fundamentals to commercial systems. *Appl. Microbiol. Biotechnol.* **60**, 523-533.

Timson, D. (2007). Galactose metabolism in *Saccharomyces cerevisiae*. *Dynamic Biochem. Proc. Biotechnol. Mol. Biol.* **1**, 63-73.

Torres, J., Di Como, C. J., Herrero, E. & De La Torre-Ruiz, M. A. (2002). Regulation of the cell integrity pathway by rapamycin-sensitive TOR function in budding yeast. *J. Biol. Chem.* **277**, 43495-43504.

Tozzi, M. G., Camici, M., Mascia, L., Sgarrella, F. & Ipata, P. L. (2006). Pentose phosphates in nucleoside interconversion and catabolism. *FEBS J.* **273**, 1089-1101.

Truman, A. W., Millson, S. H., Nuttall, J. M., King, V., Mollapour, M., Prodromou, C., Pearl, L. H. & Piper, P. W. (2006). Expressed in the yeast *Saccharomyces cerevisiae*, human ERK5 is a client of the Hsp90 chaperone that complements loss of the Slt2p (Mpk1p) cell integrity stress-activated protein kinase. *Eukaryotic Cell* **5**, 1914-1924.

Truman, A. W., Kim, K.-Y. & Levin, D. E. (2009). Mechanism of Mpk1 mitogen-activated protein kinase binding to the Swi4 transcription factor and its regulation by a novel caffeine-induced phosphorylation. *Mol. Cell. Biol.* **29**, 6449-6461.

Tsaponina, O., Barsoum, E., Aström, S. U. & Chabes, A. (2011). Ixr1 is required for the expression of the ribonucleotide reductase Rnr1 and maintenance of dNTP pools. *PLoS Genet* **7**, e1002061.

Tucker, C. L. & Fields, S. (2003). Lethal combinations. *Nature Genet.* **35**, 204-205.

Uetz, P., Giot, L., Cagney, G., Mansfield, T. A., Judson, R. S., Knight, J. R., Lockshon, D., Narayan, V., Srinivasan, M., Pochart, P., Qureshi-Emili, A., Li, Y., Godwin, B., Conover, D., Kalbfleisch, T., Vijayadamodar, G., Yang, M., Johnston, M., Fields, S. & Rothberg, J. M. (2000). A comprehensive analysis of protein-protein interactions in *Saccharomyces cerevisiae*. *Nature* **403**, 623-627.

Ugbogu, E. A., Wippler, S., Euston, M., Kouwenhoven, E. N., de Brouwer, A. P., Schweizer, L. M. & Schweizer, M. (2013). The contribution of the nonhomologous region of Prs1 to the maintenance of cell wall integrity and cell viability. *FEMS Yeast Res.* **13**, 291-301.

Ullman, B. & Carter, D. (1997). Molecular and biochemical studies on the hypoxanthine-guanine phosphoribosyltransferases of the pathogenic haemoflagellates. *Int. J. Parasitol.* **27**, 203-213.

van Drogen, F. & Peter, M. (2002). Spa2p functions as a scaffold-like protein to recruit the Mpk1p MAP kinase module to sites of polarized growth. *Curr. Biol.* **12**, 1698-1703.

van Pel, D. M., Stirling, P. C., Minaker, S. W., Sipahimalani, P. & Hieter, P. (2013). *Saccharomyces cerevisiae* genetics predicts candidate therapeutic genetic interactions at the mammalian replication fork. *Genes Genomes Genet.* **3**, 273-282.

Vavassori, S. (2005). An investigation of the influence of impaired PRPP production on the physiology of *Saccharomyces cerevisiae*. *PhD thesis*: School of Life Sciences, Heriot-Watt Univesity, Edinburgh.

Vavassori, S., Wang, K., Schweizer, L. M. & Schweizer, M. (2005a). In *Saccharomyces cerevisiae*, impaired PRPP synthesis is accompanied by valproate and Li+ sensitivity. *Biochem. Soc. Trans.* **33**, 1154-1157.

Vavassori, S., Wang, K., Schweizer, L. M. & Schweizer, M. (2005b). Ramifications of impaired PRPP synthesis in *Saccharomyces cerevisiae*. *Biochem. Soc. Trans.* **33**, 1418-1420.

Vidalain, P. O., Boxem, M., Ge, H., Li, S. & Vidal, M. (2004). Increasing specificity in high-throughput yeast two-hybrid experiments. *Methods* **32**, 363-370.

Walker, G. M. (1998). Yeast Growth. In Yeast Physiology and Biotechnology: Pp 101-202. Chichester: John Wiley & Sons Ltd.

Wang, K., Vavassori, S., Schweizer, L. M. & Schweizer, M. (2004). Impaired PRPP-synthesizing capacity compromises cell integrity signalling in *Saccharomyces cerevisiae*. *Microbiology* **150**, 3327-3339.

Wang, K. (2005). The involvement of PRPP synthetase in cell integrity signalling in *Saccharomyces cerevisiae*. *PhD thesis*: School of Life Sciences, Heriot-Watt Univesity, Edinburgh.

Watanabe, Y., Takaesu, G., Hagiwara, M., Irie, K. & Matsumoto, K. (1997). Characterization of a serum response factor-like protein in *Saccharomyces cerevisiae*, Rlm1, which has transcriptional activity regulated by the Mpk1 (Slt2) mitogen-activated protein kinase pathway. *Mol. Cell Biol.* 17**,** 2615-23.

Wen, K. K. & Rubenstein, P. A. (2009). Differential regulation of actin polymerization and structure by yeast formin isoforms. *J. Biol. Chem.* **284**, 16776-16783.

Wilkiewicz, A. (2010). Investigation of the phenotypical stress responses of a *Saccharomyces cerevisiae* strain mutated to mimic Arts syndrome. *BSc Honours project:* School of Life Sciences, Heriot-Watt Univesity, Edinburgh.

Wojda, I., Alonso-Monge, R., Bebelman, J.-P., Mager, W. H. & Siderius, M. (2003). Response to high osmotic conditions and elevated temperature in *Saccharomyces cerevisiae* is controlled by intracellular glycerol and involves coordinate activity of MAP kinase pathways. *Microbiology* **149**, 1193-1204.

Yabuki, Y., Kodama, Y., Katayama, M., Sakamoto, A., Kanemaru, H., Wan, K. & Mizuta, K. (2014). Glycogen synthase kinase-3 is involved in regulation of ribosome biogenesis in yeast. *Biosci. Biotechnol. Biochem.* **78**, 800-805.

Yan, G., Lai, Y. & Jiang, Y. (2012). The TOR complex 1 is a direct target of Rho1 GTPase. *Mol. Cell* **45,** 743-53.

Yao, R., Zhang, Z., An, X., Bucci, B., Perlstein, D. L., Stubbe, J. & Huang, M. (2003). Subcellular localization of yeast ribonucleotide reductase regulated by the DNA replication and damage checkpoint pathways. *Proc. Natl. Acad. Sci. USA.* **100**, 6628-6633.

Ye, P., Peyser, B. D., Pan, X., Boeke, J. D., Spencer, F. A. & Bader, J. S. (2005). Gene function prediction from congruent synthetic lethal interactions in yeast. *Mol. Syst. Biol.* **1**, 2005 0026.

Ye, Y., Zhu, Y., Pan, L., Li, L., Wang, X. & Lin, Y. (2009). Gaining insight into the response logic of *Saccharomyces cerevisiae* to heat shock by combining

expression profiles with metabolic pathways. *Biochem. Biophys. Res. Commun.* **385**, 357-362.

Yip, T.-T., Nakagawa, Y. & Porath, J. (1989). Evaluation of the interaction of peptides with Cu(II), Ni(II), and Zn(II) by high-performance immobilized metal ion affinity chromatography. *Anal. Biochem.* **183**, 159-171.

Yoshida, S., Bartolini, S. & Pellman, D. (2009). Mechanisms for concentrating Rho1 during cytokinesis. *Genes Develop.* **23**, 810-823.

Young, C. L., Britton, Z. T. & Robinson, A. S. (2012). Recombinant protein expression and purification: A comprehensive review of affinity tags and microbial applications. *Biotechnol. J.* **7**, 620-634.

Young, E. (2012). Are various Prs5 mutants capable of interacting with Rim11? *BSc Honours project*: School of Life Sciences, Heriot-Watt Univesity, Edinburgh.

Zhang, J., Zhou, B., Zheng, C. F. & Zhang, Z. Y. (2003). A bipartite mechanism for ERK2 recognition by its cognate regulators and substrates. *J. Biol. Chem.* **278**, 29901-29912.

Zhao, C., Jung, U. S., Garrett-Engele, P., Roe, T., Cyert, M. S. & Levin, D. E. (1998). Temperature-induced expression of yeast *FKS2* is under the dual control of protein kinase C and calcineurin. *Mol. Cell. Biol.* **18**, 1013-1022.

Website cited;

http://www.candidagenome.org/
http://kinase.com/scerevisiae
www.matrixscience.com
http://www.ncbi.nlm.nih.gov/pubmed
http://www.phosphogrid.org
http://www.phosphopep.org
www.piercenet.com
http://www.yeastgenome.org